POLITECNICO DI MILANO
Department of Civil and Environmental Engineering
Master of Science in Civil Engineering

EXPERIMENTAL INVESTIGATION ON SOIL-FOUNDATION INTERACTION UNDER CYCLIC AND MONOTONIC LOADING

Supervisor:
Prof. Andrea Galli

Master Dissertation of:
Ehsan Sanglakh Ghouchan Atigh -779966

Academic Year 2013-2014

To my beloved family

And my love.

Acknowledgments

First and Foremost, I would like to express my sincere gratitude and deepest appreciation to my advisor Professor Andrea Galli for the continuous support of my Master dissertation that shaped my research, for his patience, motivation, enthusiasm, and immense knowledge. His guidance helped me in all the time of research and writing of this thesis.

Many friends have helped me stay sane through these difficult years. Their support and care helped me overcome setbacks and stay focused on my graduate study. I greatly value their friendship and I deeply appreciate their belief in me.

Last but by no means least, a special heart-felt gratitude to my family and my love. Words cannot express how grateful I am to my father, my mother, my sisters, my brother and my love for all of the sacrifices that they've made on my behalf. Their candidly love and support throughout, in these years as always, for which my mere expression of thanks does not suffice.

Abstract

With the ever growing interest in performance-based approaches to seismic design, there is now an increasing awareness of the effects of the interaction between the foundation and the superstructure and its role on the overall seismic capacity of the system.

In the classical seismic design approach according to capacity principle, it is generally recognized that any damage to the foundation should be avoided, while the nonlinear capacity of the system is exploited at the superstructure level alone.

One of the most important challenge and criteria that must always be considered in the design of structures is to correctly predict all the structure movements and find out the movement limitation that structure can resist. To get a correct prediction and safe design all the displacements and forces induced by the nature or even by human factors on the structure must be analyzed and taken into account carefully. Many cyclic loads of different nature may affect civil and environmental structures, such as wind effect, sea-wave actions and earthquake. From the geotechnical point of view and by considering the soil-structure interaction these extreme and complex loading paths can cause large irrecoverable and plastic deformation in the soil. Sometimes these loads become the dominant factor in the design and may cause significant changes in the structure of the soil, even causing a shear rupture, heave, void deformation and important compaction. Hence the analytical and experimental modeling under such a complex loading paths requires to analyze a post-yielding behavior for both soil and foundation response. It is then evident the importance of studying effects of cyclic loads on the foundation, but empirical data are still far from sufficient, both for shallow and deep foundation.

This thesis deals with soil-foundation interaction by considering shallow and foundation under cyclic loads. The work is divided into two parts:

1- ***Experimental works:***

This part has been performed by means of the small scale experimental set up available at the geotechnical laboratory of the department of the civil and environmental engineering at Politecnico di Milano. This machine is capable to apply cyclic or monotonic, horizontal and vertical loads. In this study loose Ticino River sand was used, with the relative density about 40%. Several types of cyclic tests were performed.

The experimental results have been interpreted in terms of generalized stress-strain variables, by studying and quantifying in particular (i) the global stiffness and damping properties of the foundation system and their evolution with cycling, (ii) the ratcheting phenomenon along both vertical and horizontal directions, and (iii) the coupling effect between vertical and horizontal loads. This latter issue, in particular, plays an important role even at low number of cycles, i.e. when the behaviour of the system is often considered in the design practice to be linear elastic, since it has been observed that the average stiffness of the system remarkably depends on the loading direction. The results appear to be particularly useful in the light of a reliable displacement-based design procedure for the deep foundation, as required by the current design standards.

2- ***Numerical Interpretation by Using the Macro-Element:***

A Soil-foundation interaction modeling approach is presented, with an emphasis on the macro- element model. The present part is aimed at giving a contribution to the description of the mechanical response of the system by presenting the results of a small scale experimental campaign on different kinds of foundations. By studying initially monotonic tests results, by considering the generalized stress path, regarding each monotonic test, it is possible to analytically define the interaction domain by means of macro-element approach for the different geometries of the foundation. In the monotonic part, the coupling between vertical and horizontal direction is presented by studying the kinematic of the system, and also it is confirmed that the system is non-associated. After defining the interaction domain, a deeper investigation on the response to several cyclic loading paths, combining vertical and horizontal loads, will be presented. The experimental results will be interpreted in particular in terms of the average stiffness and of the damped energy of each cycle, as well as in terms of the accumulation of permanent displacements during cycling. A clear increase in stiffness and decay in dissipated energy will be observed after applying number of cycles, and influence of the loading path and the type of the foundation has been studied.

Key Words: Soil-Foundation Interaction, Deep Foundation, Shallow Foundation, Macro Element Approach, Interaction Domain, Monotonic Loading, Cyclic Loading, Ratcheting Phenomena, damping Factor, Average Stiffness, Dissipated energy, Pseudo Dilatancy.

Sommario

Con il crescente interesse per gli studii basati sulle prestazioni di progettazione antisismica, vi è oggigiorno una crescente consapevolezza degli effetti dell'interazione tra la fondazione e la sovrastruttura e il suo ruolo della complessiva capacità sismica del sistema.

Nel classico approccio della progettazione antisismica secondo il principio della capacità, è generalmente riconosciuto che dovrebbe essere evitato qualsiasi danno alla fondazione, mentre la capacità non lineare del sistema viene sfruttata a livello della sola sovrastruttura.

Uno dei più importanti criteri che deve sempre essere considerato nella progettazione delle strutture è quello di prevedere correttamente tutti i movimenti e di trovare lo spostamento limite che la struttura può subire. Per ottenere una stima corretta e un progetto che rispetti i parametri di sicurezza devono essere analizzati e presi in considerazione attentamente tutti gli spostamenti e le forze dovuti dalla natura e dai fattori antropologici sulla struttura. Carichi ciclici di diversa natura possono influenzare le strutture civili ed ambientali, come l'effetto del vento o le azioni dovute dalle onde del mare e del terremoto. Dal punto di vista geotecnico considerando l'interazione terreno-struttura questi percorsi di carico estremi e complessi possono provocare deformazioni irreversibili e plastiche nel terreno. Talvolta questi carichi diventano il fattore dominante nella progettazione e possono causare cambiamenti significativi nel suolo, provocando perfino rotture a taglio, sollevamento, deformazioni e compressioni. Da qui la modellazione analitica e sperimentale sotto tali complessi percorsi di carico richiede di analizzare il comportamento del suolo e della fondazione dopo il cedimento. E 'quindi evidente l'importanza dello studio degli effetti dei carichi ciclici sulla fondazione, ma i dati empirici non sono ancora sufficienti per studiare la parte superficiale e profonda della fondazione.

Questa tesi si occupa dello studio dell'interazione tra fondazione e terreno considerando la superficie e la fondazione sotto carichi ciclici. Il lavoro è diviso in due parti:

1- ***Lavori sperimentali:***

Questo esperimento è stato eseguito su piccola scala presso il laboratorio di geotecnica del dipartimento di ingegneria civile e ambientale del Politecnico di Milano. Lo strumento utilizato è in grado di applicare carichi ciclici o monotoni, orizzontali e verticali. In questo studio è stata usata la sabbia sciolta del fiume Ticino, con densità relativa di circa il 40%. Sono stati eseguiti vari tipi dis proves cicliche.

I risultati sperimentali sono stati interpretati in termini di variabili generalizzate sforzo-deformazione, studiando e quantificando in particolare (i) la rigidità globale e lo smorzamento del sistema di fondazione e la loro evoluzione durante l'applicazione del carico ciclico, (ii) accumulo ciclico di deformazioni di lungo la direzione verticale ed orizzontale, (iii) l'effetto del mutuo accoppiamento del carico orizzontale e verticale. Quest'ultimo problema, in particolare, gioca un ruolo importante anche sotto un basso numero di cicli, vale a dire quando il comportamento del sistema è ancora in campo elastico lineare, in quanto è stato osservato che la rigidità media del sistema dipende notevolmente dalla direzione di carico. I risultati appaiono particolarmente utili alla luce di uno spostamento basato sulla procedura di progettazione per la fondazione profonda, come richiesto dagli standard odierni.

2- ***Interpretazione numerica attraverso i macroelementi:***

Viene presentato un approccio di modellazione di interazione fondazione-terreno, con l'accento sul modello dei macro-elementi. La presente parte mira a dare un contributo alla descrizione della risposta meccanica del sistema presentando i risultati di una campagna sperimentale su piccola scala condotta su diversi tipi di fondazioni. Studiando inizialmente i risultati dei test monotoni, considerando il percorso di stress, riguardo ogni prova monotona, è possibile definire analiticamente il dominio di interazione mediante l'approccio dei macro-elementi per le diverse geometrie della fondazione. Nella parte monotona, l'accoppiamento tra la direzione verticale ed orizzontale viene presentato studiando la cinematica del sistema, conferma che il sistema è non associato. Dopo aver definito il dominio di interazione, sarà presentato un approfondimento sulla risposta a diversi percorsi di carico ciclici, combinando carichi verticali ed orizzontali. I risultati sperimentali saranno interpretati in particolare in termini di sovrapposizione degli spostamenti permanenti dovuti dal ciclo. Un chiaro aumento della rigidità e una diminuzione dell'energia dissipata viene osservata dopo in certo numero di cicli, così viene studiata l'influenza del percorso di carico sulla fondazione.

Parole Chiave: Interazione Terreno-Fondazioni, Fondazioni Profonde, Fondazioni Superficiali, Aproccio per Macro Elemento, Dominio di Interazione, Carico Monotono, Carico Ciclico, Accumulo Ciclico di Deformazioni, Fattore di Smorzamento, Rigidezza Media, Energia Dissipata, Pseudo Dilatanza.

Table of Contents

List of figures

List of Tables

Preface

Chapter's overview

This thesis deals with soil-foundation interaction by considering shallow foundation with different configuration of piles under monotonic and cyclic loading. This dissertation includes experimental works and mechanical interpretation by using macroelement. This work is aimed at giving a contribution to description of the mechanical response of the system by presenting the results of the small scale experimental tests on shallow foundation. Some parameters that were not considered in previous studies, are taking into account such as: dissipated energy, average stiffness and etc. outlined below a brief description of each chapter.

❖ Chapter 1 - Fundamental concepts

This chapter presents the outline of the study, an introduction into the problem along with the essential background information for the problem and basic concepts of the macroelement model.

❖ Chapter 2 – Literature review

This chapter will present a literature review and description of the previous studies on soil-foundation interaction and give a background into why this study is required.

❖ Chapter 3 – Description of experimental device

This chapter will present the complete description of the experimental device which is available at the geotechnical laboratory of the department of the civil and environmental engineering at Politecnico di Milano that has been used in order to perform the tests.

❖ Chapter 4 – Experimental results on a shallow foundation with pile and interpolations

This chapter will present the final results and mechanical interpolations from the monotonic and cyclic tests. Within this chapter different comparisons have been performed and

some crucial parameters provided by interpolating in order to compare the behavior of the soil in different situations under different kind of loading with different configuration of the piles.

❖ Chapter 5 – Conclusion

This chapter will make a final conclusion on the behavior of the soil under shallow foundation with pile. In addition this chapter will present the overall deductions from different parameters, tables and figures within previous chapters.

1

Fundamental concepts

1.1 Engineering Problems

One of the most important challenge and criteria that must always to be considered in the design of structures is to correctly predict all the structure movements and find out the movement limitation that structure can resist. To get a correct prediction and safe design all the displacements and forces induced by the nature or even by human factors on the structure must be analyzed and taken into account carefully. Many cyclic loads of different nature may affect civil and environmental structures, such as wind effect, sea-wave actions and earthquake. From the geotechnical point of view and by considering the soil-structure interaction these extreme and complex loading paths can cause large irrecoverable and plastic deformation into the soil. Sometimes these loads become the dominant factor in the design and may cause significant changes in the structure of the soil, even causing a shear rupture, heave and important compaction. Hence the analytical and experimental modeling under such a complex loading paths requires to analyze a post-yielding behavior for both soil and foundation response. It is then evident the importance of studying effects of cyclic loads on the foundation, but empirical data are still far from sufficient, both for shallow and deep foundation.

Non-linarites can develop in case of soil-foundation interaction, such as:

1-Geometric nonlinearity: such as the separation of the foundation from the soil or uplift phenomena in case of shallow foundation. Overturning can occur only when the structure rotation is sufficiently large to displace the center of gravity of the foundation. The uplift phenomena can cause rocking motion, which can be considered as the geometric nonlinearity. Since the ductility of the superstructure will be reduced while the rocking motion will take place, many authors such as Hounser (1963), Meek (1978) and Chopra and Yim (1985), reported the benefit of the uplifting on the performance of the supported structure.

2-Interface inelasticity: such as sliding at soil-foundation interface. This can happen when the lateral loading exceeds the frictional resistance of the foundation. As it is mentioned by Newmark (1965) the sliding usually does not induce any failure but permanent deformation can be

induced by these phenomena.

3-Mechanical nonlinearity: such as mobilization of bearing capacity failure mechanism in supporting soil. In static large factor of safety are applied to be far enough from the bearing capacity failure. In seismic analysis sort of plastic hinge will be introduced which can limit the transmitted load by limiting capacity of the foundation and make the superstructure separated by the ground motion. This concept may provide an alternative method of in-ground seismic isolation: the so-called rocking isolation.

1.2 Outline of the study

This study aims at experimentally exploring the behaviour of a small scale shallow foundation on loose dry sand, subject to vertical and horizontal cyclic loads. The experimental results have been interpreted in terms of generalized stress-strain variables, by studying and quantifying in particular (i) the global stiffness and damping properties of the foundation system and their evolution with cycling, (ii) the ratcheting phenomenon along both vertical and horizontal directions, and (iii) the coupling effect between vertical and horizontal loads. This latter issue, in particular, plays an important role even at low number of cycles, i.e. when the behaviour of the system is often considered in the design practice to be linear elastic, since it has been observed that the average stiffness of the system remarkably depends on the loading direction.

The results appear to be particularly useful in the light of a reliable displacement-based design procedure for the deep foundation, as required by the current design standards.

1.3 Background Information

Safe design of deep foundation subject to cyclic loads still represents an open issue for engineers and researchers, since it requires several complex non-linear phenomena (such as ratcheting, rocking and uplift mechanisms of the foundation, coupling among the different loading components) to be accounted for. All these features become even more important when dynamic loads have to be considered in the design, like in case the structure must be verified against severe environmental loads (e.g. wind loads on tall buildings, or sea-wave actions on offshore structures). Such non-linear and inelastic effects, however, are not necessarily detrimental, but they can even be beneficial for the foundation, in particular when seismic actions are considered, since they reduce the ductility demand on the superstructure and allow (theoretically) to design the foundation as a seismic isolator. Rigorous numerical modelling approaches, like finite element or discrete element methods, are nowadays available for design

purposes, but they are still quite demanding both from an economic and a computational point of view, and they cannot be considered yet as a standard design tool for geotechnical and structural engineers, in particular when a pre-dimensioning of the system is required. Moreover, even sophisticated numerical codes are not always able to capture some of the above cited features of the soil-foundation interaction and require advanced constitutive rules or very refined calibration procedures in order to get satisfactory quantitative results.

Since late ’80 an alternative (and innovative, at that time) interpretative framework has been proposed (Nova andMontrasio1991) for describing the behaviour of the system in terms of generalised stress-strain variables. In the last two decades several models have been proposed in order to analytically describe the generalized constitutive relationship for a macro element, based on different theoretical approaches, like classical strain hardening elastoplasticity, hypo plasticity, multi mechanism models, and accounting even for complex loading paths and complex geometries. More recently, a new soil-foundation contact interface model, based on the tracking of the deformed geometry of the soil beneath the foundation has been proposed (Gajan and Kutter, 2009). Beyond a validation or a critical discussion of such modelling approaches, the present study is aimed at giving a contribution to the description of the mechanical response of the system by presenting the results of a small scale experimental campaign on a model shallow foundation. Starting from the experimental work published by Nova, di Prisco, Sibilia (2003; Nova and Maugeri editors), a deep investigation on the response to several cyclic loading paths, combining vertical and horizontal loads, will be presented. The experimental results will be interpreted in particular in terms of the average stiffness and of the damped energy of each cycle, as well as in terms of the accumulation of permanent displacements during cycling. This approach (although the presented results are referred to small scale tests, and a robust verification on large scale experimental campaign will be required before upscaling them to the actual design of a real scale structure) can be interpreted into the light of the current design standards, which require a displacement based approach (Priestley et al. 2007;Calviand Sullivan 2009). These methodologies have been proposed in the last decade within the framework of a “performance based design”, aimed at verifying the structure not only in term of the strength with respect to a single action (or to a combination of them), but mainly in terms of the permanent displacements that the structure is required to accommodate. Such approaches are essentially based on non-linear equivalent iterative procedures, capable of taking into account (i) the decay of the stiffness and (ii) the evolution of the damping of the foundation with increasing displacement. Both of these quantities are generally expressed by means of abaci, whose analytical expressions can be easily implemented into the design procedure. Nevertheless, the design abaci do not explicitly take into account the evolution of stiffness and damping with the increasing number of cycles, nor the coupling effect of combined vertical and horizontal loads acting on the system. Moreover, a large amount of experimental and theoretical works have been devoted to the study of the behaviour of the foundation under cyclic rocking moment

(representative of systems like tall buildings, offshore structure, etc...), but fewer results are available for describing the response of the system under pure horizontal cyclic loads. The present study gives a contribution to the current knowledge on this point, by experimentally investigating the evolution of the representative quantities during cycling for different generalised loading paths.

1.3.1 Foundation

Foundations are designed to have an adequate load capacity with limited settlement. Construction of structures involves setting up of foundation which is the lowest part of a building or a bridge and which transmits weight to underlying soil. The soil being a relatively weak material the load is required to be transferred at an increased volume and area in order to prevent over settlement within the soil structure or gross failure. There are two classes of foundations; shallow foundations and deep foundations.

Shallow foundations are often called footings which represent the simplest form of load transfer from a structure to the ground beneath. They are typically constructed with generally small excavations into the ground (they are usually embedded about one meter or so into soil) and do not require specialized construction equipment or tools, and are relatively inexpensive. In most cases, shallow foundations are the most cost-effective choice to support a structure.

There are four main types of shallow foundations (Figure 1-1): isolated spread footings, combined footings, strip footings and mat footings, but the most common for a building structure is spread footing. Overall the design of a footing is based on the allowable bearing capacity which is the maximum pressure that a soil structure can be subjected to by a foundation before overstressing and failure occurs.

Deep foundations are used to transfer a load from a structure through an upper weak layer of soil to a stronger deeper layer of soil. It ensures stability of the structure. Historically, piles built of wood, later steel, reinforced concrete, and pre-tensioned concrete. Sometimes these foundations penetrate bedrock.

There are many types of deep foundations including driven piles, drilled shafts, caissons, geo- piers, and earth stabilized columns (Figure 1-2). Large buildings such as skyscrapers typically require deep foundations.

1.3.1.1 Shallow Foundation

A shallow foundation is a footing planned to take a shape of rectangle or square which supports columns, other structures and walls. In shallow foundations generally consider that bears at a depth less than about two times the foundation width. Shallow foundations principally distribute structural loads over large areas of near-surface soil or rock to reduce the intensity of the applied loads to levels tolerable for the foundation soils. The design and layout of spread footing is controlled by several factors, foremost of which is the weight (load) of the structure it will support as well as penetration of soft near-surface layers, and penetration thought near surface layers likely to change volume due to frost heave or shrink-swell. These foundations are common in residential construction that includes a basement, and in many commercial structures. But for high rise buildings they are not sufficient.

Shallow foundations are used in many applications in highway projects when the subsurface conditions are appropriate. Such applications include bridge abutments on soil slopes or embankments, bridge intermediate piers, retaining walls, culverts, sign posts, noise barriers, and rest stop or maintenance building foundations. Footings or mats may support column loads under buildings. Bridge piers are often supported on shallow foundations using various structural configurations.

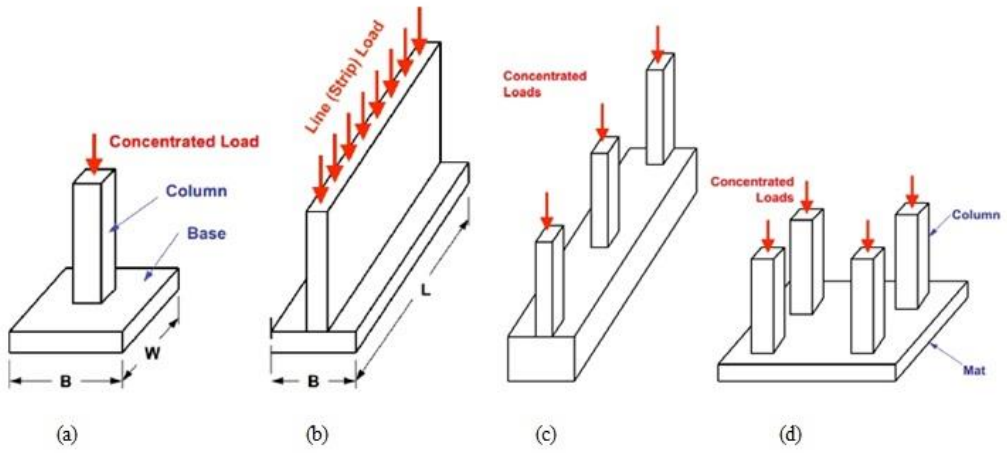

Figure 1-1: Different types of shallow foundations: (a) Spread Footing, (b) Strip Footing, (c) Grade Beams, (d)Mat Footing.

1.3.1.2 Deep foundation

A deep foundation is used to transfer the load of a structure down through the upper weak layer of topsoil to the stronger layer of subsoil below.

Deep foundations are used for structures or heavy loads when shallow foundations cannot provide adequate capacity, due to size and structural limitations. Some of the common reasons of using deep foundations are very large design load, a poor soil at shallow depth or site constrains (like property lines). While shallow foundations rely solely on the bearing capacity of the soil beneath them, deep foundations can rely on end bearing resistance, frictional resistance along their length, or both in developing the required capacity. Geotechnical engineers use specialized tools, such as the cone penetration test, to estimate the amount of skin and end bearing resistance available in the subsurface.

There are different types of deep footings including impact driven piles, drilled shafts, caissons, helical piles, geo-piers and earth stabilized columns. . When the foundation is less than 6 meters deep it is called semi-deep. Beyond that it is called a deep foundation. The naming conventions for different types of footings vary between different engineers.

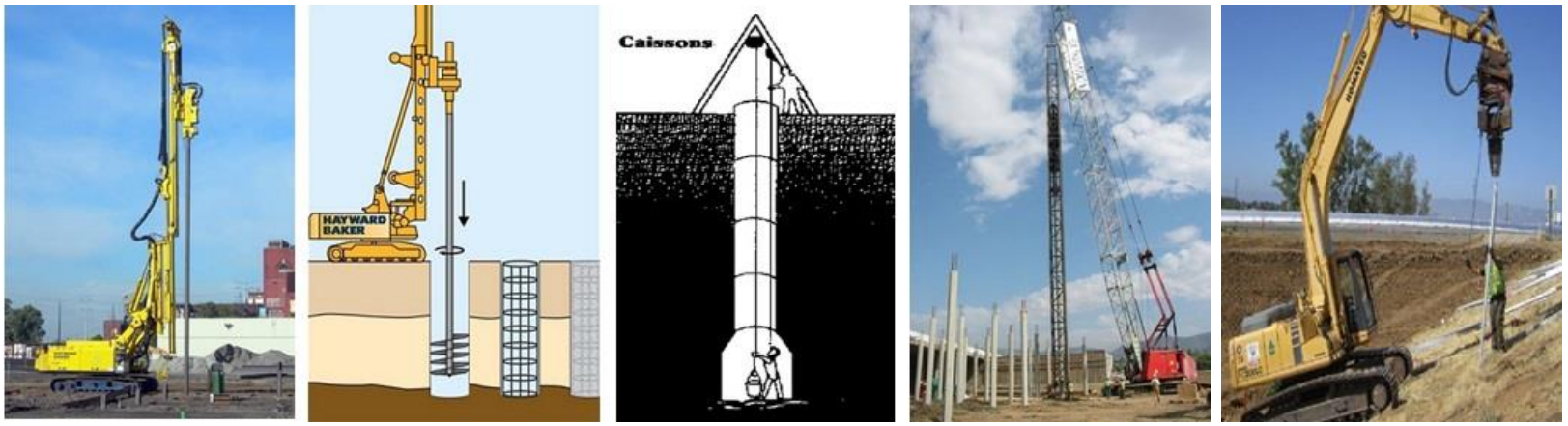

(a) (b) (c) (d) (e)

Figure 1-2: Different kind of deep foundations: (a) driven piles, (b) drilled shafts, (c) caissons, (d) earth stabilized columns, (e) geo-piers.

1.3.2 Macro-Element Approach

In fact most part of the design procedure takes place by considering separately the structure and geotechnical problem, which means either they neglect the geotechnical problem or once the structural problem is solved, the geotechnical issue will be considered, but this uncoupling may be not correct or even safe (di Prisco et al. 2004).

Not many studies consider these two factors all together. One of the possibilities to study in a coupled manner can be small or large scale experimental tests. On the other hand this interaction can be successfully considered by macro-element theory (Butterfiel and Ticof (1979), Georgiadis and Butterfield (1988), Nova and Montrasio (1991), Paolucci, (1997), Gottardi, Houlsby and Butterfield (1999), Martin and Houlsby (2001), Cremer et al. (2001 and 2002) and di prisco et al. (2003a and b) and it is useful because consider the generalized velues.

The aim of the macro-element is to model the near field soil-foundation behavior. In this concept the entire soil-foundation system is considered as a one single element located near the foundation area, which is introduced to analyze the non-linear and irreversible behavior of soil-foundation interaction that can takes place at the near field zone.

The basic idea of the macro-element is to following the analysis of the non-linear behavior of shallow foundation with the plasticity theory of the Roscoe and Schofield (1956 and 1957).

In fact this theory is expanded by Nova and Montrasio (1991) in a case of shallow strip footing on sand under monotonic loading with an isotropic hardening elasto-plastic law to define the bearing capacity of the foundation in a vertical, horizontal and overturning moment plane. This bearing capacity is defined as a yield surface in a plasticity model. And a kinematic of the system has been introduced by a plastic flow rule, non-associated flow rule in sand. So many factors can have an effect on this capacity, for instance, different loading path, different foundation shape and different soil properties.

1.3.3 Interaction Domain in V-H space

In macro-element theory, proposed by Nova and Montrasio (1991) for a rigid strip footing the experimental tests have been performed on a small scale prototype of a strip foundation (plane strain conditions) that can be subject to a generalized loading system composed of vertical (V) and horizontal (H) forces and to an overturning moment (M), and undergo a generalised displacement represented by the vertical (v) and horizontal (u) displacements and by the rotational settlement (θ), as sketched in figure (1-2) with reference to

the central point O of the foundation. For the sake of simplicity the distance b between the line of application of the horizontal load H and the point O is assumed to be negligible, so that H does not influence the overturning moment M.

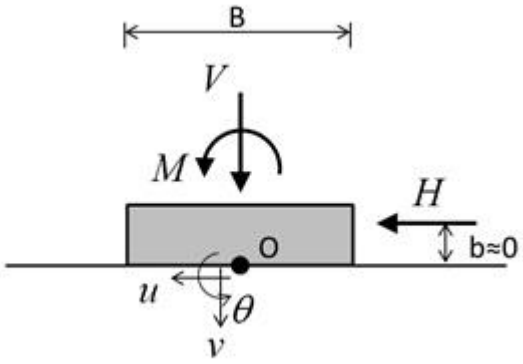

Figure 1-3*:* Footing under the generalized stress variables; the vertical force (V), the horizontal force (H) and the overturning moment (M) and generalized displacement represented by the vertical (v) and horizontal (u) displacements and by the rotational settlement (θ).

These quantities can be lumped into a generalised stress vector Q and a generalised strain vector q, representing the static and kinematic variables of the system, respectively (superscript index T stands for transpose operator).

$$Q = \left[V \quad H \quad M/B\right]^T, \quad q = \left[v \quad u \quad \theta \cdot B\right]^T. \qquad \text{Eq 1.1}$$

Within the theoretical framework of the macro element approach, the behaviour of the whole system can then be described by means of an elastoplastic constitutive relationship between Q and q:

$$\dot{Q} = \begin{bmatrix} \dot{V} \\ \dot{H} \\ \dot{M}/B \end{bmatrix} = \begin{bmatrix} K_V & K_{HV} & K_{MV} \\ K_{VH} & K_H & K_{MH} \\ K_{VM} & K_{HM} & K_M \end{bmatrix} \cdot \begin{bmatrix} \dot{v} \\ \dot{u} \\ \dot{\theta} \cdot B \end{bmatrix} = K^{ep} \dot{q} \qquad \text{Eq 1.2}$$

Where matrix K^{ep} plays the role of incremental elastoplastic stiffness for the soil-foundation system (dots are not intended as derivative with respect to time, but only as increments).In particular, in the following the attention will be restricted to simplified conditions were:

1. The rotation of the foundation is prevented (i.e. $\dot{\theta} = 0$),

2. The components V and H only of the generalised stress vector Q are controlled by the user, and

3. No values of the moment M are recorded.

Consequently, from a conceptual point of view, the generalized constitutive equation for the macro element (equation 1.2) can be simplified and, in the following, it will be applied in the form:

$$\begin{bmatrix} \dot{v} \\ \dot{u} \end{bmatrix} = \begin{bmatrix} K_V & K_{HV} \\ K_{VH} & K_H \end{bmatrix}^{-1} \cdot \begin{bmatrix} \dot{V} \\ \dot{H} \end{bmatrix} \quad \text{Eq 1.3}$$

The failure locus proposed by Nova and Montrasio (1991) is obtained in two steps. Initially pure vertical load applied to the foundation in order to define the limit load by means of two different techniques. Unlevelled technique which is the vertical load increase in steps until the system reaches to the failure load (V_M), and in the second technique, after each step of increasing vertical load, sand surface was levelled so that the free surface was always kept at the same level as the base of footing. This step allows the limit load to be defined and also it is possible to model the vertical load-vertical displacement curve by the best fitting approach proposed by Butterfield (1980):

$$\frac{V}{V_M} = 1 - \exp\left(-\frac{R_0 v}{V_M}\right) \quad \text{Eq 1.4}$$

Where, $R_{o,}$ is the initial slope of the vertical load-vertical displacement curve (Figure 1-4).

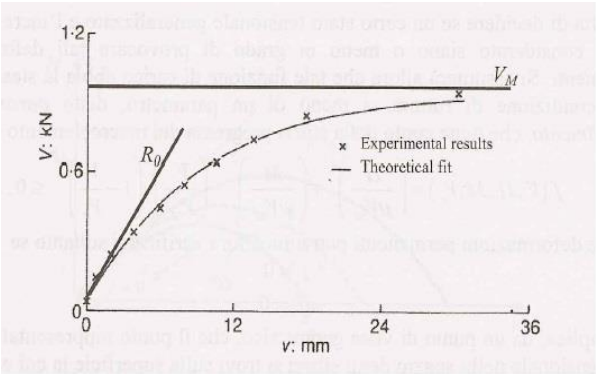

Figure 1-4: Vertical load versus vertical displacement experimentally obtained by Nova and Montrasio (1991), theoretical curve obtained by means of equation 2.1 (Butterfield, 1980).

For the second step to find the failure locus, a series of the tests have been performed with vertical and horizontal loads. In this case the failure point is conducted where initially the vertical load applied until a certain value and then the horizontal load applied at a constant vertical load until the failure load or in the other case both horizontal and vertical load increased in a proportion to each other (Figure 1-5).

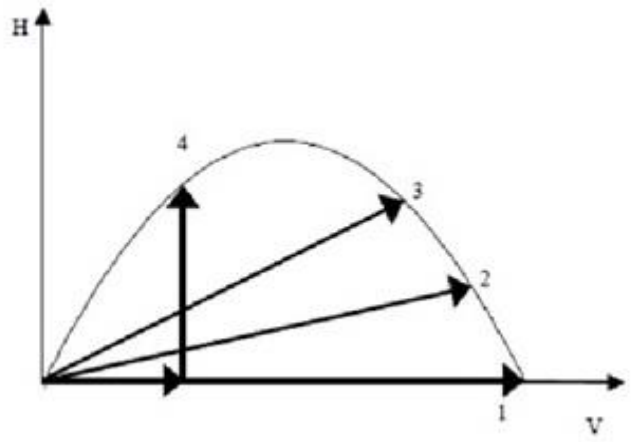

Figure 1-5: Procedure of applying loads to obtain failure locus.

Figure 1-6 shows the interaction diagram at failure between the vertical load (V) and Horizontal load (H) normalized with respect to the maximum vertical load (V_M) obtained by Nova and Motrasio (1991).

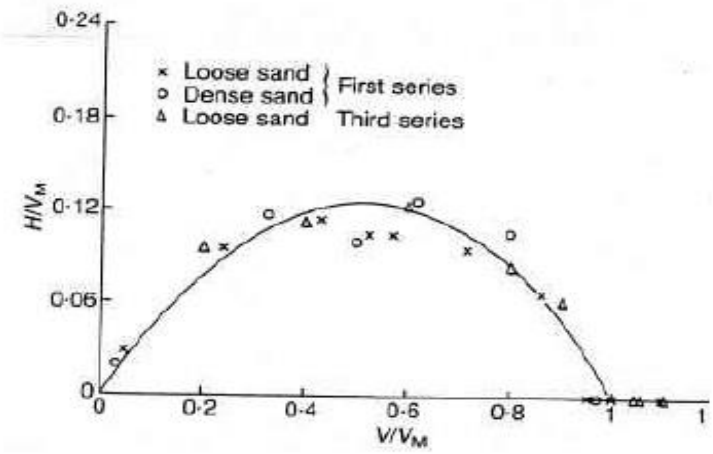

Figure 1-6: Failure Locus for inclined load (Nova and Montrasio, 1991**).**

According to Nova and Montrasio (1991) the best way to fit the obtained failure points in the V-H plain is:

$$\mathbf{F(V,H,V_M) = \frac{H}{\mu V_M} - \frac{V}{V_M}\left(1 - \frac{V}{V_M}\right)^{\beta} = 0} \qquad \text{Eq 1.5}$$

μ, and β are the constitutive parameters and. In particular μ is the traditional soil- foundation friction coefficient, and it is linked to foundation roughness. From experience in laboratory experiments, it can be evaluated as (Nova and Montrasio 1997):

$$\boldsymbol{\mu = \tan \emptyset + 0.72\ \frac{z}{B}} \qquad \text{Eq 1.6}$$

Where φ is the soil friction angle and B is the foundation width. For a small vertical Loads failure occurs when (Nova and Montrasio 1991):

$$\boldsymbol{H = \mu V} \qquad \text{Eq 1.7}$$

Parameter β controls the shape of the interaction domain and maximum horizontal load, if β is equal to 1 the domain described by a parabolic shape and H is maximum in $V = {}^{V_m}/_{2}$. Experimental results are better fitted if β is chosen as 0.95 (Nova and Montrasio, 1991).

Another series of tests have been performed by Nova and Montrasio (1991) by an eccentric vertical loads and the new interaction diagram were defined between the overturning moment (M) and the vertical load. The analytical description for this new failure locus also can be defined in a similar way of the equation 1.5 as follow:

$$F(V, M, V_M) = \frac{M}{\psi B V_M} - \frac{V}{V_M}\left(1 - \frac{V}{V_M}\right)^{\beta} = 0 \qquad \text{Eq 1.8}$$

ψ is non dimensional constitutive parameter which can be selected according to the failure value under eccentric loading; e.g., ψ=0.33 according to the Meyerhof theory (1953), or ψ=0.48 according to Vesic (1970).

1.3.4 Definition of cyclic loading

The term 'cyclic loading' suggest a system of loading which exhibits a degree of regularity both in magnitude and its frequency. Loading system which are approximately cyclic in this sense are indeed encountered in practice. Many machines and even offshore structures, for example, transmit fairly rhythmic stress pulses to their foundations.

1.3.4.1 Cyclic loading

The basic macro-element formula has been further modified by pedretti (1998) and di Prisco et al. (2003) by considering the foundation under cyclic loading by taking into account the model with isotropic hardening with the bounding surface elasto plastic model. For the first time the bounding surface plasticity was defined by Dafalias and Hermann (1982) and it is used instead of loading surface. Here the image point P (Figure 1-7 and 1-8) is defined within the surface which is associated by the specific mapping rule to the point I_P on the surface. At this time the plastic modules will be defined. As a function of the distance between the point P and the image point I_P, so the size of the plastic modules is various by changing the distance between these two points. di Prisco et al. (2003a) define the bounding surface according to the loading-reloading response and gives a continue variation of the plastic modules, while the virgin loading response is defined according to the hardening rule and this model coincide with the Nova and Montrasio model. Pedretti (1998) validated this model by experimental cyclic tests on loose and dense sand, and di Prisco et al. (2003a) defined the purely elastic region similar to the concept of the elastic bubble introduced by the Al Tabbaa and Wood (1989). This model has been declared

that the behavior is fully reversible limited to the sort of ice-cream cone (figure 1-7 and 1-8) within the surface limited by the bounding surface, already defined in monotonic loading as already seen also in Nova and Montrasio macro-element. The cone is defined by the position of the center of the spherical cap, A_1, and by its radius that is a fix quantity. The angle at the cone apex, the origin of axes, is determined by the continuity condition between the cone and the spherical cap. Assume now that a point P_1 on the surface of the ice-cream represents the current state of stress, and that the stress increment P_1P_2 is such that plastic strains occur. It is assumed that these strains are given by:

$$dq^P = \Lambda(Q_1)\emptyset(\delta, \rho_k)\frac{\partial_g}{\partial_Q}(Q_1) \qquad \text{Eq 1.9}$$

In Equation 1.9, the plastic multiplierΛ, as well as the gradient of the plastic potential$\frac{\partial_g}{\partial_Q}$, are Calculated in the image point I_1, as if the stress point were on the bounding surface. The image point is determined by the intersection of the bounding surface with the straight line A_1P_1 (mapping rule). The matrix ϕ is a diagonal matrix, the role of which is that of a weight function. For its definition, which is rather complex, the interested reader can refer to di Prisco et al. (2003).

As far as the evolution of the loading-unloading locus is concerned, three possibilities Exist:

1. Irreversible strains do not occur and the current stress point is within the zone S of Figure 1-6. In this case the elastic domain does not evolve.

2. Irreversible strains do not occur but the current stress point belongs to the border between zones R and S defined in Figure 1-6. In this case the elastic domain evolves and shrinks. The center of the ice-cream cone, point A_1, shifts along the straight line connecting it with the axes origin, while the current stress point remains on the inner border between zones R and S.

3. Irreversible strains take place. Point A_1 shifts along the straight line connecting it with the image point on the boundary surface previously defined, while the current stress point belongs to the outer border of the sphere.

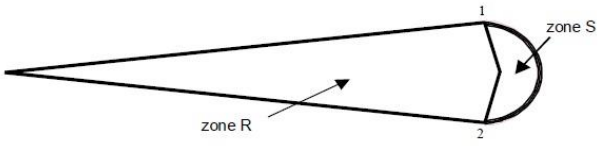

Figure 1-7: the unloading-reloading domain: definition of zones S and R.

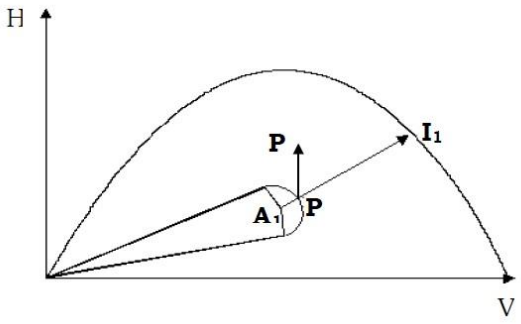

Figure 1-8: bounding surface and domain fully elastic behavior.

1.3.5 Ratcheting phenomena

For large number of cyclic loads applied to the foundation, while there is not any damage observed, the irreversible displacement will be accumulated at a decreasing rate, and a sort of stabilization takes place (Figure 1-9). The experimental work by di Prisco et al. (2003a), already observed such phenomena and confirmed experimentally that the results are affected by the amplitude of the cycles, generalized stress path and the image point which already discussed (see Figure 1-7 and 1-8).

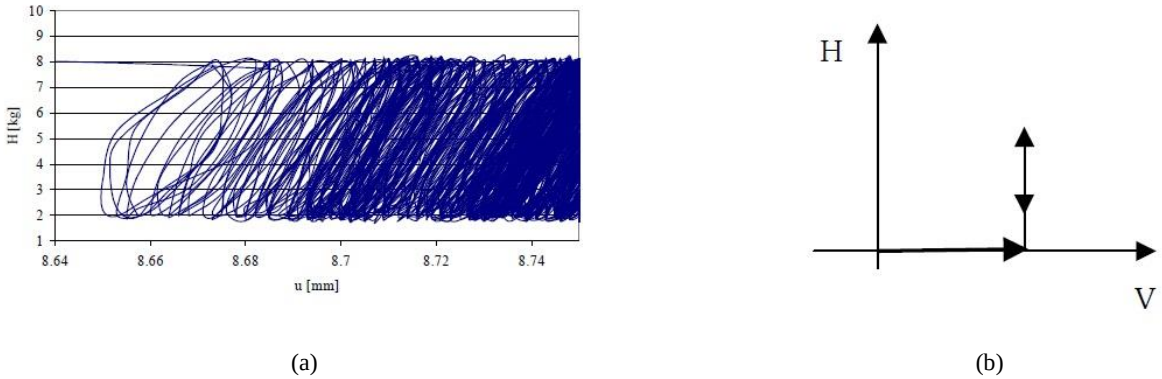

(a) (b)

Figure 1-9: Experimental results (di Prisco et al. 2003a) obtained by keeping constant the vertical load and apply horizontal cyclic load; (a) horizontal load versus horizontal displacement , (b) generalized strength path.

It is quite difficult to find an approach capable quantitavely to define the ratcheting Phenomenon. di Prisco (2012) in the research based on multi-mechanism viscoplasticity assumption defines elasto plastic constitutive relationship as below:

$$\dot{\varepsilon}_{ij} = \dot{\varepsilon}^{el}_{ij+} \dot{\varepsilon}^{vp}_{ij+} \dot{\varepsilon}^{c}_{ij+} \dot{\varepsilon}^{r}_{ij}$$ Eq 1.10

Where the first term will describe response of material at a very small strain rate referring to the elastic/reversible strain and the second term is for the small strain rate of the mechanical response of material, and these two parameters control typical standard cyclic response and show that when the cyclic amplitude is small, irreversible strain do not develop and the typical shake down response is reproduced (Figure 1-10).

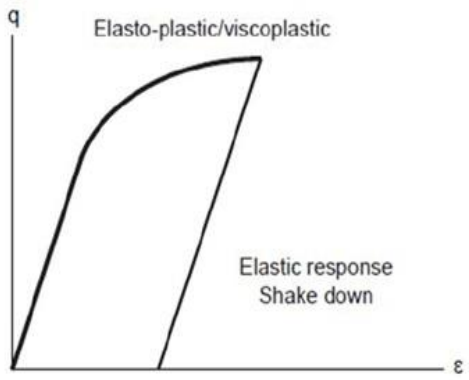

Figure 1-10: Mechanical response of the system in case of shake down (di Prisco, 2012) .

The third parameter controls the dissipation of energy and reduction in stiffness due to the change of the size of the cycles. By adding this parameter it is possible to generalize the ideal plastic adaptation where no accumulation of irreversible displacement will take place (Figure 1-11).

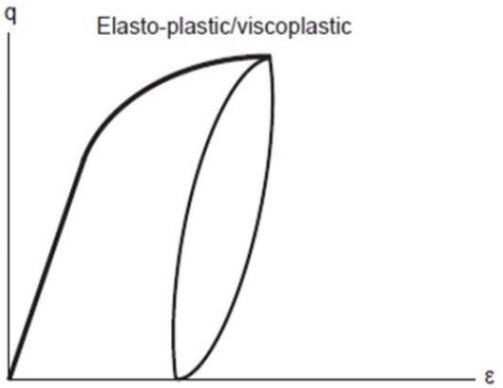

Figure 1-11: Mechanical response of the system in case of an ideal-plastic adaption (di Prisco, 2012).

The last term will describe the ratcheting phenomena and the coupling between these Mechanisms cause the progressive accumulation of irreversible strain due to repeated loading and unloading.

In fact mentioned parameter which concerns the ratcheting phenomena can be described in three ways (Figure 1-12):

1. First it can produce this accumulation with the same rate, in the case of no coupling between the principal plastic mechanism and the one that introduce the ratcheting phenomenon.

2. Second it can be stabilized and the rate of accumulation will be decreased and sort of positive hardening can be take place.

3. The ratcheting can produce continually increase in the accumulation rate.

In case of granular material as already discussed in experimental work with di Prisco (2003a) the second case is suitable which employed the isotropic hardening and non-associated flow rule.

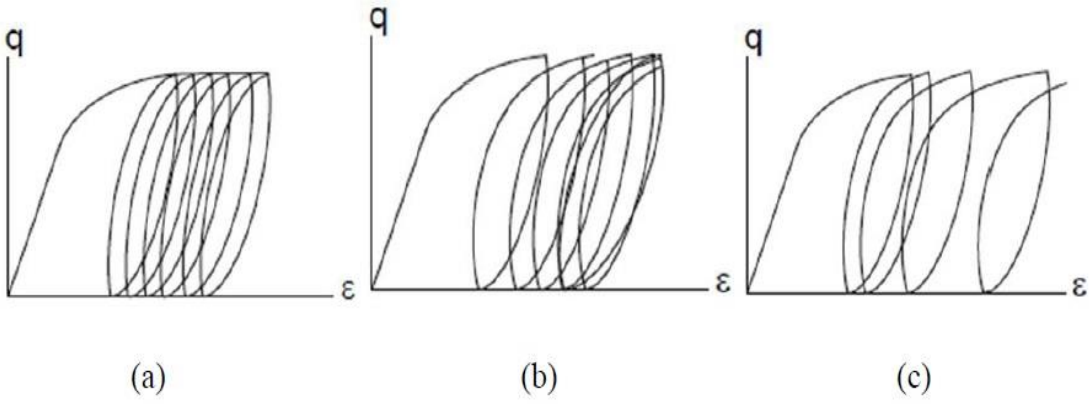

Figure 1-12: Mechanical response of the system; (a) Perfect ratcheting, (b) Progressive stabilization, (c) Increase the accumulation (di Prisco, 2012).

1.3.6 Stiffness and damping factor

Many experimental results, by taking into account the well-known concepts for secant stiffness (K), and damping ratio (η) observed a clear decay in stiffness K and increase in η after applying cyclic load and having horizontal or even rocking displacement. Damping ratio (η) which is calculated as a ratio between dissipated energy "D" and the stored elastic energy "Δw" (Equation 1.11), (Figure 1-13 d). It must be noted that these abacus are affected by the amplitude of the cycles.

$$\eta = \frac{D}{4\pi\Delta W} \qquad \text{Eq 1.11}$$

The example of the results illustrated in the figure 1-13 refers to the sand. In case of stiffness K, it is normalized with respect to the initial small strain stiffness K_0. In the same plot, the numerical results employing the macro-element concept which is developed by di Prisco et al. (2003a) are also reported. It is shown that even for the small foundation rocking angle such as 0.001 rad the rotational secant stiffness of the foundation reduces by a percentage varying from 40% to 60%, depending on the relative density of the soil.
Damping factor values vary between 5% and 10% for rotations up to 0.001 rad, while they increase significantly for higher rotations up to about 20% for dense sands and 30% for medium dense sands. As already discussed when the rocking angle is sufficiently high, the uplift dominates the response of the system and damping ratio will not be observed any more. It must be mentioned that we didn't consider these types of tests in this study.

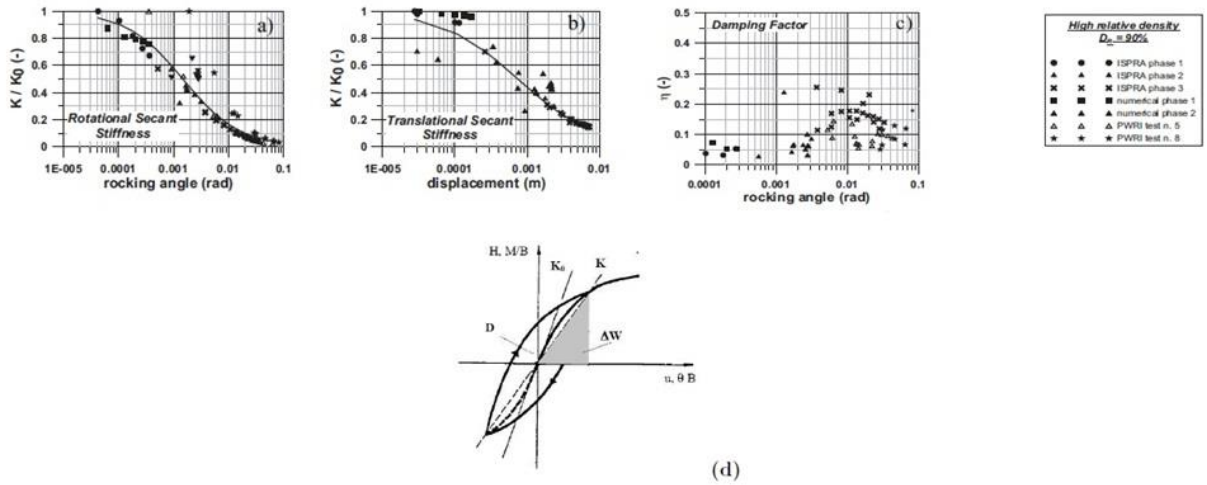

Figure 1-13: (a) Normalized rocking, (b) translational stiffness, (c) damping factor for Dr = 90% (Paolucci et al.2007) at increasing values of rocking angle and horizontal displacement, respectively, (d) definition of rocking/translational stiffness and damping factor.

1.4 Summary

The objective of this chapter was to give an introduction and basic concepts of the content of the studies and works which are presented within this dissertation. It is quite evident from this chapter that there are many aspects and fundamental concepts which need to be considered during this study. The following chapter presents literature review of the past studies that have been related within the topics of this thesis.

2

Literature review

2.1 General overview

In this chapter, a summary of previous works that have been done, on the subject of "Soil-foundation interaction under cyclic loading" for a footing on shallow and deep foundations throughout the past years is presented. The aim of these studies was to realize more exactly the difference of behavior of the soil, foundation and structures under cyclic loads. It is worth to mention that the extent of researches performed in this field is not very wide.

2.2 Introduction

During the last several decades, seismic soil-structure interaction has been a major topic in earthquake engineering since it is closely related to the safety evaluation of many important engineering projects, such as nuclear power plants, to resist earthquakes. The significance of the interaction has long been recognized because of the massive and stiff nature of the structure and, often, soil softness. In recent years the importance of dynamic soil-structure interaction to earthquake behaviors of high arch dams has also been realized, since the effects of energy radiation through the infinite canyon and the non-uniform ground motions on the dam response may be significant. Nuclear power plants and high arch dams are only two examples for which dynamic soil-structure interaction is important and needs to be seriously considered in engineering practice.

Safe design of strip footings subject to cyclic loads still represents an open issue for engineers and researchers, since it requires several complex non-linear phenomena (as ratcheting, rocking and uplift mechanisms of the foundation, coupling among the different loading components) to be accounted for. All these features become even more important when dynamic loads have to be considered in the design, like in case the structure must be verified against severe environmental loads (e.g. wind loads on tall buildings, or sea-wave actions on offshore structures). Such non-linear and inelastic effects, however, are not necessarily detrimental, but

they can even be beneficial for the foundation (Paolucci 1997; Pecker 1998, Martin and Lam 2000; Makris and Roussos 2000; Pecker and Pender 2000; Faccioli et al. 2001; Gazetas et al. 2003; 2007; Gajan et al. 2005; Paolucci et al. 2008; Kawashima et al. 2007; Gajan and Kutter 2008; Chatzigogos et al. 2009; Anastasopoulos et al. 2009), in particular when seismic actions are considered, since they reduce the ductility demand on the superstructure and allow (theoretically) to design the foundation as a seismic isolator. Rigorous numerical modelling approaches, like finite element or discrete element methods, are nowadays available for design purposes, but they are still quite demanding both from an economic and a computational point of view, and they cannot be considered yet as a standard design tool for geotechnical and structural engineers, in particular when a pre- dimensioning of the system is required. Moreover, even sophisticated numerical codes are not always able to capture some of the above cited features of the soil-foundation interaction and require advanced constitutive rules or very refined calibration procedures in order to get satisfactory quantitative results.

The use of piles beneath shallow foundation is a suitable solution to increase the bearing capacity and to reduce the settlement. This situation is used when the structural load is shared between the shallow foundation and piles that are structurally connected. Piles as settlement reducers were first proposed by Burland et al. (1977). The overall design objectives are to provide sufficient ultimate resistance and to distribute the load into the soil-pile interaction (Poulos et al. 2001, Xiao et al. 2004, Zheng et al. 2008, Paniagua et al. 2009, and Choi et al. 2009).

In the literature there are several different studies available (Gerber et al. 2003, Remaud et al. 1998, Ilyas et al. 2004, Matlock and Reese et al. 1960, Broms et al. 1964, Poulos et al. 1971, and Boulanger et al. 1999 and etc.) dealing with experimental tests on pile group. They are generally divided into three types, full-scale tests, centrifuge model and small scale model tests. Full-scale tests provide of course the most accurate results but, there are not too much works on the full-scale tests due to the high costs. Therefore many studies available concern the model tests.
It must be mentioned that also there are lots of studies that consider different situation of loading, most of these studies used piles in 3 main configurations, which means in-line arrangement (the piles aligned in the direction of load), side-by-side arrangement (the piles are aligned normal to the direction of load) and in box arrangement (consists of multiple in- line or side-by-side arrangement).

In case of full-scale tests some studies can be cited, for instance Brown et al. (1988) determined the lateral load behavior conducted the 3x3 pile group in dense sand. He concluded that group pile deflect significantly more than isolated single pile when loaded to similar average load per pile. This fact now is generally accepted and is proved by many authors such as Rollins et al. (1998). Rollins et al. (2006) performed full-scale test, to investigate group interaction effects with respect to the pile spacing on laterally loaded pile groups. Cyclic lateral load tests

were performed on 3x5, 3x4 and 3x3 pile group with 3.3D, 4.4D and 5.65D pile spacing. Rollins et al. (2006) confirmed that the lateral load resistance was a function of pile spacing. While decreasing the pile spacing from 5.65D to 3.3D, group interaction effect became more and more important.

Beside the full-scale tests, centrifuge test is one of the most widely used methods. The basic theory behind the centrifuge modeling is increasing the g-force to physical model in order to produce identical self-weight stresses in the model and prototype (Gerber 2003). Many studies used centrifuge model tests, such as McVay et al. (1998), which evaluated the behavior of laterally loaded pile in sand, and concluded that group response is independent of soil density, but mainly a function of group geometry and row position. In this field other researches can be named Remaud et al. (1998), Ilyas et al. (2004) and etc.

On the other hand many studies are available in the in the small scale model tests since it is low cost and less time consuming. In this context can be cited even the research by Cox et al. (1984) which performed tests on both single and group pile subject to laterally cyclic tests. Groups of three and five piles with a spacing of 0.5D, 1D, 2D, 3D and 5D were considered. Piles were arranged both in side by side and in line configuration. Cox et al. (1984) concluded that for the in line configuration, the load distribution depends on the pile group horizontal displacement and the effect of the group piles increase by the increasing of the number of the piles in a line from three to five. Another study was conducted by Rao et al. (1998) in order to determine the influence of the rigidity on the laterally loaded pile group. Other studies in this configuration were performed by, Brown and Reese (1985), Shibata et al. (1989), Liu (1991), Adachi et al (1994), Franke (1998).

All the mentioned studies were agreed that the most significant parameters affected to the group piles behavior are: pile spacing, group arrangement, group size, pile-head fixity, soil type and density. Pile spacing is the most dominant factor affecting the pile group behavior; group effects are negligible when the pile spacing is bigger than 6D.

One of the standard ways for quantifying group interaction effects is a group efficiency factor, $G_{e,}$ which is defined in equation 2.1 as the average lateral capacity per pile in a group divided by the lateral capacity of single pile (Parkash 1990).

$$G_e = \frac{(Q_u)_g}{n\,(Q_u)_s} \qquad \text{Eq 2.1}$$

Where $(Q_u)_g$ is the ultimate lateral load capacity of the group, *n* is the number of piles

in the group and the $(Q_u)_s$ is the ultimate lateral load capacity of a single pile. For the sake of brevity the results of cited references are summarized in the figure 2-1. This figure shows the effects of the pile spacing (S = the ratio between the pile diameter and center to center of the pile in a direction of the load) on the factor G_e. Factor G_e is increasing by increasing the pile spacing. However the other factors such as the piles configurations also affected this factor.

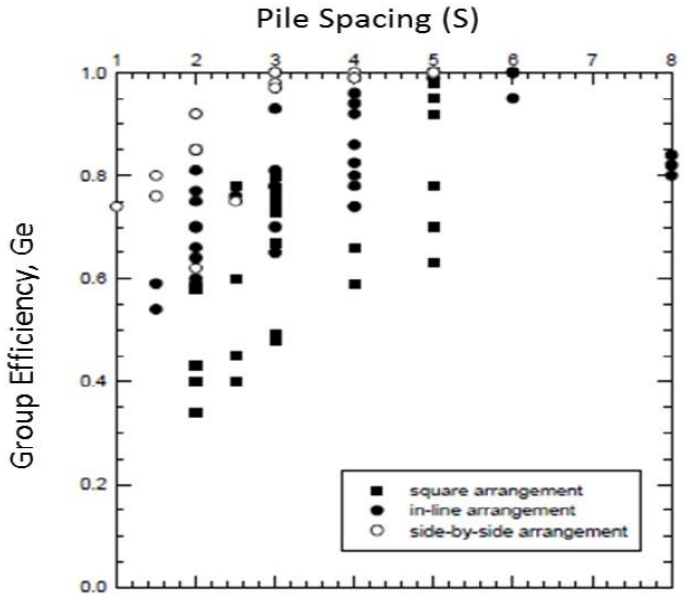

Figure 2-1: Group efficiency factor versus pile spacing for different foundation configurations (square arrangement, in-line arrangement and side by side arrangement).

2.3 Previous studies

The seismic behavior of the foundations and structures and their interaction by soil was mainly investigated through lots of studies during the last decades and has led to the development of various solutions and views. Full-scale tests are the most definitive means for determining mentioned purpose. After that, numerical analysis comes second to experimental processes in reliability and flexibility. It makes it possible to observe the effects of changing the different parameters (e.g. sand level, loading direction, boundary conditions, etc.) Nevertheless, numerical methods require specialized software skills. On the other side, empirical methods are characterized by simplicity but are usually limited in their applicability to specific test types.

In the following the focus is on demonstrating some main parts of other studies that are in this field and are related to this thesis in order to show the importance of this topic.

2.3.1 Shallow footing under cyclic loading (by C. di Prisco, R. Nova& A. Sibilia)

2.3.1.1 Introduction

Many and various are in nature the cyclic loading (seismic actions, wind storms, undercurrents and so on) which may affect civil structures (chimneys, towers, off-shore structures, etc.). In such conditions, in the analysis of the dynamic mechanical response of these civil structures, a crucial role is played by the mechanical response of the foundation-soil system which is stressed by inclined and eccentric cyclic loads. For this reason, Eurocode EC8 (§.5-4-1) prescribes, in the design of important structures, the analysis of the non-linear mechanical behavior of soils in order to calculate irreversible displacements due to seismic actions.
This can be done in various ways. For instance, it is possible to subdivide the structure, the foundation and the soil in a mesh of finite elements; each characterized by an appropriate constitutive law, and then analyzes the whole dynamic problem. Since soil behavior is highly non-linear, however, an analysis with a realistic soil model would be time-consuming. Furthermore, due to the intrinsic complexity of the problem, the quality of the numerical solution is not necessarily better than the quality of simpler model solutions. An alternative way consists in lumping the soil compliance in few discrete springs and dashpots that constrain the movement of the foundation. The springs are usually assumed to behave elastically, while the viscous dashpots are responsible for modelling the dissipation, both geometrical and mechanical, of the soil.

This latter method is clearly much more economic, but has important limitations. The linear behavior of the springs and dashpots implies the uncoupling of the effects of the external actions on the foundation displacements. For instance, the cyclic action of a rocking moment and a horizontal shear force do not cause any vertical settlement of the foundation, at variance with the actual behavior.

The aim of this paper was to show that it is possible to overcome this difficulty by abandoning the conceptual framework of elasticity of springs. We shall make reference instead to a strain-hardening elastoplastic theory, which allows such coupling effect to be correctly described. The system of springs will be therefore substituted by a macroelement (Nova and Montrasio (1991)) connecting generalized stresses (forces and overturning moment acting on the foundation) and the corresponding (in the work equation) generalized strains (displacements and rotation). This is similar to what it is usually done for the constitutive law of an elementary volume of soil in terms of stresses and strains. In such a

way it is possible to take directly into account the mechanical dissipation of energy associated with irreversible strains. In this case, therefore, the system of dashpots will be responsible only of the modelling of the geometrical damping due to the radiation of the cyclic excitation from the surface into the soil half space.

Theoretical predictions will be compared to experimental data obtained by means of laboratory tests on small-scale models subject to quasi-static cyclic inclined loading at variable frequencies, cycle amplitudes, load histories and load paths. The large number of tests allowed a critical review of the constitutive assumptions of the model and its progressive refinement.

2.3.1.2 Experimental test results

The experimental device allows us to perform any load path defined in the domain of Figure (2-2a) with the constraint that both V (vertical load) and H (horizontal load) are positive. Since the rigid footing length coincides approximately with the caisson width, the displacements orthogonal to the glass walls are prevented. Both the horizontal and vertical forces are centered. As a consequence, the small scale model footing may be assumed to work as a shallow strip footing.

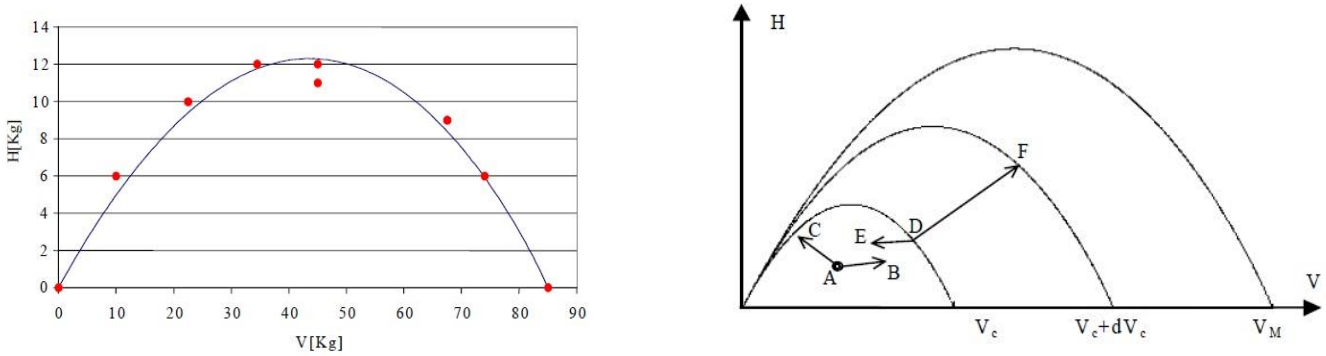

(a) (b)

Figure 2-2: (a) Experimental failure locus, (b) definition of the elastic domain and its evolution.

In the following, both monotonic and cyclic tests, during which the load is changed with time accordingly to a sinusoidal rule, will be considered. In this latter case, the amplitude as well as the frequency f_r of the load were kept constant.

All the experimental test results illustrated in the following (Capozza & Generali (1999)) were obtained on very loose Hostun RF sand specimens (Dr=30%). In order to describe the collapse locus, monotonic tests were performed (figure 2-2a).

These consist of two distinct paths:

(i) Radial path, characterized by a fix value of the obliquity H/V,
(ii) Vertical path characterized by a continuous increase in the H value and by a constant V Value. The different tests are characterized by different initial V values. These are reached during a first load phase, during which V is increased, while H is kept nil.

The footing collapse is obtained by imposing, thanks to the artificial removal of the laterally flowing material, the footing level to be coincident with the ground level.

As was observed by others (e.g. Nova & Montrasio (1991)), the failure locus does not depend on the chosen load path. In Figure 2-2(a), the mathematical expression of the plotted curve interpolating the failure data coincides with that introduced by Nova and Montrasio.

The cyclic tests were next performed. These are characterized by a first phase during which the loads are monotonically incremented, along one of the load paths defined above, and a second phase during which the loads are cyclically changed according to one of the following paths:
(a_C) H = constant, (V*-A) <V< (V*+A),
(b_C) V = constant, (H*-A) <H< (H*+A),
(c_C) H/V = constant, (H*-A) <H< (H*+A);

Where A is the load cycle semi-amplitude, while H* and V* are the coordinates of the medium point P*. The mechanical response of the footing- soil system was analyzed by changing the load amplitude, the load frequency and, in particular, the position of P*.
Finally, the importance of the point P* position with respect to the failure locus previously defined has been discussed. Four points were considered. These are plotted in Fig 2-9(a), in the H-V plane, together with the failure locus previously defined. In Fig 2-9(b) and c the u, v displacements versus the cycle number, relative to the different P* points, are compared to each other. The dramatic dependency of the mechanical response on the point P* position is clearly shown.

2.3.1.3 Modeling soil-structure interaction: the elasto-plastic- strain-hardening macroelement (Nova & Montrasio (1991))

Consider the strip foundation of width B, subject to a vertical load V, a horizontal load H and an overturning moment M. The variables, conveniently adimensionalised, can be collected in a vector Q of generalized stresses, while the corresponding generalized

displacement variables can be collected in a vector **q**;

$$\boldsymbol{Q}=\begin{Bmatrix}\xi\\ h\\ m\end{Bmatrix}=\frac{1}{V_m}\begin{Bmatrix}V\\ H/\mu\\ M/(\psi\cdot B)\end{Bmatrix}\qquad \boldsymbol{q}=\begin{Bmatrix}\eta\\ \varepsilon\\ \zeta\end{Bmatrix}=V_m\begin{Bmatrix}v\\ \mu\cdot u\\ \psi\cdot B\cdot\theta\end{Bmatrix} \qquad \text{Eq 2.2}$$

where μ and ψ are two constitutive parameters, V_m is the collapse load obtained when H=M=0 and is the foundation rotation. Such variables, which are connected to each other through the work equation, can be incrementally related by a generalized compliance matrix C:

$$d\boldsymbol{q}=C\,d\boldsymbol{Q}\,. \qquad \text{Eq 2.3}$$

Soil behavior is non-linear and irreversible, in fact. Furthermore C depends on the generalized stress state, on the direction in the stress space of the stress increment vector, and on the 'history' of the macroelement, via a set of hidden variables. In the simplest case such set reduces to a single variable ρ_c, controlling the size of the domain within which the behavior of the macroelement is considered to be linear elastic, for the time being, at least. If a stress point is within the elastic domain, e.g. point A in Fig 2-2(b), where only horizontal and vertical forces have been considered for the sake of simplicity, any increment of generalized stress (such as AB or AC) will give rise to recoverable strains. The foundation will experience the same elastic behavior when the generalized stress state is on the boundary of the domain, such as in point D, and the stress increment is directed inwards, e.g. as for the DE path. On the contrary, when the stress increment is directed outwards, e.g. in the case of the DF path, the generalized strains will be partly irreversible. They can be derived following the theory of elastoplasticity.
Given a loading function *f* in the dimensionless 3D space ξ-h-m which defines the elastic domain, and a plastic potential (Nova & Montrasio (1991)):

$$f(\boldsymbol{Q},\rho_c)=h^2+m^2-\xi^2\cdot\left[1-\left(\frac{\xi}{\rho_c}\right)\right]^{2\beta}=0 \qquad \text{Eq 2.4}$$

$$g\left(\boldsymbol{Q},\rho_g\right)=\lambda^2h^2+\chi^2m^2-\xi^2\cdot\left[1-\left(\frac{\xi}{\rho_g}\right)\right]^{2\beta}=0 \qquad \text{Eq 2.5}$$

Where λ, χ, β are constitutive parameters, ρ_C is the state variable, while ρ_g is a dummy variable. The gradient to g defines the direction of the irreversible part of the generalized strain increment $d\boldsymbol{q}^{p}$. Once the hardening rule is introduced:

$$d\rho_c\left(d\boldsymbol{q}^{pl}\right) = (1-\rho_c)\frac{R_o}{V_m^{\,2}}\left[d\eta + \left(\frac{\alpha|d\varepsilon|}{\mu}\right) + \left(\frac{\gamma|d\zeta|}{\psi}\right)\right] \qquad \text{Eq 2.6}$$

And the consistency rule is fulfilled, i.e. $df = 0$, it is possible to derive the plastic generalized strain increments. When plastic generalized strains occur, the value of ρ_C is updated and the elastic domain size increases. When ρ_C reaches the unit value no further hardening is possible. The associated yield locus is therefore the failure locus.

In equation 2.6, the variables α, γ and R_0 are constitutive parameters. In particular, R_0 gives the initial stiffness of the load-displacement curve.

The amount of plastic strain experienced is clearly governed by all the other parameters appearing in equations 2.2-2.6, which control the shape of the yield locus, of the plastic potential, and the amount of hardening. Although these parameters should be in principle determined case by case, it is shown in Nova and Montrasio (1991) that many of them can be taken as material constants, so that only the variables R_0, V_m, and μ are relevant. Furthermore they can be related to traditional soil constants, such as the 'elastic' modulus, the friction angle or the relative density (Montrasio and Nova (1997)).

2.3.1.4 Numerical simulations

As was illustrated in §.3, in order to obtain the failure locus, various monotonic quasi-static experimental tests were performed in the laboratory. These allowed the calibration of the constitutive parameters of the original Nova Montrasio (1991) model roughly described in §.4, which are collected in Table1-1. As is shown in Figure 2-3, a good agreement between experimental data and numerical simulations is obtained.

α	β	γ	λ	μ	χ	ψ	V_m(kN)	R_o(kN/m)
2.81	1.2	1.71	0.12	0.615	0.286	0	0.9	45

Table 2-1: Calibrated parameters of the original monotonous Nova-Montrasio (1991) constitutive model (loose sand homogeneous stratum).

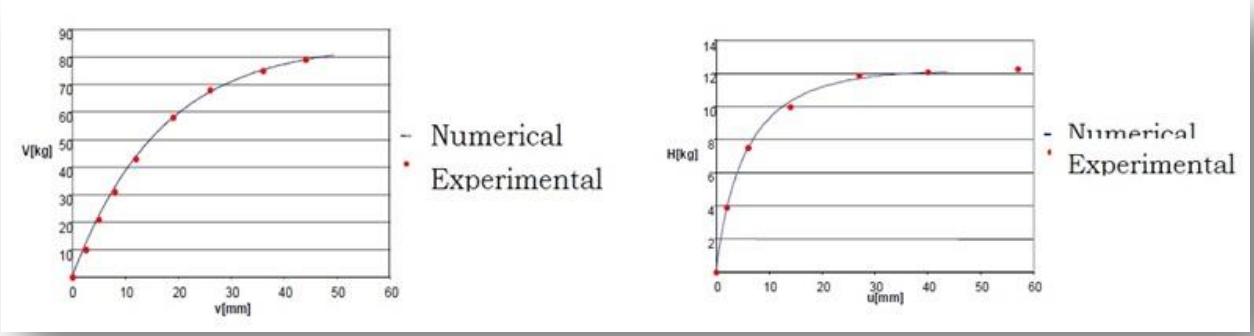

Figure 2-3: Calibration tests; comparison between numerical simulations and experimental data.

Figure 2-4 shows the numerical results concerning the case of a small scale railway embankment subject to cycles of unloading-reloading of the vertical force, whose experimental data have been illustrated in Figure 2-5. The direct comparison between experimental data and numerical results in a semi- logarithmic plane is shown in Fig 2-6. The relative constitutive parameter values are reported in Table 2-2.

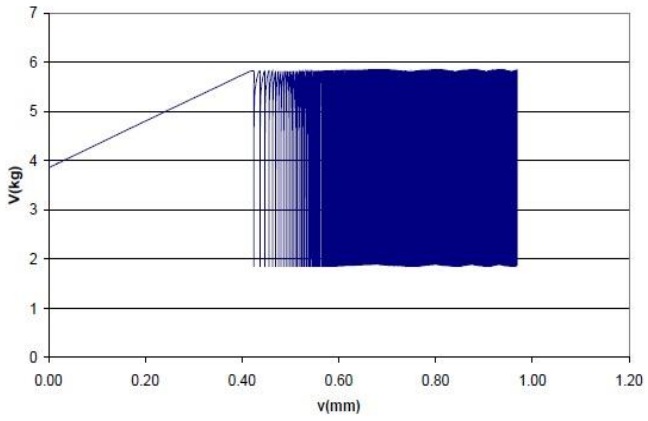

Figure 2-4: Simulated mechanical response to the load path (H=0, variable).

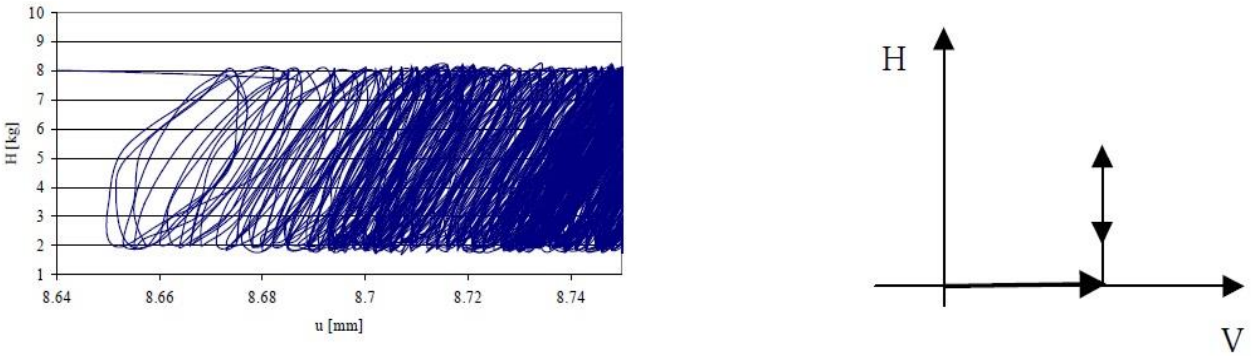

Figure 2-5: Experimental results: horizontal displacements under constant vertical loading (V=450 kN) and cyclic horizontal load.

α_η	$\alpha_{\varepsilon\zeta}$	K_η	$K_{\varepsilon\zeta}$	φ
300	20	50	100	0.01

Table 2-2: Additional constitutive parameters (loose sand homogeneous stratum).

In Figure 2-6, the hysteresis cycles obtained by performing path (b_C) type tests are illustrated. By changing the position of point P* defined in Figure 2-7 of section 3, the mechanical response changes abruptly. In Figure 2-8 the relative numerical results are illustrated. They should be compared to the experimental data of Fig 2-9 (a). From these figures, we may derive that the presented constitutive model is capable of reproducing the main features of the cyclic mechanical behavior of the footing-soil system:

1. The model is able to reproduce the hysteretic behavior of the foundation, that is particularly relevant for horizontal loading;
2. Even though vertical loading is kept constant, vertical displacements increase with the number of cycles;
3. The irreversible displacements increase with the cycle amplitude;
4. Dependency of the mechanical response on the position of P* is quite well reproduced;
5. The dissipated energy decreases with the number of cycles.

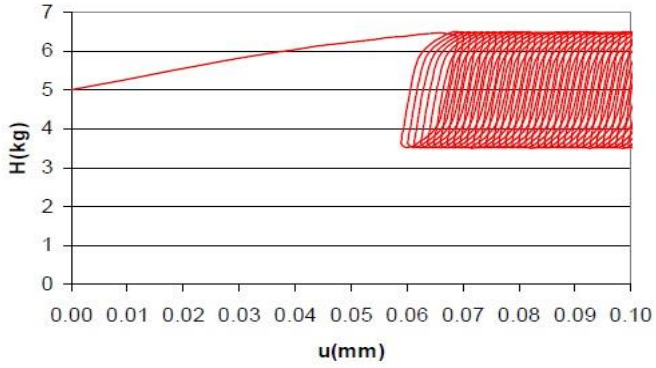

Figure 2-6: Load path (b_C); hysteresis loops.

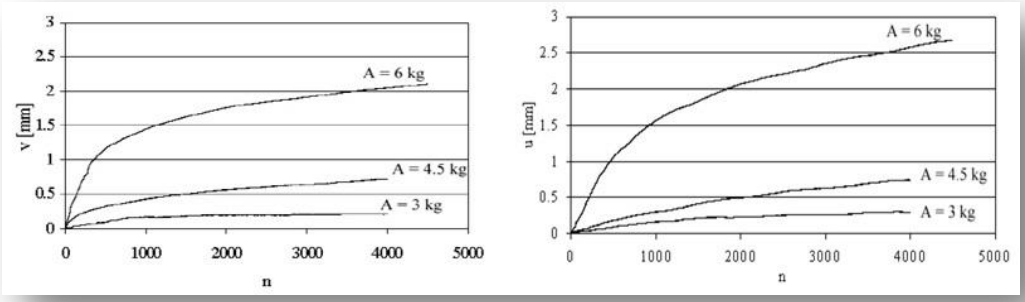

(a) (b)

Figure 2-7: Dependency on cycle amplitude of the experimental response during path (b_C) (V=220 kN, H cyclically changing, H^*=50 kN); (a) vertical displacements, (b) horizontal displacements, as a function of The number of cycles n.

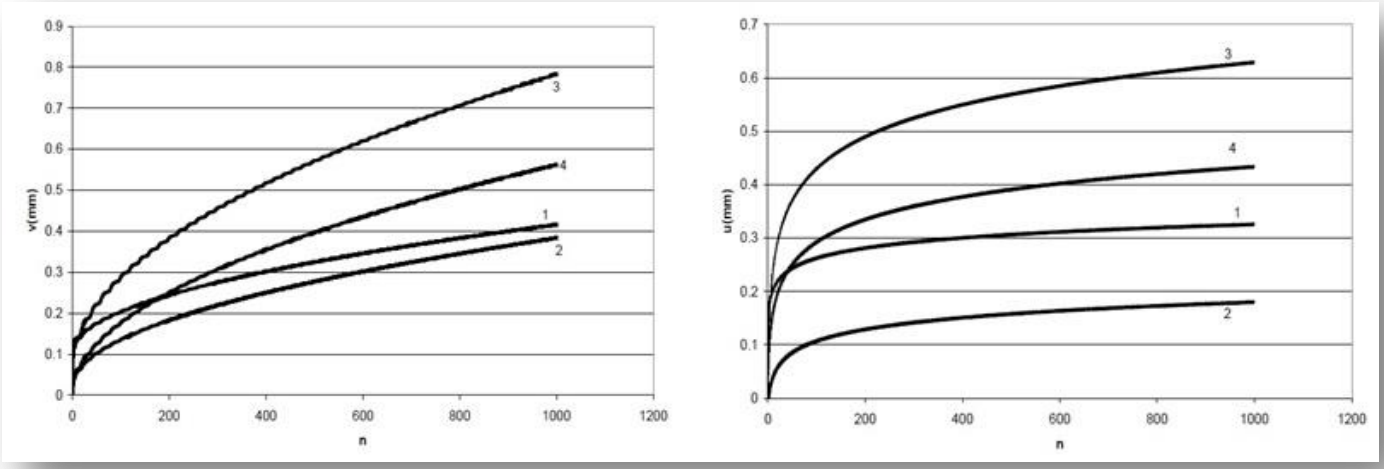

(a) (b)

Figure 2-8: (a) vertical displacements, (b) horizontal displacements, as a function of the number of cycles n.

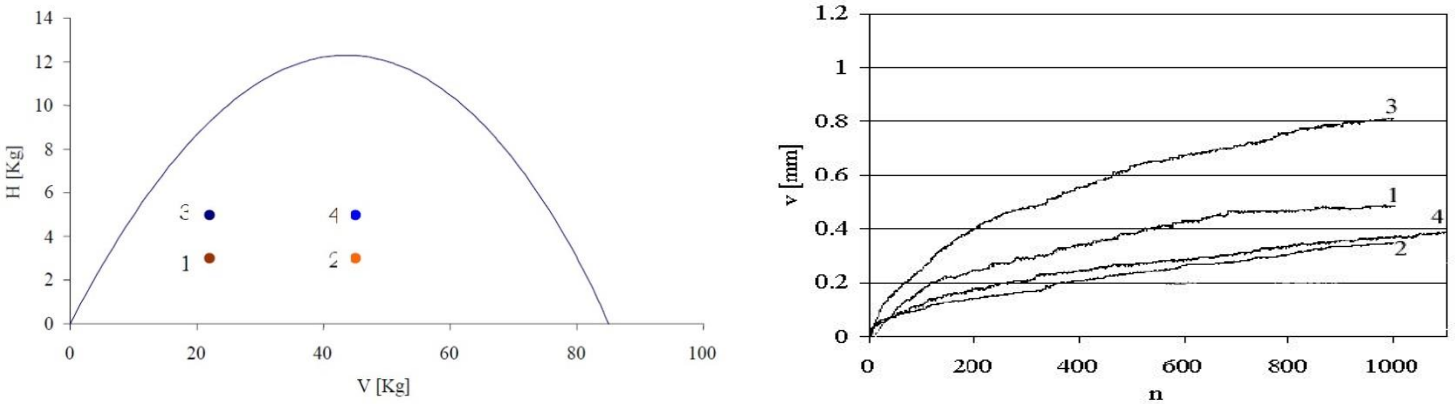

(a) (b)

Figure 2-9: Dependency on P_i* position of the system experimental behavior; (a) failure locus and P_i* point positions, (b) vertical displacement as a function of number of cycles.

Finally, in Figure 2-10 it is shown the behavior of a plinth, 1 m wide, founded on dense sand, subject to a constant vertical load, cyclic horizontal force and a n overturning moment (after Pedretti (1998)). The relative constitutive parameters are collected in Tab2-3. The overturning moment and the horizontal force are linked by proportionality constant. Once again it is apparent that, with the proposed method, it is possible to capture the essential features of the model test results in a satisfactory way. In this case both the memory surface and the ρ_k variable play a negligible role. In fact, the cycles are symmetric, i.e. there is a periodic change of the H and M sign, and very few are the cycles performed.

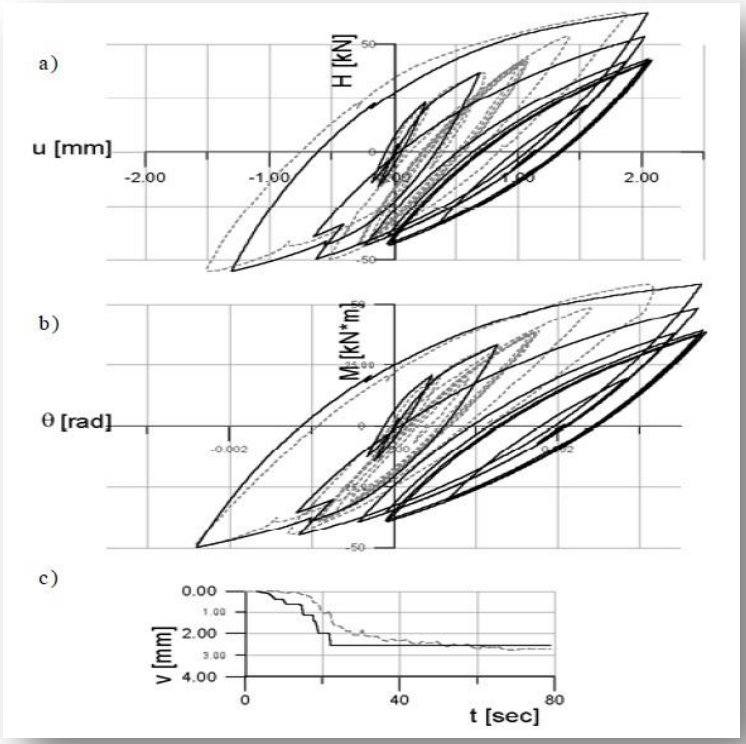

Figure 2-10: Comparison of measured (dotted lines) and calculated (full lines) displacements of a real scale foundation under cyclic horizontal loading and overturning moment with constant vertical load (experimental data after Pedretti (1998)); (a) horizontal displacement; (b) rotation; (c) accumulated vertical settlement.

α	β	γ	λ	μ	χ	ψ	α_η	$\alpha_{\varepsilon\zeta}$
2.83	0.95	1.71	0.8	0.8	0.286	0.4	4	20

Table 2-3: Constitutive parameters (dense sand homogeneous stratum).

2.3.1.5 Conclusion

In order to analyze the dynamic behavior of structures under cyclic loading, it is necessary to model the interaction of the structure with the foundation soil. To do that in a relatively, simple way, it is possible to lump the stiffness and the damping exerted by the soil in springs and dashpots with appropriate mechanical characteristics. To model phenomena such as hysteresis, ratcheting, and the coupling between horizontal displacements, rotations and settlements, it is necessary to employ a coupled system of springs. This can be achieved by conveniently defining a macroelement, which connects forces and displacements. Generalized stresses and generalized strains are linked by a strain hardening theory of plasticity. Such theory should be modified, however, to take cyclic phenomena into account. This was shown here starting from the idea of a bounding

surface and the formulation of an appropriate mapping rule.

In order to appropriately define the constitutive law, a small scale experimental apparatus was conceived and realized. Although from a qualitative point of view and by disregarding load eccentricity, the experimental test results highlighted the mechanical response of the system under cyclic loading.

It was shown that the experimental behavior of model foundations subject to various types of quasi-static cyclic loading can be successfully matched by means of a model based on the generalized plasticity theory. In particular, the dependency of the cyclic mechanical system response on the permanent loads applied to the rigid footing was successfully reproduced.

2.3.2 Large scale soil-structure interaction experiments on sand under cyclic loading (by Paolo Negro, Roberto Paolucci, Stefanio Pedretti & Ezio Faccioli)

2.3.2.1 Introduction

The seismic behavior of shallow foundations has been mainly investigated through pseudo-static analysis of the bearing-capacity reduction due to seismic forces [Sarma and Iossifelis, 1990; Pecker and Salençon, 1991; Paolucci and Pecker, 1997a and 1997b], and the evaluation of the earthquake-induced settlements [Richards et al., 1993; Paolucci, 1997]. However, these investigations have been scarcely supported by parallel experimental investigations, essential to check the analytical procedures.

Laboratory tests encounter several major difficulties for a sound experimental analysis of this complex, nonlinear dynamic soil-structure interaction problem, such as:

1. Careful control of soil properties: the deposition procedure and the saturation (if required) of the soil specimen must be carefully conducted and checked;
2. Boundary conditions: the boundaries of the testing apparatus should be enough removed from the foundation so to prevent any constraint on the development of failure mechanisms. Besides, flexible boundaries should be used, with well calibrated properties to reproduce free-field boundary conditions;
3. Scale problems: large-scale tests are more expensive, involve a very large amount of material, and cannot be repeated easily, while the use of scaling laws in small-scale tests is questionable when applied to the grain size of soil materials, especially for strongly non-linear problems with pore-pressure build up;

4. Seismic loads: both seismic actions transmitted by the superstructure (vertical and shear force, plus overturning moment) and soil inertia effects should be taken into account simultaneously.

It is impossible to cope with all of these requirements with the same testing apparatus. Centrifuge testing has encountered a notable success in the recent years. An interesting description of a centrifuge test setup for validation of innovative concepts in foundation engineering is reported by [Garnier and Pecker, 1999]. Another potentially useful apparatus for testing geotechnical structures is the shear stack mounted on the shaking table of the University of Bristol [Taylor et al., 1994], that allows to perform large-scale experiments and to closely simulate free-field boundary conditions.

A programme of large-size, cyclic loading experiments has been designed in the framework of the TRISEE Project (3D Site Effects and Soil-Foundation Interaction in Earthquake and Vibration Risk Evaluation), funded by the European Commission, to investigate the non-linear interaction between shallow foundations and the supporting soil under seismic loading. The basic set-up of the experiments consists of a shallow foundation lying on a saturated sand of known properties, and excited by a time-varying horizontal force and moment, which simulate the inertial forces transmitted to the foundation by the superstructure. The soil mass is at rest, so that the wave propagation and inertia effects in the soil are neglected with respect to the dynamic structural inertia forces transmitted by the foundation. In fact, theoretical work on seismic bearing capacity of shallow foundations [Pecker and Salençon, 1991; Paolucci and Pecker, 1997a and 1997b] has shown the soil inertia has a negligible influence on the failure loads.

The tests have been carried out with two different soil relative densities ($Dr \approx 85\%$ and $Dr \approx 45\%$), that are representative of high density (HD) and low density (LD) soil conditions. The latter can be considered as a lower bound for design of shallow foundations in practice, since the presence of sands at lower density generally leads the engineer to other design solutions.

2.3.2.2 Description of the experimental set up

The experimental prototype consists of a stiff concrete caisson filled with medium dense sand (Ticino sand, [Bellotti et al, 1996]), and of a steel mock-up, representative of a concrete shallow foundation (Figure 2-11). The caisson has dimensions 4.60 m by 4.60 m in plan and 4 m in height, while the foundation is 1 m by 1 m in plan. The lateral boundaries of the caisson are rigid and waterproof. While the bottom boundary is far enough from the foundation to avoid any interference with the possible failure mechanisms, the rigid lateral boundaries may have a significant influence on the bearing capacity of the foundation on dense sand, which should be

taken into account in the interpretation of experimental results. On the contrary, the effect of the lateral constraints on the development of permanent displacements and rotations is less important, except at failure.

The foundation is made of steel, and has a concrete interface with the underlying soil that ensures a high friction resistance to horizontal loads. As shown in Figure 2-11, the foundation is embedded 1 m in the sand, corresponding to a lateral overburden of about 20 KPa. A 1 m high steel framework was placed around the foundation to retain the sand.

The vertical load is transmitted by an air cushion system designed to keep the force constant throughout the test. A hydraulic actuator, acting 0.9 m above the foundation level, transmits to the foundation the prescribed time- varying horizontal force or displacement.
Details on the reconstitution and saturation of the soil samples, on the assessment of soil properties and on the instrumentation are reported elsewhere [Jamiolkowski et al., 1999]. Full saturation of the soil mass could not be attained.

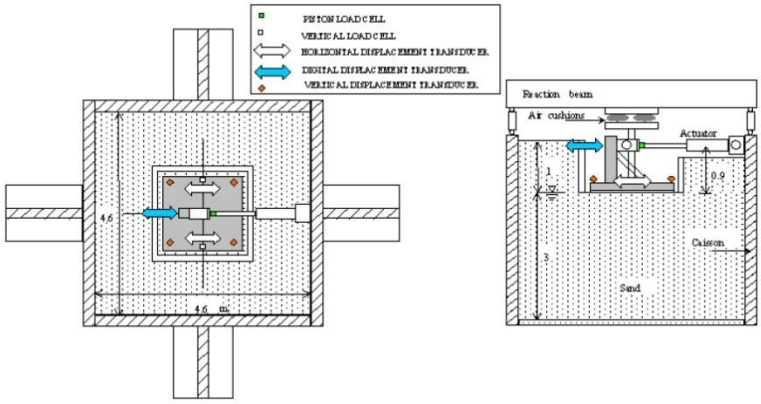

Figure 2-11: scheme of the experimental set up.

The HD and LD specimens were subjected to a similar test sequence, consisting of the application of the design- level vertical load (which was kept constant throughout the whole loading sequence), and of three subsequent loading phases reproducing different levels of horizontal excitation. The design values for the vertical load were 300 kN and 100 kN for HD and LD specimens, corresponding to design pressures of 300 kPa and 100 kPa, respectively. These are typical design values for foundations on medium to dense sands, and are governed by admissible settlement requirements. The resulting static safety factor was found to be about 5 in both conditions. It means the bearing capacity safety factor against the vertical load (V_m) is equal to 5 in H-V space.

After the static loading phase, the final vertical settlement experienced by the foundation

was about 7 mm for HD, and about 16 mm for the LD soil conditions. Details on the settlements resulting from the application of the static load alone are provided elsewhere [Jamiolkowski et al., 1999].

After completion of the static loading, the horizontal cyclic loading was applied in three phases, as follows.

Phase I

A series of small-amplitude force-controlled cycles was applied first, to identify the onset of significant non- linear behavior in the soil. The cycles were sine-shaped, with frequency f=0.5 Hz. Their amplitude was gradually increased up to about 5% of the vertical load, to obtain evidence of stiffness degradation and development of hysteresis loops.

Phase II

The foundation was then subjected to an earthquake-like time history of horizontal force and overturning moment transmitted by the hydraulic actuator at 0.9 m height. The horizontal force was adapted from the base- shear time history measured on a four-story RC building, designed according to EC8 and tested at the ELSA laboratory [Negro et al., 1996]. The peak of the seismic input was scaled to a seismic coefficient (horizontal force divided by vertical force) of about 0.2 (Figure 2-12). The combination of seismic coefficient and height of application of the horizontal force (h=0.9m) was such that a compressive stress was maintained everywhere on the foundation interface. The absolute value of the force peak was of about 60 kN and 20 kN for the HD and LD tests respectively. To preserve the accuracy in the force-control system, the original time scale was expanded. For the first (HD) test, the time scale was expanded by a factor of 6, whereas for the second one (LD) the original time scale was expanded by a factor of 3. The original time history of horizontal force had a fundamental frequency of about 0.8 Hz. The resulting diagram of horizontal force was, instead, characterized by a fundamental frequency of 0.13 Hz and of 0.27 for the HD and the LD test respectively.

Phase III

Finally, sine-shaped displacement cycles of increasing amplitude were imposed to the top of the structure, up to the attainment of a limit threshold of the foundation resistance. The test was displacement-controlled in order to avoid excessive movement of the system close to its ultimate capacity. Pairs of cycles (f=1/6 Hz) were used for HD test and single cycles (f=1/3 Hz) for LD test.

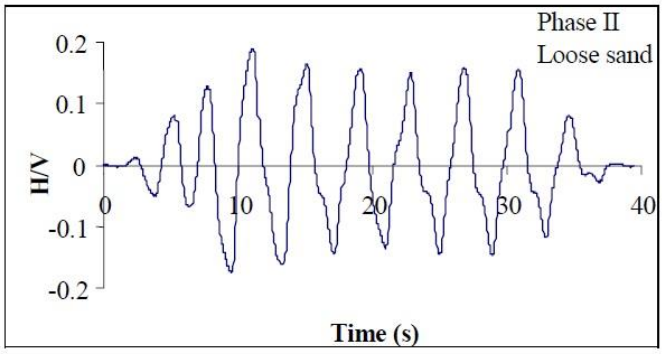

Figure 2-12: Phase II: time-history of horizontal force.

2.3.2.3 Test results

Phase I

The application of force-controlled cycles of small amplitude resulted in substantially similar behavior in the two tests. As shown in Figure 2-13. For the overturning moment vs. rocking, hysteresis loops are rather stable and denote a limited amount of dissipation. The rocking stiffness for the HD case is more than twice that in the LD case. The final settlement of the foundation after this loading phase was about 0.15 mm in both HD and LD cases, denoting that for low values of the seismic coefficient (up to about 0.05 g) the non-recoverable part of foundation displacement and rocking is negligible.

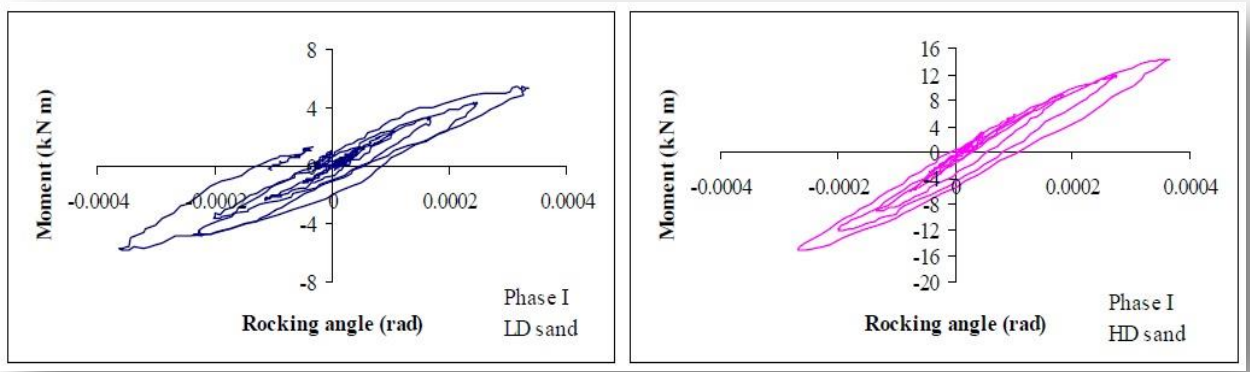

Figure 2-13: Phase I: overturning moment vs. rocking for LD (left) and HD (right) soil conditions.

Phase II

This is the most meaningful loading phase for analyzing the foundation behavior under earthquake loading. Some representative results are illustrated in Figures 2-14 and 2-15, namely the overturning moment vs. rocking diagrams and the vertical settlements, respectively. In both HD and LD cases, the largest cycle corresponds to the peak of horizontal force, while the subsequent cycles are essentially contained inside this loop. During the most severe loading cycle, stiffness reduces to about 30% of the initial value for the HD case and to about 20% for the LD case. However, as shown in Figure 2-14, the initial stiffness is gradually recovered during subsequent cycles.

In this loading phase the seismic coefficient did not exceed 0.2, the permanent deformations of the foundation are significant, especially in terms of rocking. Recalling that a foundation rotation of 2 mrad is considered as a threshold value for the onset of cracking on the superstructure (e.g. [Lambe and Whitman, 1969]), this value is slightly exceeded during several cycles in the HD case, while in the LD case the peak rocking reaches 6 mrad. According to Eurocode7 [EC7, 1994], the latter value is the relative rotation likely to cause an ultimate limit state. The permanent value in the LD case at the end of the loading phase is about 2 mrad. Vertical settlements experienced by the foundation are less severe than rocking in terms of serviceability limit state. However, for LD conditions, the final settlement is about 10 mm, that is about 60% of the vertical settlement under the static loading phase. For HD conditions the increment with respect to static loading is about 30%.

These results stress the need of improving the accuracy of current predictions of foundation settlements and rocking during earthquakes; the indication is that the movements may attain significant values, possibly beyond serviceability limit states, even under a moderate seismic excitation as the one considered in these tests.

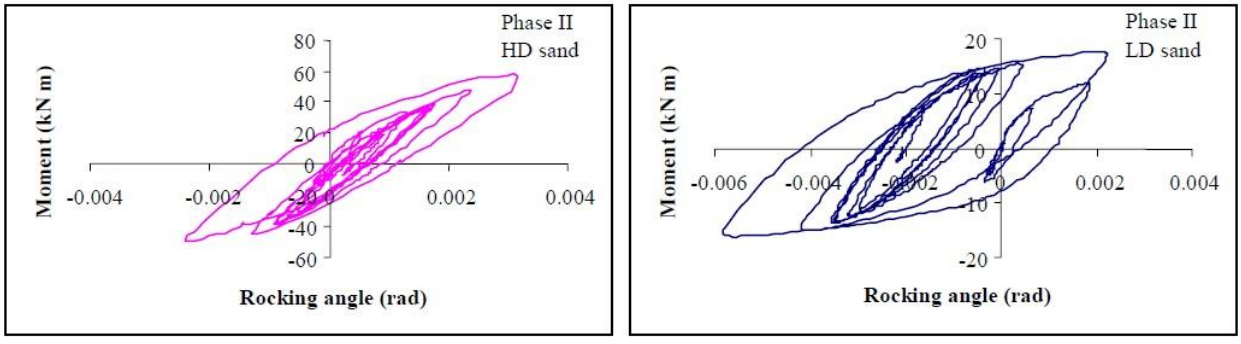

Figure 2-14: Phase II: Overturning moment vs. rocking for HD and LD conditions.

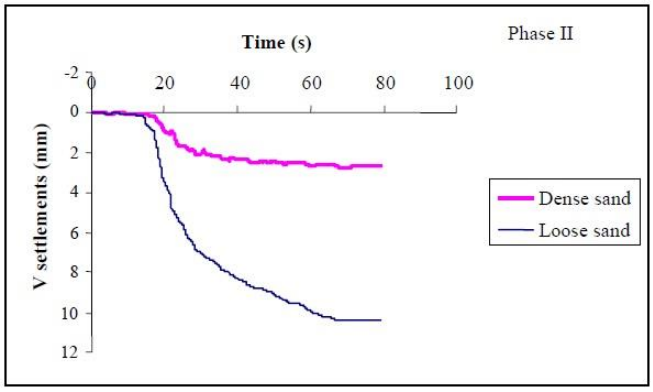

Figure 2-15: Phase II: Vertical displacement of the foundation.

Phase III

During this phase, displacement-controlled cycles with increasing amplitude were applied to the foundation with the aim of reaching the ultimate foundation resistance.

The loops described by the curves of overturning moment vs. rocking (Figure 2-16) are remarkably regular, with a characteristic s-shape for the HD case. Theoretical modelling of the experiment [Pedretti, 1998], has shown that such shape can be explained in terms of foundation uplift under eccentric loading. During uplift, the stiffness of the system degrades significantly but, as soon as the eccentric load decreases, the contact at the soil-foundation interface increases correspondingly and the rocking stiffness recovers. This effect does not appear for LD conditions, since "punching" is the prevailing failure mode of the foundation in low to medium dense conditions [Vesic, 1973]: the foundation sinks into the sand and uplift effects are prevented.

Foundation punching in LD conditions is well illustrated in Figure 2-17, with settlements that tend to increase linearly, probably due to the progressive expulsion of sand from underneath the plate toward the sides during the sinking of the foundation. A linear increase of settlements is seen to occur also for HD conditions, but final values in this case do not exceed 20 mm.

In Fig 2-18 foundation settlements are plotted as a function of the seismic coefficient k_h. A limit value of k_h slightly lower than 0.4 is found, both for HD and LD soil conditions. However, the interpretation of such value in terms of seismic bearing capacity should be considered with care, even in the HD case. First, the lateral boundaries of the concrete caisson are too close to the foundation for a shear failure mechanism to completely develop, so that the resulting bearing capacity should increase with respect to the theoretical value. Second, the experiments were carried out in dynamic conditions, that generally leads to an increase of the bearing capacity with respect to the conventional monotonic loading (Vesic, 1973).

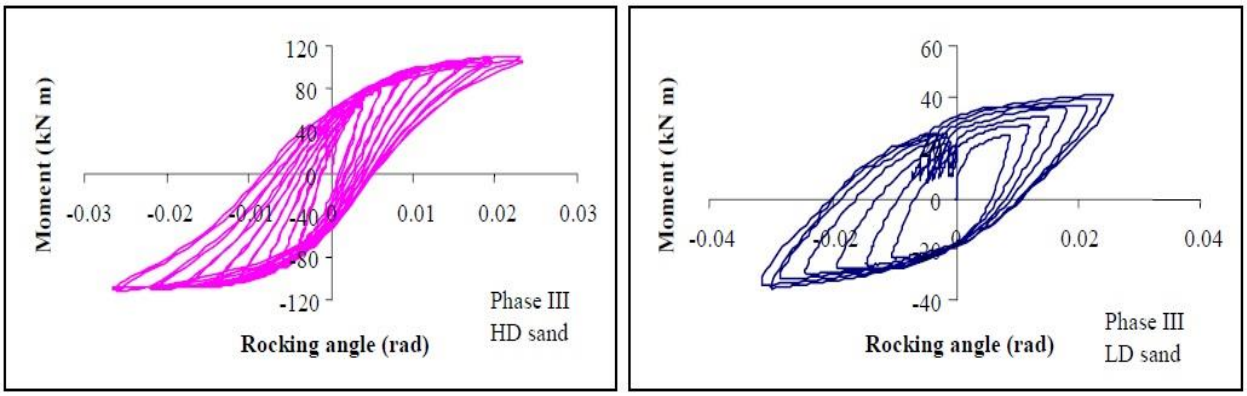

Figure 2-16: Phase III: Overturning moment vs. rocking for HD and LD conditions.

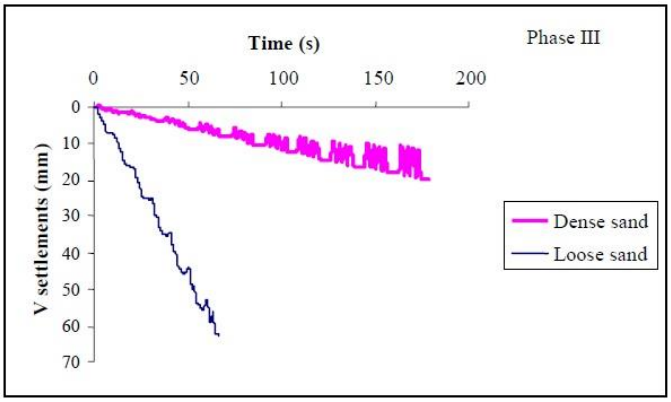

Figure 2-18: Phase III: Foundation settlements.

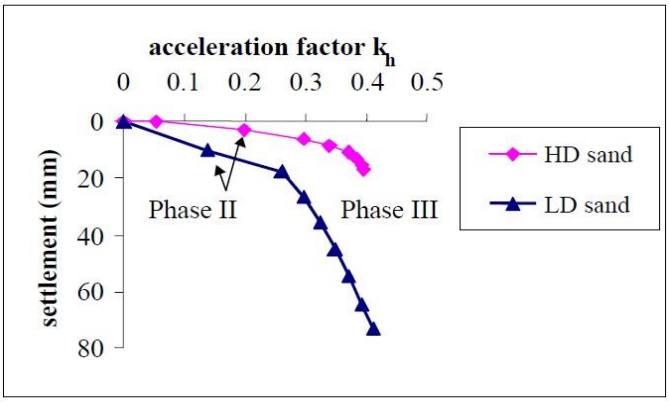

Figure 2-17: Comparison of foundation settlements in HD and LD soil conditions as a function of the seismic coefficient ($k_h=H_{max}/V$).

2.3.2.4 Conclusion

We have explored the capabilities of an experimental approach for the analysis of soil-structure interaction effects during seismic loading. The main advantages are the following: a) small-scale modelling; b) accurate determination of soil properties; c) application of realistic time histories of horizontal force and overturning moment. On the other side, a) soil inertia forces are not taken into account, b) lateral and bottom boundaries are close to the foundation and cannot reproduce completely free-field conditions, c) repetition of the experiment involves the treatment of a large amount of soil material.

The results illustrated herein have been obtained with two almost completely saturated soil specimens, characterized by relative densities Dr≈ 45% (LD) and Dr≈ 85% (HD), subjected to the same loading phases: 1) small amplitude cycles; 2) earthquake-like force-controlled excitation; 3) cyclic displacements up to foundation failure.

While a thorough investigation of these results is still under way, one important indication of the tests is the relevance of permanent deformations of shallow foundations even during the moderate seismic excitation used in the earthquake-like loading phase (seismic coefficient k_h=0.2). The vertical settlements observed are an important fraction (from 30% to 60%) of the static ones, and may play a relevant role in the development of differential settlements between adjacent points of the same structure. Rocking values are the most significant ones. Permanent values at the end of excitation reach 2 mrad for LD conditions, while peak values in the transient phase reach about 2 mrad for HD and 6 mrad for LD conditions. The attainment of such values can affect significantly the serviceability of the structure.

The results are considered to be very accurate and provide a useful basis for a number of investigations on dynamic soil-structure interaction, such as: a) validation of non-linear constitutive models for soil-structure interaction analyses; b) validation of current methods for assessing the seismic bearing capacity of shallow foundations and of the simplified approaches for calculation of permanent deformations; c) analysis of the effect of uplift of shallow foundations; d) check of the currently used formulas for spring and dashpot coefficients of shallow foundations.

2.4 Summary

It was tried in this chapter to describe two different papers that are related to the topic of this thesis in order to show the importance of the investigating on such a kind of experiments. It was evident that there are still many aspects and full experiments that require consideration throughout the duration of this project. The most important difference between this study and other studies that have been done before is considering some mechanical properties such as average stiffness (K_H), dissipated energy (E_d) and pseudo dilatancy (ψ_{cyc}) which able us to study the behavior of the soil under cyclic and monotonic loads more accurately. Next chapter will provide description to the experimental device that have been used in order to the do the several tests to evaluate the behavior of the soil-foundation interaction under cyclic loading.

3

Description of experimental device

3.1 General overview

In this chapter a description on the experimental device which is available at the geotechnical laboratory of the department of the civil and environmental engineering at Politecnico di Milano will be presented. This small scale apparatus is capable of applying cyclic or monotonic, horizontal and vertical loads to the foundation. This apparatus was originally designed for the shallow foundation but by modifying some parts of the system, it can be possible to apply different foundation configurations such as piles or shallow foundation with piles.

3.2 Experimental set up

The experimental apparatus consists of a rigid steel frame (composed of 12 H140 shaped beams), which is fixed and used as a main body (Figure 3-1).

(a) (b) (c)

Figure 3-1: (a) front view of the loading steel frame and of the testing box, (b) upper view of the loading steel frame, (c) displacement transducers at the beginning of the tests.

The main body is consisting of the following parts:

3.2.1 Main box

This box (90 cm wide, 40 cm height and 20 cm deep) is filled with medium dense sand (Ticino river sand) via a controlled pluviation method and it is laterally confined by two tempered glass walls (10mm thickness) that can be considered sufficiently rigid and smooth to prevent any out of plane displacement and any shear stress to develop at glass-sand interface.

Figure 3-2*:* Main box.

3.2.2 Sand reservoir

A sand reservoir, with the size of 300 cm width, 47 cm depth and 125 cm length (Figure 3-3a) is placed above the rigid steel frame, and its vertical position can be modified in order to precisely control the falling height. The reservoir is equipped at its bottom with an appropriate grid (Figure 3-3b). The dimension and the spacing of the holes in the grid, as well as the falling height, have been accurately calibrated in order to precisely control the final relative density of the sand within the testing box.

A wooden connection element, which is placed between the sand reservoir and the testing box, is equipped with two sand stream spreaders (Figure 3-3c), which are inserted to limit the

formation of whirls during the pluviation and to make uniform the sand stream, in order to have a regular sand pluviation process, capable of creating homogeneous sand layers within the testing box.

(a) (b) (c)

Figure 3-3: (a) sand reservoir, (b) grids employed to control the pluviating procedure, (c) wire mesh introduced to prevent whirls during the pluviation of the sand.

3.2.3 Spreader caisson

A spreader caisson is provided for the system, which is placed between the main box and the sand reservoir box (Figure 3-4), so it makes the sand fall in the uniform way, and it makes possible to have regular and homogeneous sand. The final step to prepare the sample consists in regulating the sand level by means of a vacuum cleaner and it must be considered that this action must not make any disturbance to the soil.

Figure 3-4: spreader caisson.

3.2.4 Loading system

The loading system allows applying two independent loading components along vertical and horizontal direction, respectively, without inducing any overturning moment on the model foundation. The loads are applied by means of two double acting Bellofram air cylinders connected to a pressure control panel giving an independent regulation line for each of the two chamber of every cylinder. In both cylinders the air pressure of right chamber is controlled by a proportional 4-20 mA control valve while air pressure in the left chamber is regulated by a long-term stable manually driven pneumatic regulator. . It is worth noting that the entire loading system can be moved forward and backward with respect to the testing box so that no disturbance is induced during the pluviation phase.

Figure 3-5: loading system.

3.2.5 Displacement transducer

The rigid displacements of the model foundation are recorded by two estensimetric displacement transducers with an estimated average precision of ±0.05mm.

The positioning of the transducer takes place thanks to a bar fixed to the supporting frame by means of bolts and it makes it possible to rotate.

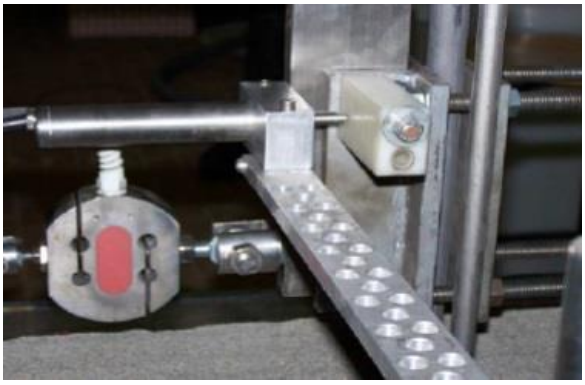

Figure 3-6: displacement transducer.

3.2.6 Load cell

Each piston includes two load cells for horizontal and vertical directions, at the connection between cylinder rod and its extension needed to reach the model foundation at the middle of the testing box. Horizontal load cell allows measuring an applied force up to 1.961 KN with an estimated precision of ±1.5 N and Vertical load cell has a 0.96 KN capacity with an estimated precision of ±0.5 N.

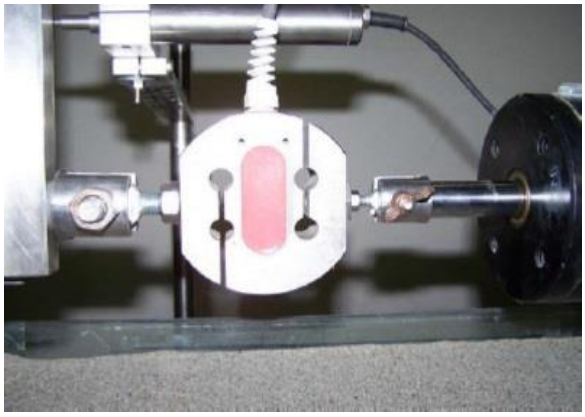

Figure 3-7: load cell.

3.2.7 Lab view environment

The whole system is controlled by dedicated software (developed in the LabVIEW® environment), handling the data pre-processed by a 16 bit A/D converter. A low-noise power supply device for all transducers has been also designed to improve measurement reliability.

Figure 3-8: lab view.

3.3 Calibration

The calibration of the instruments is crucial for a correct interpretation of the data during the tests.

The tools that allow us to collect the data of interest for our tests are:

1. Displacement transducer for the measurement of foundation displacements.
2. Pressure transducer for measuring the pressure exerted by the piston on the foundation.
3. Load cell to measure the load transmitted to the foundation.

The purpose of calibration is to find the factor for each instrument which translates the variation of microvolt initially measured by the electronic devices to the appropriate measuring unit relative to the type of instrument. For example, for the displacement transducer, the calibration allows to determine how many microvolts correspond to the actual displacement in millimeter. In this way, by inserting the appropriate values identified by this calibration, the values read from the computer will be directly expressed in millimeters. This

value will be showed in kilogram for the load cell and in Kilopascal for the pressure transducer.

3.3.1 Calibration of the displacement transducer

For calibrating displacement transducer, the micrometer is used which allows to measure the movement of the transducers with the high accuracy.

The procedure is to turn the micrometer manually until the desired displacement, then put the corresponding number in the computer which already has microvolt data sent by the displacement transducer. In this way we can have the function between the millimeter and microvolt data for each step, that for the best calibration it shows the linear line relation between these two parameters (Figure 3-9b).

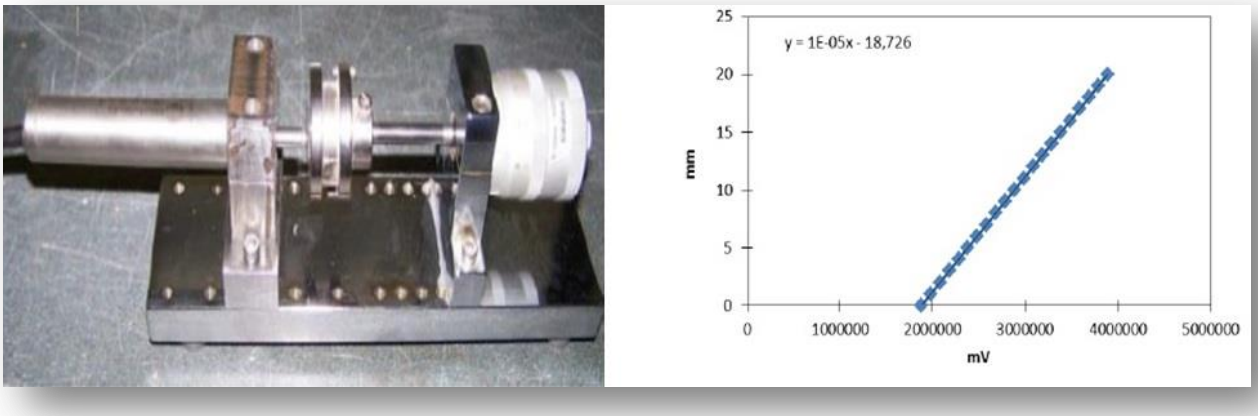

(a) (b)

Figure 3-9: (a) displacement transducer attached to the micrometer, (b) relation between displacement (mm) and microvolt.

3.3.2 Calibration of the load cells

The purpose of this calibration is similar to the previous case, which means to find the bind between the microvolt (real data sent to the computer) and the corresponding force value.

As it can be seen in figure (3-10), the load cell will be placed in the frame suitably made for this purpose, to connect the load cell with the bar which is possible to put the weights on that and also prevent of any rotation. The first reading in microvolt is relating to the load cell without

applying load, after that for each step 10 Kilogram load will put on manually.

As it was discussed before, two kinds of load cell was used, the one with maximum load 100 Kilograms and another one with 200 Kilograms limit, which the linear relationship Between microvolt and corresponding kilogram data for each load cell shows below:

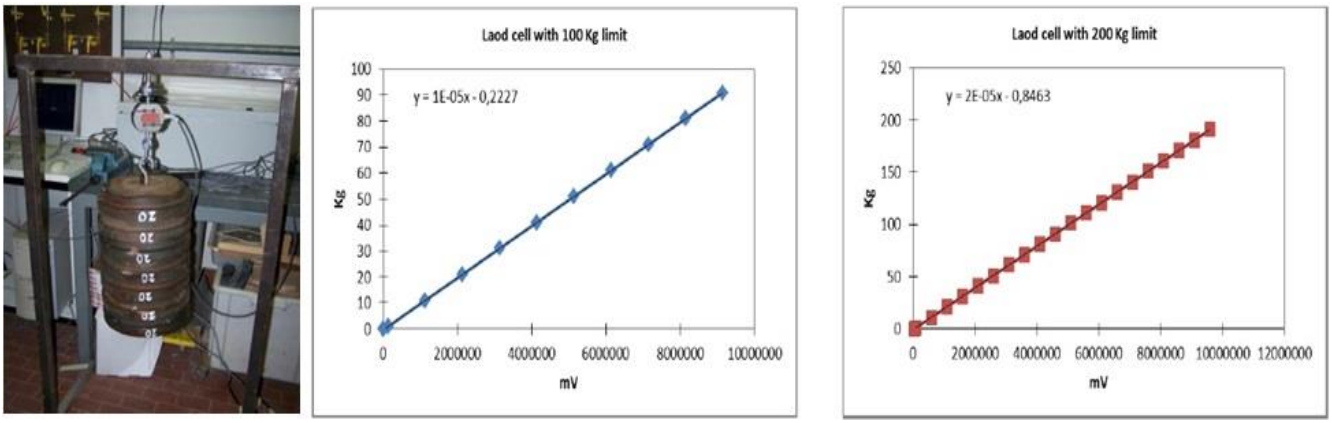

(a) (b) (c)

Figure 3-10: (a) calibration the load cell, (b) Relation between load (kg) and microvolt for load cell with 100 Kg limit, (c) Relation between load (kg) and microvolt for load cell with 200 Kg limit.

3.3.3 Calibration of the air pressure cell

In order to calibrate the air pressure cell, a manual pump calibration will be used. The principle of operation is by means of plastic tubing with low deformability. The two cells are connected to the pump pressure available for quick and easy generation of hydraulic pressures (Figure 3-11). All the tubes and connections must be saturated by means of pure oil to apply the hydraulic pressure. After making all the connection saturated by the oil, we will increase the hydraulic pressure in each step until it reaches the limit of the pressure cells which it is equal to 1000 KPa.

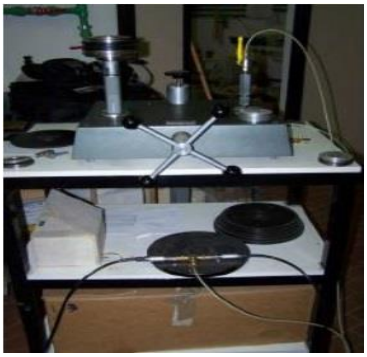

Figure 3-11: Pressure cells connected to the pump for generating hydraulic pressures.

3.4 Different kind of foundations

Two types of foundations including shallow foundation and shallow foundations with piles have been used in order to perform the tests.

3.4.1 Shallow foundation

In this part a model steel footing with the dimension of 10 cm wide, 3 cm thick and 19 cm long has been used. According to the unit weight of the steel used for the foundation, Self-weight of the foundation is equal to 4.71 Kg.

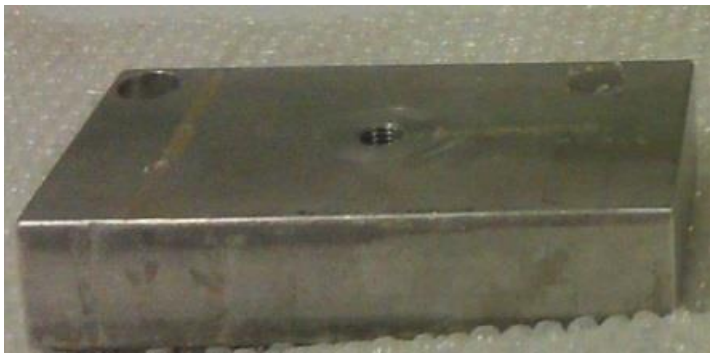

Figure 3-12: steel footing.

Sand paper is glued in the bottom part of the foundation, to introduce a realistic friction at the soil-foundation interface.

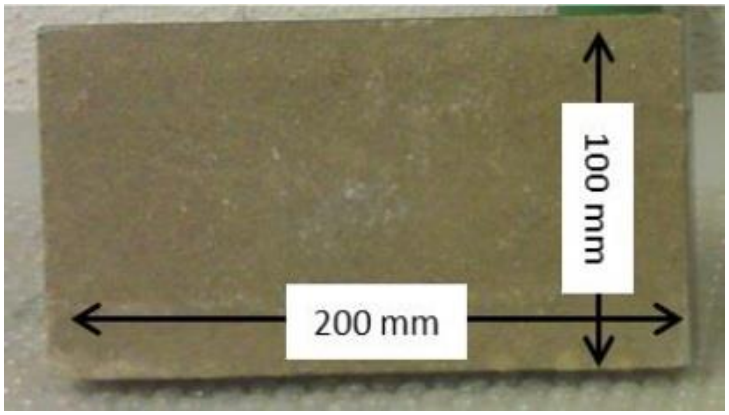

Figure 3-13: bottom view of the steel footing.

3.4.1.1 Installing the shallow foundation

For the shallow foundation the vertical load in addition to the horizontal load have been applied, so the connection parts must be organized in order to produce the capability that foundation can have vertical and horizontal movements without any rotation.

The support is designed, which is able to be screwed to the system with four, M5 screw. it has a 25 mm hole which allow the bar that connected the foundation to the piston move freely without making any extra friction.

Figure 3-14: connection system of the shallow foundation.

3.4.2 Shallow foundation with piles

In this part the footing consists of two parts. The first part is the footing plate with the same dimension already described for the shallow foundation but with the possibility of screwing piles on the bottom part. The second part is the steel bars used as a pile with the diameter of 15 mm and 150 mm length, and each pile has a weight equal to 0.208 Kg.

In this study 4 different configurations with different number of piles will be used, referred to 1 pile in the center, 3 piles in a row, 3 piles in a column and 9 piles (Figure 3-15).

It is worth mention that a special cap designed to screw on the holes which may remain free when the number of piles used under the shallow foundation is less than 9 piles and each cap has about 0.01 Kg weight. The weights of the foundations for each configuration are reported in table 1-3.

(a) (b) (c) (d)

Figure 3-15: Shallow foundation reinforced with pile (a) Shallow foundation with 1 pile in the center (b) Shallow foundation with 3 piles in a row (piles in a line arrangement) (c) Shallow foundation with 3 piles in a column (piles are in a side by side arrangement) (d) Shallow foundation with 9 piles.

Type of the Foundation	**Shallow foundation**	**Shallow foundation plus 1 pile**	**Shallow foundation plus 3 piles in a row**	**Shallow foundation plus 3 piles in a column**	**Shallow foundation plus 9 piles**
Weight of the foundation (Kg)	4.710	4.982	5.538	5.538	6.854

Table 3-1: weight of foundations.

3.5 Granular material

The employed granular material is Ticino river sand, whose mechanical properties are listed in 3-2 (Fioravante, 2000) and whose grain size distribution is shown in 3-16. A loose sand configuration was adopted, by calibrating the eluviation procedure in order to get an average relative density within the testing box at the beginning of the test equal to 40%.

Specific gravity	G_s [-]	2,67
Average grain size	D_{50} [mm]	0,55
Uniformity coefficient	U_C [-]	1,6
Minimum unit weight	γ_{min} [kN/m^3]	13,65
Maximum unit weight	γ_{max} [kN/m^3]	16,67
Minimum void index	e_{min} [-]	0,578
Maximum void index	e_{max} [-]	0,927
Friction angle at critical state	ϕ'_{cv} [°]	34,6

Table 3-2: geotechnical characteristic of Ticino river sand.

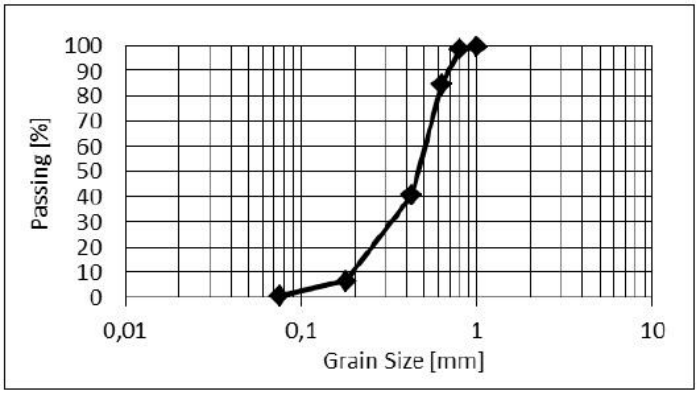

Figure 3-16: grain size distribution of Ticino river sand.

3.5.1 Relative density of sand

It is essential to correctly define the value of the relative density of the sand in the tests. As it is already mentioned, by changing the grids in the sand reservoir box (Figure 3-3c) it is possible to obtain the desire relative density of the sand. Two kinds of grids with different holes diameter and spacing between the holes have been used. According to Caloni and Savoldi (2000), a grid with the 20 mm diameter of the holes and 60 mm spacing has been used to obtain loose sand (Dr 40%) and a grid with the 4mm diameter of the holes and 25 mm spacing for obtaining the dense sand (Dr 100%).

3.6 Summary

The objective of this chapter was to describe the experimental device which is available at the geotechnical laboratory of the department of the civil and environmental engineering at Politecnico di Milano, the better explanation of the different part of this apparatus and presenting how this device works. In the next chapter the results will be presented, comparison and interpolation will be performed.

4

Experimental results on a shallow foundation with pile and interpolations

4.1 General overview

Within this chapter, it is tried to show all the results from cyclic (symmetric & asymmetric) and monotonic tests on a shallow foundation within different number of piles. The effects of different foundation configurations on the failure locus for each case as well as all nonlinear behavior of the soil-foundation interaction such as ratcheting phenomena, changing in the average stiffness and dissipated energy as well as permanent displacement due to the cyclic loading will be studied.

4.2 Introduction

In Many civil structures including offshore platforms, docks, wind turbine and bridges Piles are used in order to increase the bearing capacity and reduce the settlement of the foundation.

Besides the loads from the superstructures, piles must also resist against lateral loads, the sources of these loads can be different, such as wind, the impact of the waves, the seismic shaking, failure slope, debris flows and river currents. Most of the stresses arising from the sources mentioned earlier are coming from the nature, and potentially include cyclic effects. These issues make the interaction between the foundation and the soil to be very complex. Hence, to design safely the structure, it is important to consider the variables that affect these cyclic loading. Understanding the behavior of the piles under the complex cyclic loading is crucial for many essential engineering designs, since piles during such a loading paths can be subjected to several damages as reported in most of the earthquakes.

Although variety of methods have been proposed experimentally and theoretically for predicting the response of piles to lateral cyclic loads, but still require more investigation in

which they can predict correctly the accumulation of rotations and stiffness variations as a result of cyclic loading. This behavior has been investigated in the last decades by many authors such as Matlock and Reese (1960), Broms (1964), Poulos (1971) and Boulanger et al. (1999) which they provide the reliable procedure to design the pile. To investigate more and have wider results, other authors improve those theories by applying numerical methods and experimental tests, such as Ito and Matsui (1975), Georgiadis and Butterfield (1982), Hsiung and Chen (1997). The approach which is still frequently used by designers is based on the work of Winkler (1867), which has been used to outline the soil-structure interaction in the case of railway. In practice, analysis of laterally loaded piles is carried out using beams on non-linear Winkler springs model due to its simplicity, low computational cost and the ability to model layered soils. The mechanical behavior of the non-linear springs can be described by so call a P-y curve, which is describing the force "P" per unit length versus lateral pile deflection "y".
The approach models the response of soil-pile interaction by means of the theory of elasticity. A valid generalization of the Winkler model is then mixed by the method of the P-y curves, originally introduced by Reese & Matlock (1956) and McClelland & Focht (1958) which offers the advantage of being able to take the account of the phenomena of plasticization that occur in the soil surrounding the pile. In this case also it can be named the very first studies such as Dowrick (1977), Matlock (1970), Reese et al. (1970), API (1993), and effect of cyclic lateral loads on piles in sand by Long and Vanneste (1994) has been investigated. Rosquoët et al. (2003) see the effect of the lateral loading on the P-y curves by performing centrifuge tests. More complete research is done by Rovithis et al. (2009).

Since the Winkler method is described by theory of elasticity, in some cases, for instance when the pile applied to the long term cyclic load, has not a perfect answer. In fact originally P-y curves for cyclic loading is introduced for the ultimate lateral capacity but on the other hand the increasing in stiffness and also the accumulation of rotation during the long time cyclic loading is not at all understood in Winkler method. Or even as it is reported by Long and Vanneste (1994), for offshore piers which is subjected to the lateral loads is show much higher displacement than P-y curves suggested by Reese et al. (1974). So in this way in the few past decades some small scale experimental results has been published, due to the difficulties that you can be faced with the in situ tests of the piles. Park and Falconer (1983) reported the results obtained by using pre-stressed concrete under axial compressive load and cycles of lateral loading which simulated the seismic loading conditions, Joen and Park (1990) simulated seismic loading to apply pre-stressed concrete piles. Narasimha and Mallikarjun (1995) tested the behavior of the piles under lateral loads with different load ratios using the clay. Basack and Purkayastha (2007) investigate the behavior of the fix head or the free head model pipe pile under lateral cyclic load in Marine clay.

Leblanc et al. (2010) investigate more about the response of the rigid piles in sand due to the long term cyclic loading (8000 to 60000 cycles) and suggest some calibration for the data obtained in small-scale laboratory tests to predict correctly the real scale structure problem. In this work the method found by Briaud (1998) and Long and Vanneste (1998) to predict correctly

the accumulation of rotation and variation of pile stiffness under cyclic loading are perfectly described. Raongjant and Jong (2011) investigate seismic behavior of free head single pile in sandy soil to see the effect of different cross section of the pile and lateral load eccentricity ratio on the load-displacement hysteresis loops and energy dissipation. It also finds the influence of the relative density on the behavior of the pile. Although most of the experimental investigations are only considered by applying the lateral load, Lee et al. (2011) studied this effect by applying the combined load with driven pile in sand. More recently the Winkler method is improved by taking into account the macro-element theory following the work of Nova and Montrasio (1991). This is implied for the piles in quasi-static case by Tacirglu et al. (2006) which is considered the coupling between the frictional force, elastoplastic element for clay and the gap element and wider work by Rha and Tacirglu (2007) and in the dynamic case it is studied by Varun (2010).

4.3 Foundation configuration

Four different configurations are used in order to do the tests as follows (Figure 3-15).

- **1 pile** in center
- **3 piles in a row** (piles are in a line arrangement). The center to center pile spacing parallel to the loading direction is 33 mm which means about 2.3 times larger than the pile diameter.
- **3 piles in a column** (piles in a side by side arrangement). The center to center pile spacing is 67 mm in direction perpendicular to the load which means 4.47 pile diameters.
- **9 piles** (piles are in a box arrangement). The center to center pile spacing parallel to the loading direction is 33 mm which means about 2.2 times bigger than the pile diameter and the center to center pile spacing is 67 mm in direction perpendicular to the load which means 4.47 pile diameters.

More specific details about the different configurations of piles can be captured from previous chapter. , the dimension of the shallow strip footing is the 200 mm x 100 mm and for the rigid steel pile with the 15 mm diameter and 150 mm length have been used.

4.4 Conceptual framework of the experimental program

The experimental tests described in the following sections have been performed on a small scale prototype of a shallow strip footing with different number of piles, that can be subject to a generalized loading system composed of vertical (V) and horizontal (H) forces and the overturning moment can be created by applying these loads, and undergo a generalized displacement represented by the vertical (v) and horizontal (u) displacements and by the rotational settlement, as sketched in figure 4-1 with reference to the central point O of the foundation. For the sake of simplicity the distance b between the line of application of the horizontal load H and the point O is assumed to be negligible, so that H does not influence the overturning moment M.

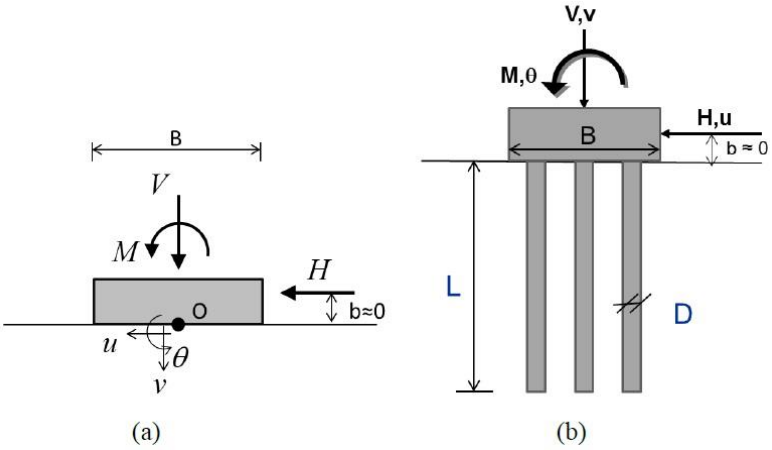

Figure 4-1: Definition of static and kinematic variables for the macro-element; (a) shallow foundation, (b) shallow foundation with pile.

These quantities can be lumped into a generalized stress vector Q and a generalized strain vector q, representing the static and kinematic variables of the system, respectively (superscript index T stands for transpose operator). More details and related equation can be captured from chapter 1 (part 1.3.3) and equations 4.1-4.3.

4.5 Defining the interaction domain

In this section, by considering the generalized stress path of each monotonic test (see chapter 1, part 1.3.3), it is Possible to configure the interaction domain for the shallow foundation with piles. Here also from the graphs regarding to the horizontal load versus horizontal displacement, the failure for horizontal load can be considered when the curve reach a perfect plateau. For the pure upward vertical loading also this ductile behavior is also visible, but unfortunately due to the machine limitation, which means the maximum displacement that displacement transducer can record and also the maximum load that the load cells can measure (chapter 3) for the pure downward vertical load, it is not possible to reach the final vertical load.

So in this case, it is necessary to define analytically the interaction domain and final limit load. This can be done by generalizing the equation derived from the Nova and Montrasio (1991) for shallow foundation (chapter 1) and also considering the results from di Prisco (2004) proposed for soil-pipe interaction and finally following the Pisano et al. (2013) for defining the new failure locus formulation for the various shapes and complex situation of soil-structure interaction (chapter 1). So in this case the following expression is used to define the failure locus analytically.

$$\frac{H}{\mu(V_{LC}-V_{LT})} = \left[\frac{V-V_{LT}}{(V_{LC}-V_{LT})}\right] \times \left[\frac{V_{LC}-V}{(V_{LC}-V_{LT})}\right]^{\beta} \qquad \text{Eq 4.1}$$

Where β and μ are the constitute parameters defining the shape of the locus and V_{LT} and V_{LC} are the bearing capacities of the foundation under the pure downward vertical load and the pure upward vertical load respectively.

4.6 Experimental tests

Monotonic and cyclic loading in horizontal and vertical directions are applied into the shallow foundation with piles on loose Ticino river sand with different configurations which is completely described in previous chapter. The tests were performed with the aim of:

1. Defining the failure condition of the system (i.e. the interaction domain of the foundation in the generalized stress space V-H);
2. Describing the coupling between horizontal and vertical directions during monotonic tests;

3. Analyzing the cyclic behavior of the system.

4.6.1 Monotonic tests

Monotonic tests are performed in two phases, in the first phase the vertical load increase until to the desired value of V_0 while the horizontal load is kept constant at zero, then in the second phase the horizontal load is increased at constant vertical load up to failure.

Figure 4-2b displays the monotonic loading path with pure vertical downward loading test. Two additional monotonic loading tests are applied; in the first case the horizontal load has been applied while the vertical load V_0 is kept at zero (Figure 4-2c) and for the second case the upward vertical loading performed until failure (V_{LT}) without applying any horizontal load (Figure 4-2d).

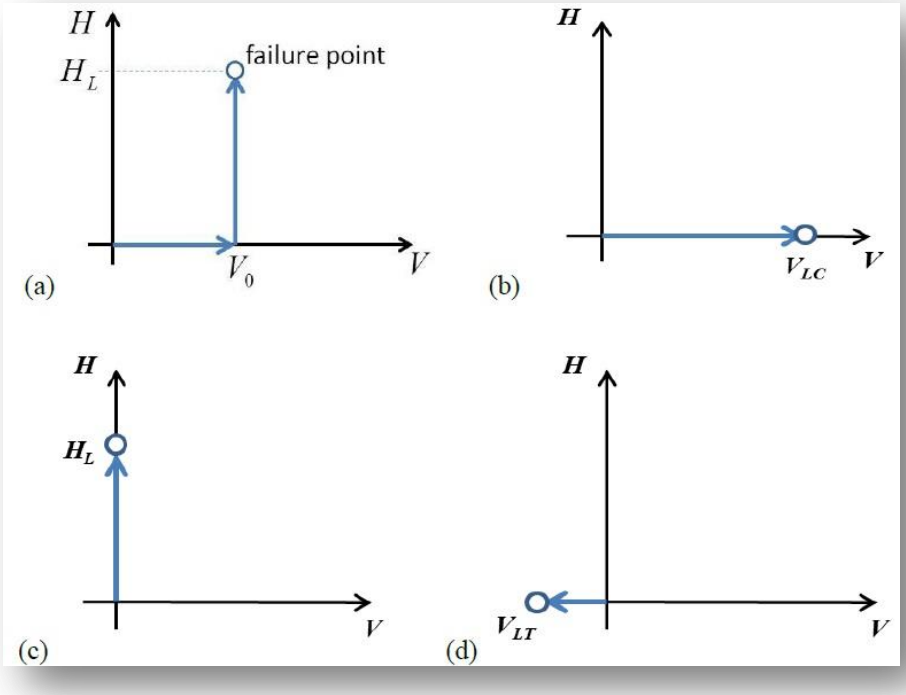

Figure 4-2: (a) Example of monotonic load, (b) Zero horizontal load and downward vertical load test, (c) Zero vertical, (d) Zero horizontal load and upward vertical load.

The complete details of the loading paths for monotonic tests are shown in Table 4-1.

Test Type	Piles Configurations	Lable	Vertical Load(KN/m)	Horizontal Load(KN/m)
Monotonic	1 pile	1pmn01	VLT = -0.20	HL = 0.00
		1pmn02	V0 = 0.00	HL = 0.42
		1pmn03	V0 = 0.79	HL = 0.86
		1pmn04	V0 = 1.21	HL = 1.09
		1pmn05	V0 = 1.63	HL = 1.22
		1pmn06	V0 = 2.01	HL = 1.34
		1pmn07	V0 = 2.84	HL = 1.55
		1pmn08	V0 = 3.20	HL = 1.65
		1pmn09	V0 = 3.96	HL = 1.64
		1pmn10	V0 = 4.79	HL = 1.45
		1pmn11	V0 = 5.21	HL = 1.35
		1pmn12	VLC = 7.47	HL = -
	3 piles in a row	3prmn01	VLT = -0.52	HL = 0.00
		3prmn02	V0 = 0.00	HL = 0.85
		3prmn03	V0 = 0.83	HL = 1.06
		3prmn04	V0 = 2.06	HL = 1.47
		3prmn05	V0 = 3.22	HL = 1.68
		3prmn06	V0 = 4.82	HL = 1.80
		3prmn07	V0 = 5.63	HL = 1.72
		3prmn08	V0 = 6.06	HL = 1.65
		3prmn09	VLC = 10.53	HL = -
	3piles in a column	3pcmn01	VLT = -0.57	HL = 0.00
		3pcmn02	V0 = 0.00	HL = 0.95
		3pcmn03	V0 = 0.85	HL = 1.43
		3pcmn04	V0 = 1.68	HL = 2.00
		3pcmn05	V0 = 3.26	HL = 2.37
		3pcmn06	V0 = 4.85	HL = 2.69
		3pcmn07	V0 = 6.08	HL = 2.58
		3pcmn08	VLC = 11.58	HL = -
	9 piles	9pmn01	VLT = -2.10	HL = 0.00
		9pmn02	V0 = 0.00	HL = 1.66
		9pmn03	V0 = 1.27	HL = 2.10
		9pmn04	V0 = 3.28	HL = 2.76
		9pmn05	V0 = 5.64	HL = 3.49
		9pmn06	V0 = 7.37	HL = 3.65
		9pmn07	V0 = 8.23	HL = 3.38
		9pmn08	VLC = 17.89	HL = -

Table 4-1: Magnitude of the vertical and horizontal loads in each test.

4.6.1.1 Results of experimental tests

The series of monotonic horizontal tests was aimed at:

1. Defining the limit condition (i.e. the interaction domain) in the V-H plane,
2. Studying the kinematic of the system during the horizontal loading phase (i.e. the coupling effect between the horizontal and vertical loads).

By considering the generalized stress path, regarding each monotonic test it is possible to configure the interaction domain. In fact it will be studied by the taking in to the account the corresponding load-displacement curves. In each case the curves show a ductile behavior, characterized by a quite well defined plateau representing the limit value of the horizontal load. By studying these limit values it was possible to define a limit condition in the V-H plane, representing the failure locus (or, in other words, the interaction domain) for the considered foundation. It must be noted that, the limit load of the uplift vertical load (V_{LT}) is obtained from the tests have been done in the case of shallow foundation with piles.

The imposed generalized stress paths concerning the monotonic tests for different Configurations of piles plus the corresponding horizontal load-horizontal displacement curves (H-u) and the vertical load-vertical displacement curves (V-v) in upward and downward direction for each configuration are shown in figures 4-3(a-c) to 4-6(a-c).

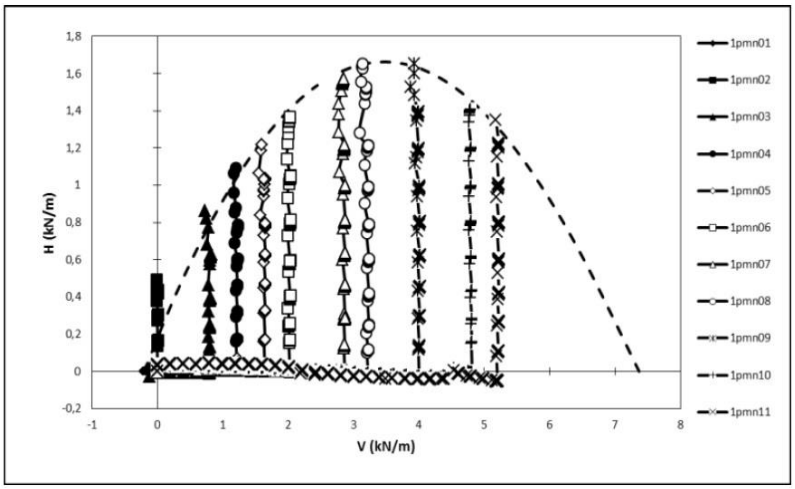

(a)

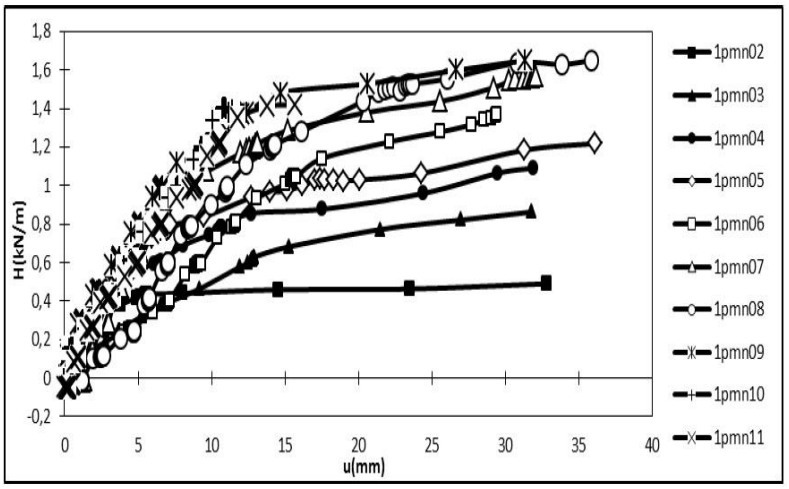

(b)

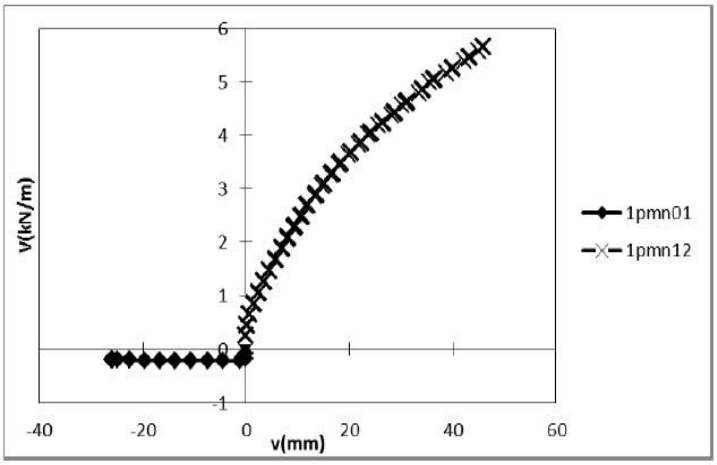

(c)

Figure 4-3: 1 pile; (a) Imposed generalized stress path for monotonic tests (dashed line represents the interaction domain calibrated according to equation 4.1), (b) Load-displacement curve in horizontal direction, (c) Load-displacement curve in vertical direction.

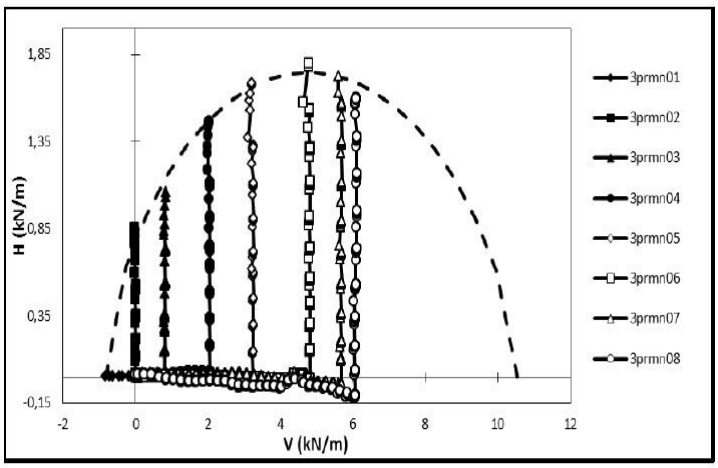

(a)

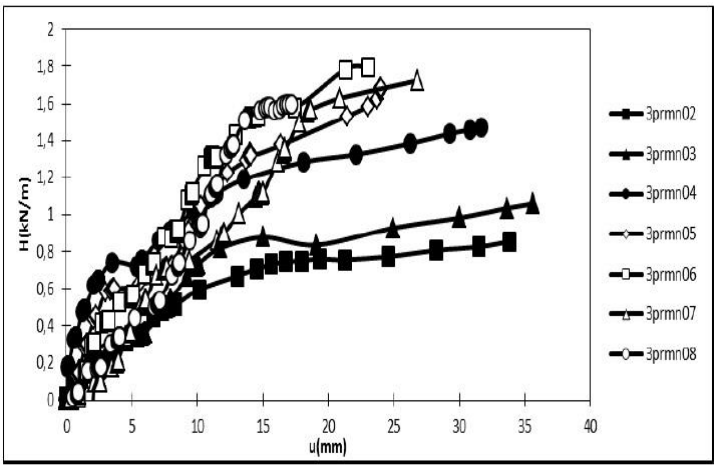

(b)

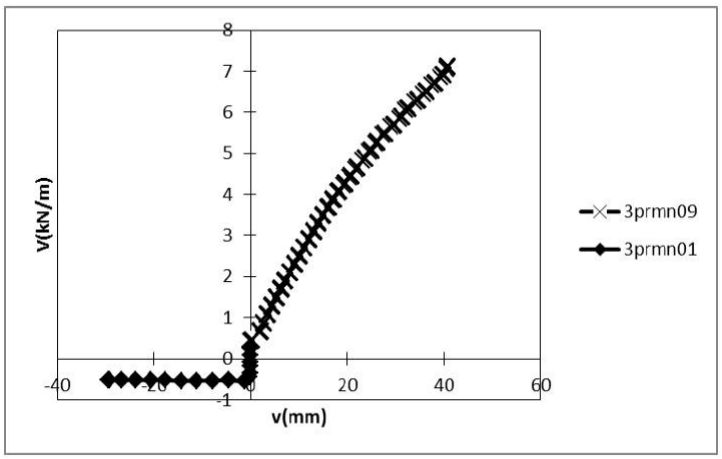

(c)

Figure 4-4: 3 piles in a row; (a) Imposed generalized stress path for monotonic tests (dashed line represents the interaction domain calibrated according to equation 4.1), (b) Load-displacement curve in horizontal direction, (c) Load-displacement curve in vertical direction.

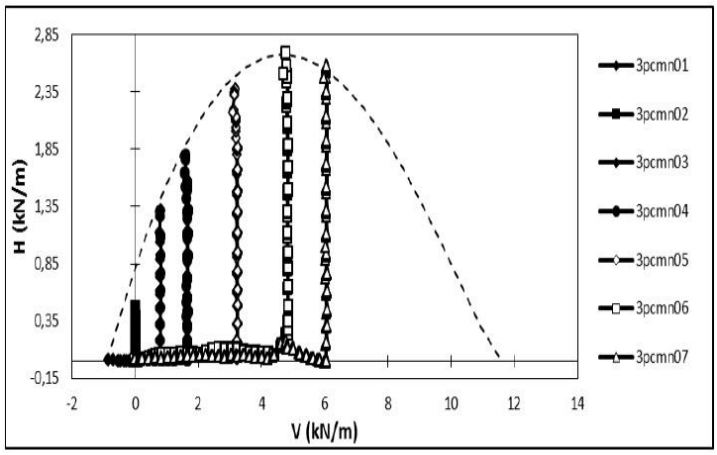

(a)

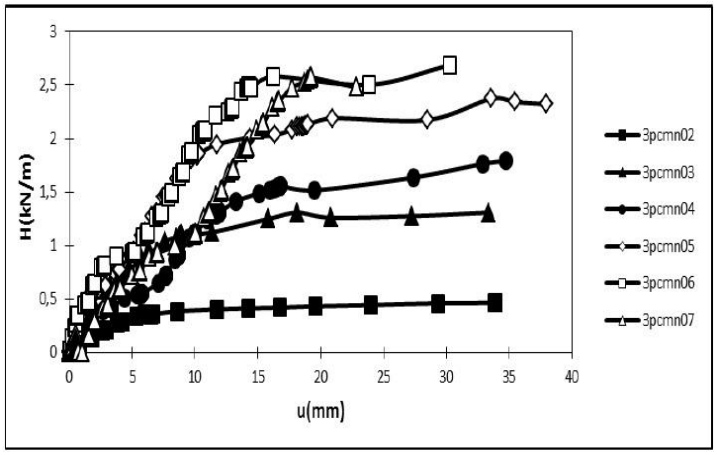

(b)

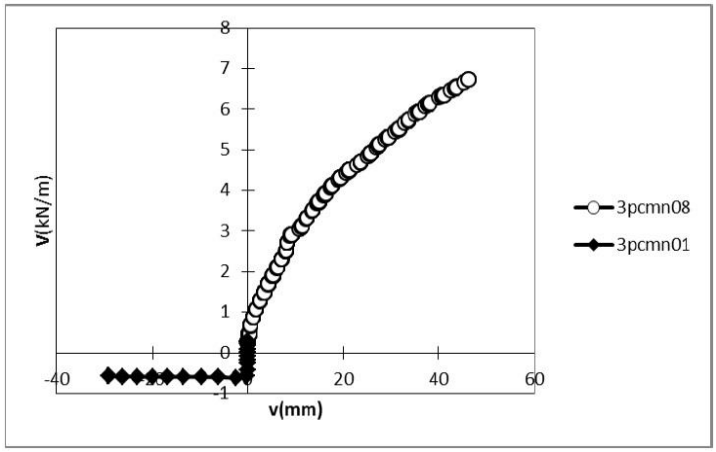

(c)

Figure 4-5: 3 piles in a column; (a) Imposed generalized stress path for monotonic tests (dashed line represents the interaction domain calibrated according to equation 4.1), (b) Load-displacement curve in horizontal direction, (c) Load- displacement curve in vertical direction.

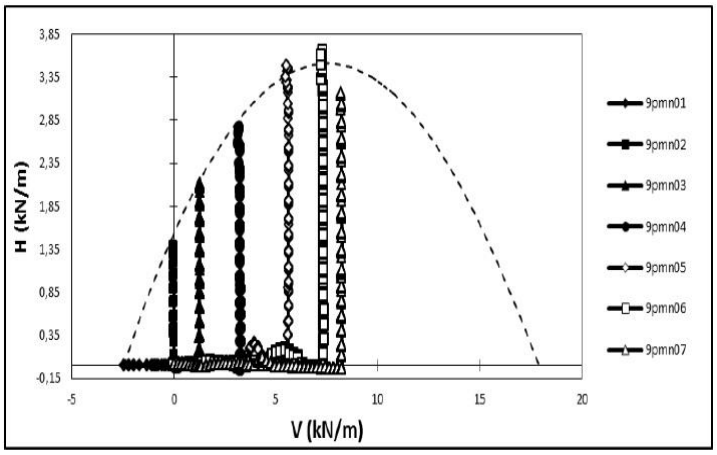

(a)

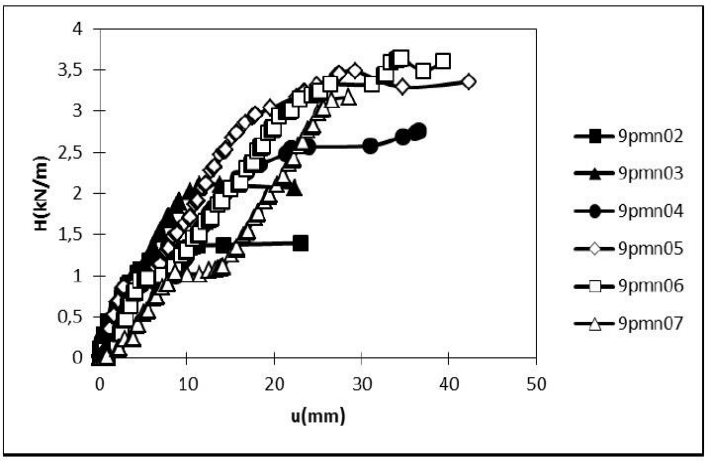

(b)

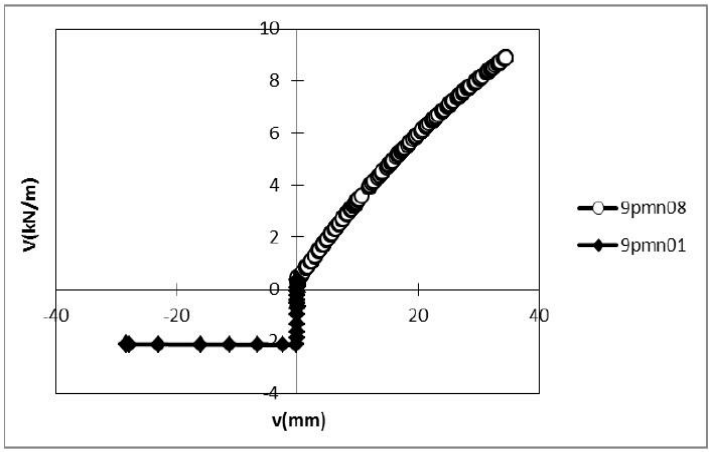

(c)

Figure 4-6: 9 piles; (a) Imposed generalized stress path for monotonic tests (dashed line represents the interaction domain calibrated according to equation 4.1), (b) Load-displacement curve in horizontal direction, (c) Load-displacement curve in vertical direction.

4.6.1.2 Interaction domain for different piles configuration

Comparison of the interaction domain for each foundation configuration are shown in figure 4-7 and the calibrated parameters by means of least square procedure of the failure points from the monotonic tests are reported in table 4-2 according to the equation 4.1.

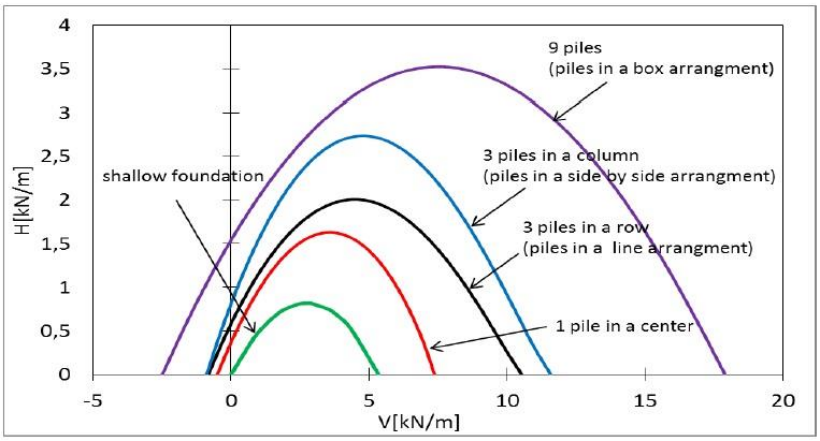

Figure 4-7: comparison of interaction domain for different foundation configuration.

Foundation Configuration	μ	β	V_{LC} *(kN/m)*
Shallow foundation plus 1 pile	0.917	1.06	7.47
Shallow foundation plus 3 piles in a row	0.775	1.28	10.53
Shallow foundation plus 3 piles in a column	0.990	1.23	11.58
Shallow foundation plus 9 piles	0.709	1.04	17.89

Table 4-2: Calibrated parameters based on equation 4.1.

Piles in a closely spaced group behave differently than a single isolated pile and a shallow foundation because of the pile-soil-pile interaction that takes place in a group piles. It is generally recognized that maximum bearing capacity of a pile in a closely spaced group are greater than the case of an individual pile because of these interaction effects. By taking into account the interaction domain obtained analytically for each configurations it is possible to see the effect of the piles under the shallow foundation (Figure 4-7). As it is obvious the smaller interaction domain is that observed for the shallow foundation, while this capacity will be increased by even using 1 pile with shallow foundation, By changing the configuration and using the shallow foundation with 3 piles in a row, while the piles are inserted in a line arrangement, there is not so much increase in case of horizontal load observed, while the downward, but on the other hand in case with the 3 piles in a column (piles are in a side by side arrangement), piles are working as a wall in front of horizontal load, due to the short spacing between the piles. Obviously the biggest interaction domain is for the case of the shallow foundation with 9 piles, this configuration is working same as a rigid block,

4.6.1.3 Coupling effect

From a kinematic point of view, the analysis of the horizontal loading phase is fundamental for describing the coupling effect between the two loading directions. in figures 4-8(a-d) and 4-9(a-d) for different configurations of shallow foundation with pile, in particular, the displacements of the foundation recorded during the horizontal loading phase are plotted in the generalized strain plane v-u (the curves do not start from the origin since v represents the cumulated vertical settlement, i.e. accounting even for the vertical settlement induced by the initial pure vertical loading phase). It can be found that all the tests show a positive vertical settlement during the horizontal load, independently of the value of the applied constant load V_0. This result can be considered consistent with the fact that relatively loose sand has been employed, which is mainly characterized by a compacting volumetric response. The trajectories can be described by means of their local steepness (measured with respect to the u-axis).

$$\psi = \frac{dv}{du} \qquad \text{Eq 4.2}$$

That can be interpreted as a sort of pseudo-dilatancy for the soil-foundation system. It appears from the trajectories of the foundation in the u-v plane during the horizontal loading phase, that the values of ψ are almost constant during the horizontal loading phase and, as a

consequence, ψ can be assumed to be mainly dependent on the current applied vertical load V, so that the following relation can be formally introduced.

$$\psi = \psi(V) \qquad \text{Eq 4.3}$$

For the presented tests, by plotting interpolation of the relationship between the Pseudo-dilatancy ψ against the imposed values of V, the ψ-V relationship shows a pronounced increasing trend, and, as a first approximation, it can be interpolated by means of simple linear function.

$$\psi = \psi_0 + \alpha \frac{V_0}{V_m} \qquad \text{Eq 4.4}$$

Where the values of V have been set to V_0 (since they are constant during the horizontal loading phase), and they have been normalized with respect to V_m. Two constitutive parameters, ψ_0 and α have been introduced, the former, ψ_0, represents the value of ψ at a (nominally) zero applied vertical load, whilst the latter, α, indicates the correlation degree between ψ and V, which they can be obtained By means of a least square procedure. The value of the ψ_0 and α which obtained from equation 4.4 for shallow foundation with piles as well as correlation coefficient (R) is reported in the table 4-3.

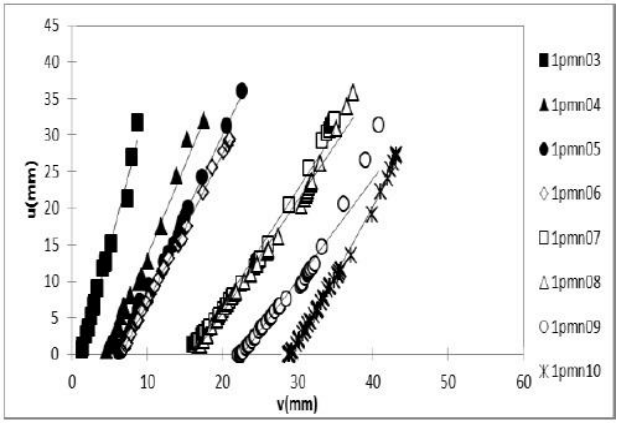

(a)

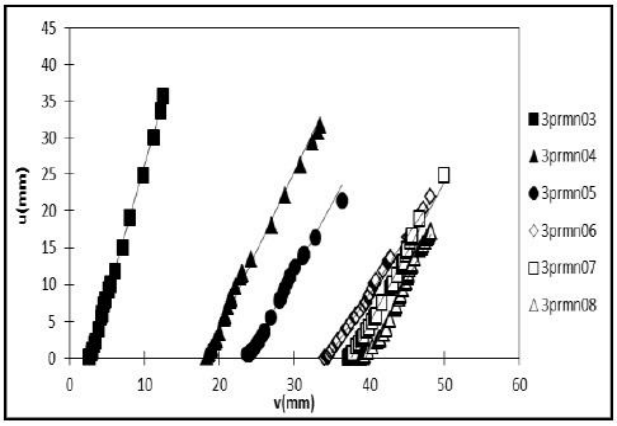

(b)

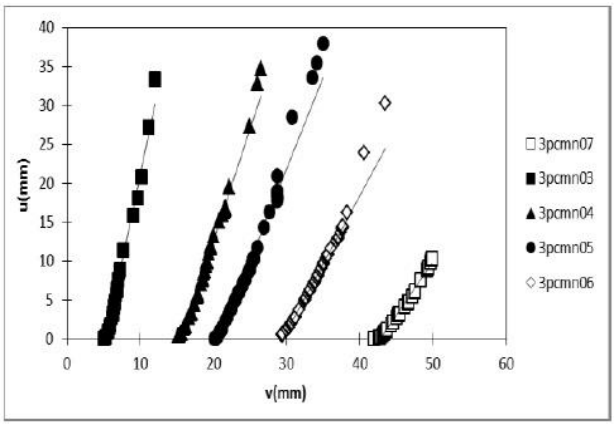

(c)

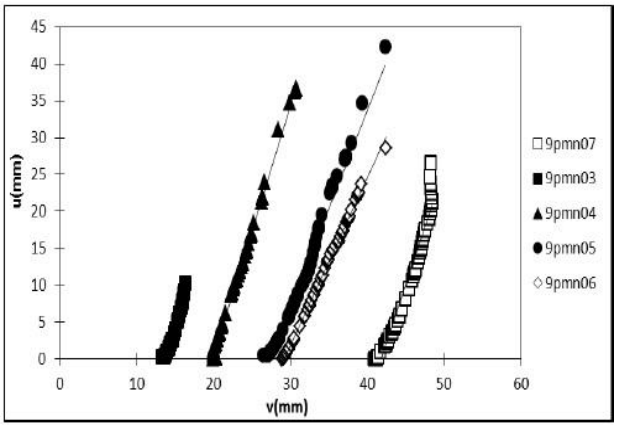

(d)

Figure 4-8: trajectoriesof the foundation in the u-v plane during the horizontal loading phase; (a) 1 pile, (b) 3piles in a row, (c) 3 piles in a column, (d) 9 piles.

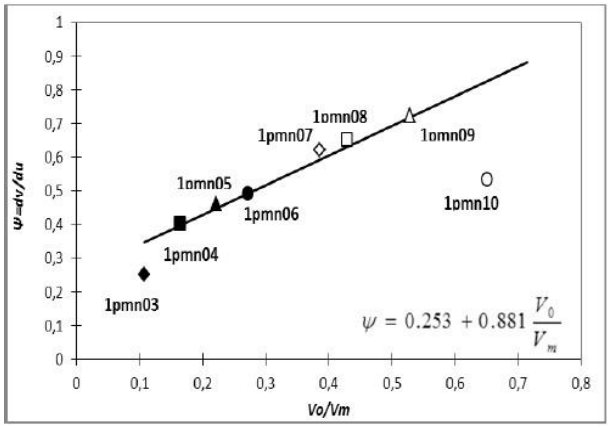

(a)

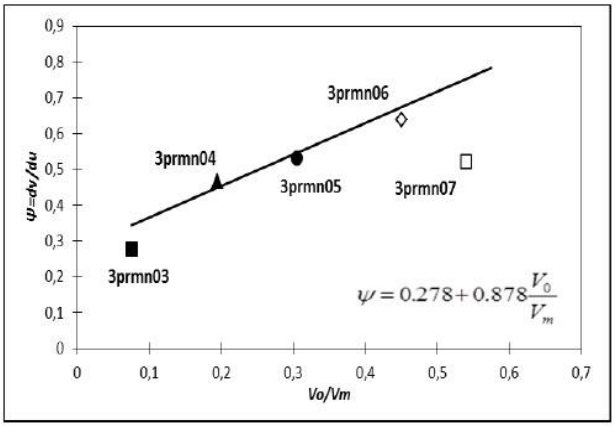

(b)

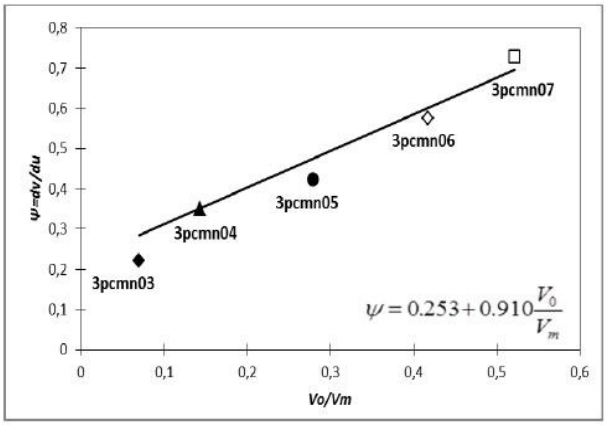

(c)

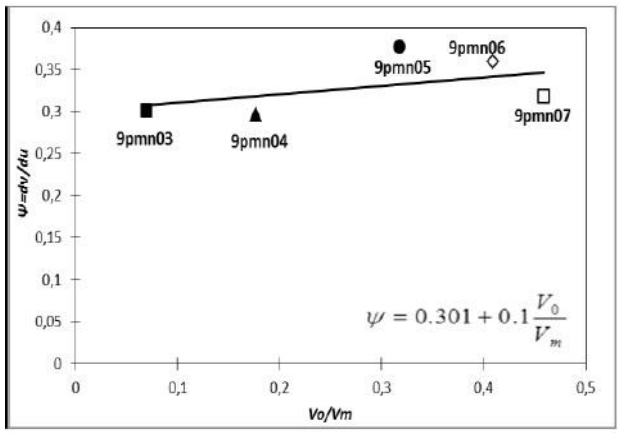

(d)

Figure 4-9: linear interpolation of the relationship between the pseudo-dilatancy ψ and the V_0/V_m ratio; (a) 1 pile, (b) 3 piles in a row,(c) 3 piles in a column, (d) 9 piles.

Foundation configuration	ψ_0	α	R^2
shallow foundation with 1 pile	0.250	0.880	0.957
Shallow foundation with 3 piles in a row	0.278	0.878	0.951
Shallow foundation with 3 piles in a column	0.253	0.910	0.978
Shallow foundation with 9 piles	0.301	0.100	0.719

Table 4-3: obtained value from equation 4.4.

4.6.1.4 Failure mechanism for shallow foundation with pile

To see the failure mechanism during the horizontal loading phase, colored sand layers have been deposited and it is possible to see the failure condition for each configuration. For the condition with shallow foundation plus piles the failure mechanism shows more and less the same behavior as the shallow foundation. Figure 4-10 shows failure mechanism for the shallow foundation plus 9 piles. As it can be seen in this figure, the failure mechanism shows that the 9 piles is working similar as single block, and it is visible how the initial position of colored layers will be changed after failure.

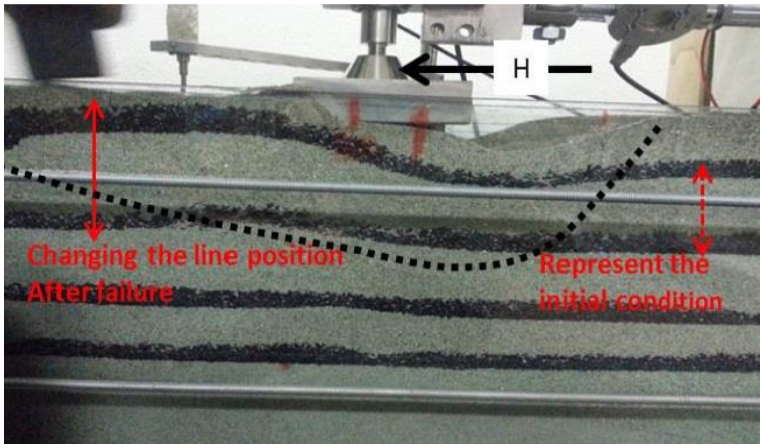

Figure 4-10: failure mechanism for shallow foundation plus 9 piles.

It is worth noting that to confirm this point, in another series of tests that have been done in geotechnical laboratory of politecnico di milano, a wooden block is prepared with the same length of the pile and same widths of the shallow footing (figure 4-11) and two tests have been done with this wooden block. By performing these two tests with wooden block, and imposing the load paths to the interaction domain and failure point obtained by the shallow foundation, it observed that the tests with wooden block perfectly shows the same results as shallow foundation plus 9 piles (figures 4-12a-d). So this is confirmed that 9 piles are working as a block in this condition for horizontal loading. But on the other hand the maximum upward vertical

loading for wooden block is much less than the shallow foundation plus 9 piles (Figure 4-12b). It must be mention that the wooden block is fixed to the plate so there is no any detachment from the plate during the vertical upward loading phase.

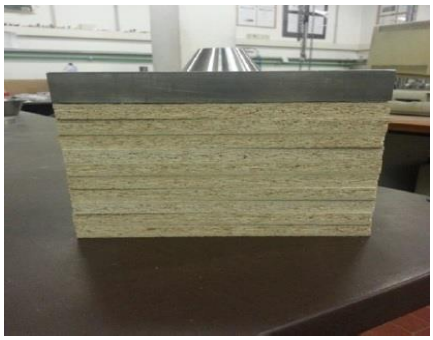

Figure 4-11: Wooden block.

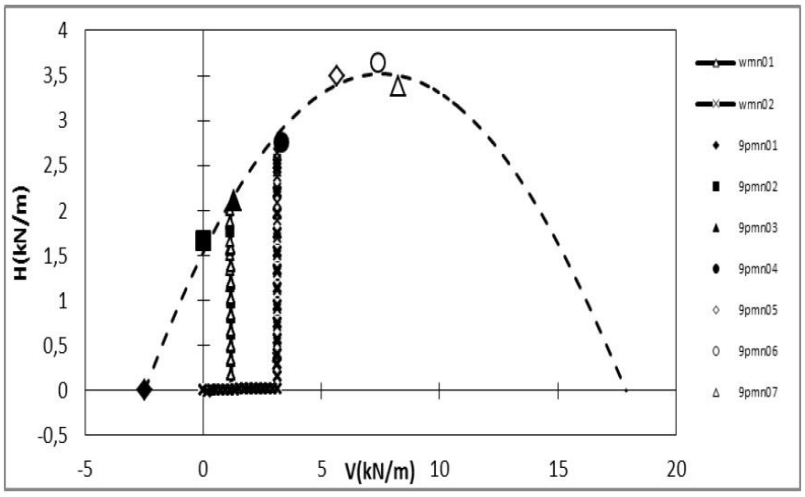

(a)

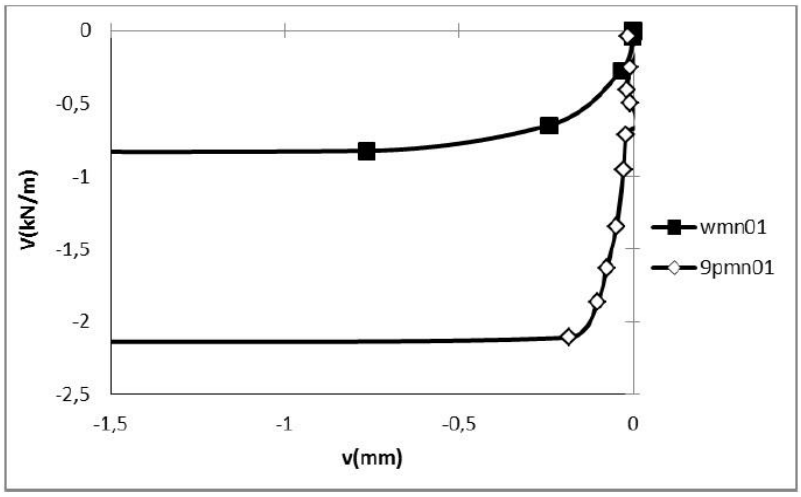

(b)

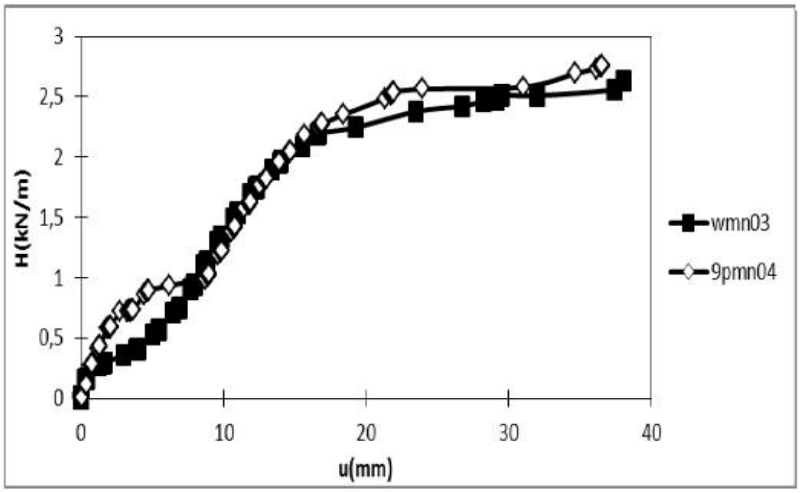

(c)

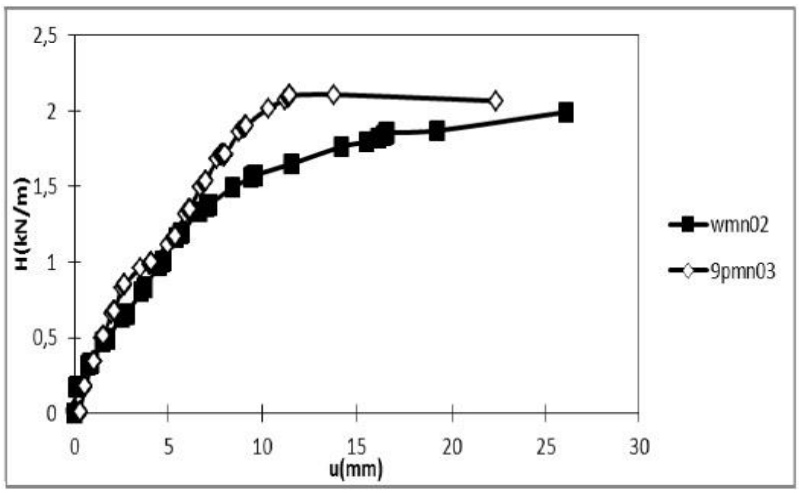

(d)

Figure 4-12: (a) Imposed generalized stress path for monotonic tests for wooden block (dashed line represents the interaction domain calibrated according to equation 4.1 For the shallow foundation plus 9 piles), (b) Load-displacement curve in vertical upward direction, comparing tests wmn01 and 9pmn01, (c) Load-displacement curve in horizontal direction, comparing tests wmn02 and 9pmn03, (d) Load-displacement curve in horizontal direction, comparing the tests wmn03 and 9pmn04.

4.6.2 Cyclic tests

Two series of cycling tests (figure 4-13a, b) were performed by initially imposing a pure vertical load up to a value V_0 and then a cyclic horizontal load of a maximum amplitude ΔH, both in asymmetric and a symmetric condition. In one case the vertical load V_0 is kept at zero value during the cyclic loading phase. Totally 5 asymmetric and 4 symmetric tests have been performed in this part.

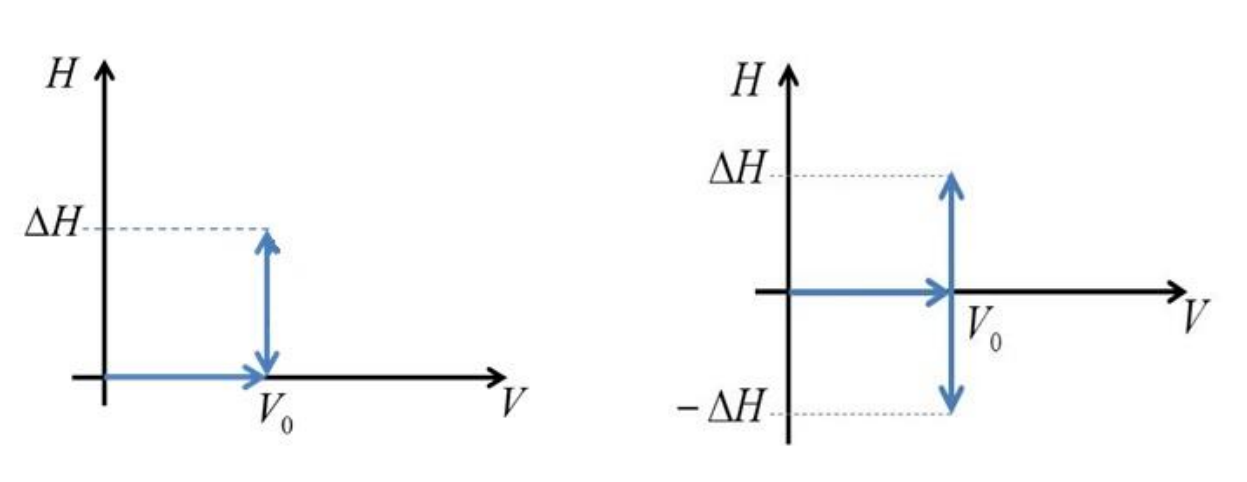

(a) (b)

Figure 4-13: (a) Example of asymmetric cyclic load (b) Example of symmetric cyclic load.

In particular, with reference to the cyclic tests, the attention will be focused on three parameters characterizing each cycle: the average stiffness K, the dissipated energy E_d (i.e. the area of each cycle) and the cumulated displacement at the end of each cycle. Required trends which are based on mentioned parameters and number of cycles that will be presented in the following, suggest the interpolating relationship in the equations 4.5-4.7. The definitions of these three quantities are schematically shown in figure 4-14 with reference to a generic cycle of the load-displacement curve H-u along the horizontal direction.

In figure 4-14 the quantity u_0 has to be intended as the horizontal displacement at the end of the monotonic phase, i.e. at the beginning of the first cycle. It is worth noting that, in case that cycles involving vertical load and vertical displacement are considered, the quantities K_V and E_{dV}, v_{max} and v_0 will be referred to, with obvious meaning of the symbols.

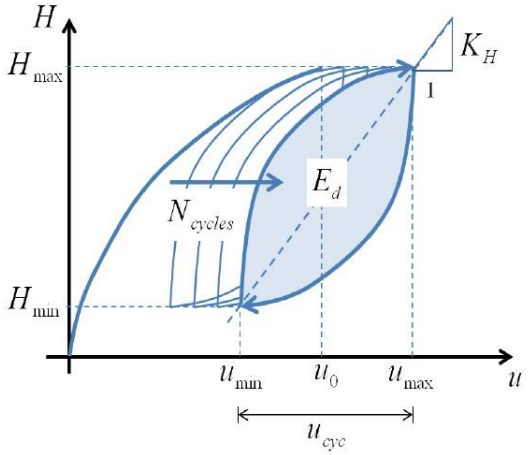

Figure 4-14: Definition of the mechanical parameters characterizing a generic loading cycle.

$$\frac{K_H}{K_{H,1}} = 1 + \alpha \cdot \left(\log_{10} N_{cyc}\right)^n \qquad \text{Eq 4.5}$$

$$\frac{E_{dH}}{E_{dH,1}} = \left(N_{cyc}\right)^{-b} \qquad \text{Eq 4.6}$$

$$\frac{v_{\max} - v_1}{B} = \beta_{cyc} \left(\log_{10} N_{cyc}\right)^m \qquad \text{Eq 4.7}$$

The complete details of the loading paths for cyclic tests are shown in Table 4-4.

Test Type	Piles Configurations	label	Max Vertical Load(KN/m)	Max Horizontal Load(KN/m)	Number of Cycles
Cyclic Asymmetric	1 pile	s1pca01	2.075	0.373	59
		s1pca02	2.125	0.698	44
		s1pca03	3.710	0.343	56
		s1pca04	3.664	0.673	44
Cyclic Symmetric		s1pcs01	0	0.367	149
		s1pcs02	2.104	0.394	59
		s1pcs03	2.120	0.789	38
		s1pcs04	3.710	0.390	50
		s1pcs05	3.771	0.775	10
Cyclic Asymmetric	3 piles in column	s3pcca01	2.078	0.379	60
		s3pcca02	2.125	0.698	44
		s3pcca03	3.710	0.343	56
		s3pcca04	3.664	0.673	44
Cyclic Symmetric		s3pccs01	0	0.367	50
		s3pccs02	2.086	0.384	158
		s3pccs03	2.130	0.769	77
		s3pccs04	3.692	0.378	156
		s3pccs05	3.771	0.777	83
Cyclic Asymmetric	3 piles in row	s3prca01	2.102	0.384	59
		s3prca02	2.124	0.688	45
		s3prca03	3.631	0.350	56
		s3prca04	3.664	0.661	41
Cyclic Symmetric		s3prcs01	0	0.383	50
		s3prcs02	2.115	0.397	49
		s3prcs03	2.097	0.767	84
		s3prcs04	3.739	0.392	50
		s3prcs05	3.738	0.762	49
Cyclic Asymmetric	9 piles	s9pca01	2.056	0.340	59
		s9pca02	2.075	0.691	45
		s9pca03	3.618	0.352	57
		s9pca04	3.664	0.661	42
Cyclic Symmetric		s9pcs01	0	0.383	50
		s9pcs02	2.096	0.398	59
		s9pcs03	2.038	0.773	80
		s9pcs04	3.673	0.380	58
		s9pcs05	3.676	0.781	93

Table 4-4: Magnitude of the maximum vertical and horizontal loads and number of cycles in each test.

4.6.2.1 Horizontal asymmetric cyclic tests

The imposed load paths of the cyclic asymmetric tests for each foundation configuration are reported in figure 4-15a-d. The corresponding load-displacement curves are plotted in figure 4-16a-d. It is worth noting that the amplitude of the horizontal load for all the tests is quiet far from the theoretical limit value, analytically determined by means of equation 4.1. Due to the laboratory errors in the unloading part of the tests, in some cases it is not possible to kept the horizontal load at the zero value, but this error is small enough to be ignored and it does not have any effect on the final results.

The graphs display the typical shape of the soil-foundation interaction under cyclic asymmetric load, which means the irreversible displacement will be accumulated but this accumulation rate will decrease after applying some cycles, and sort of stabilization in the horizontal displacement will take place.

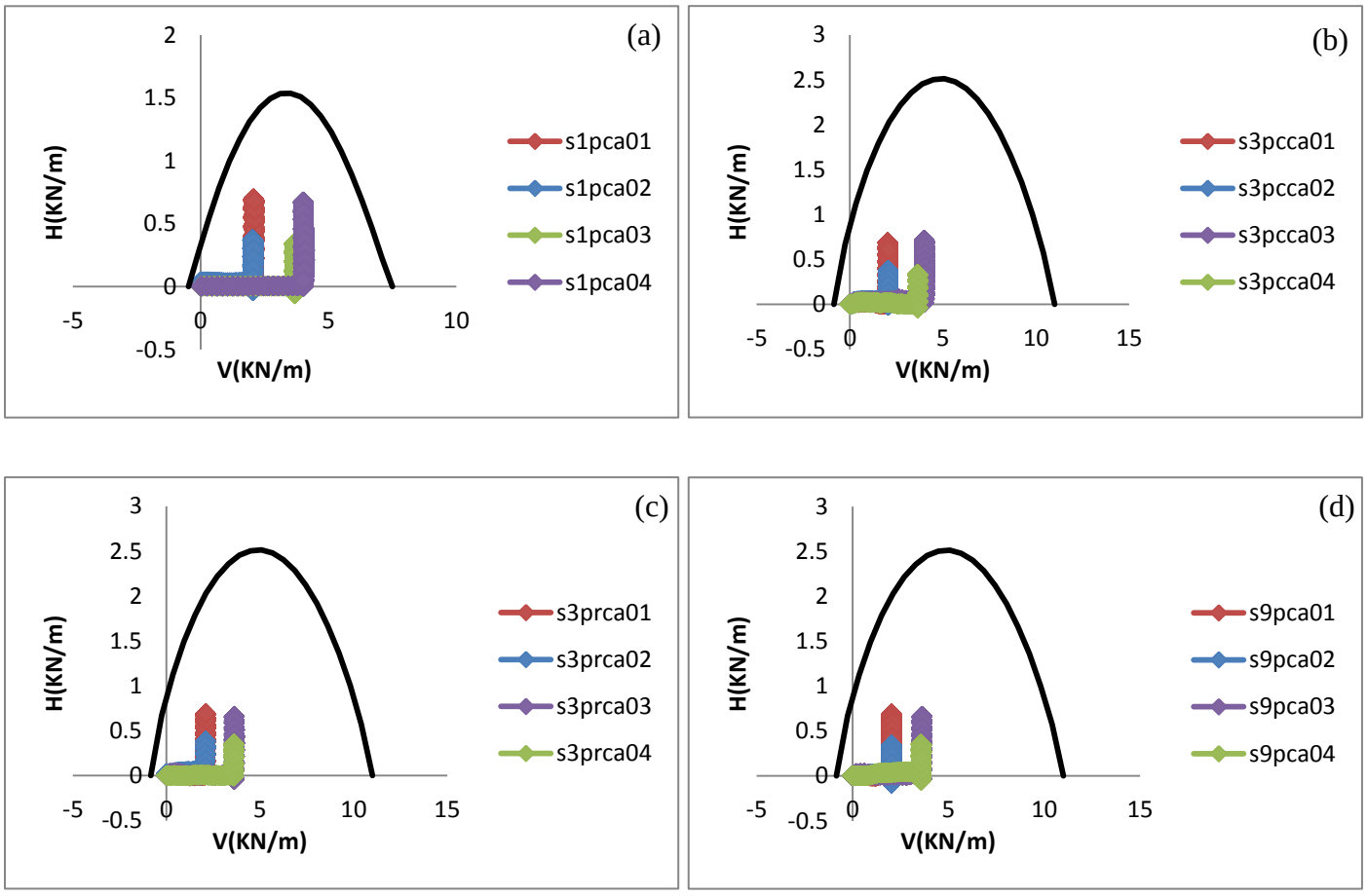

Figure 4-15: Imposed cyclic load paths for cyclic asymmetric tests; black line represents the interaction domain (a) 1 pile, (b) 3piles in a column, (c) 3 piles in a row, (d) 9 piles.

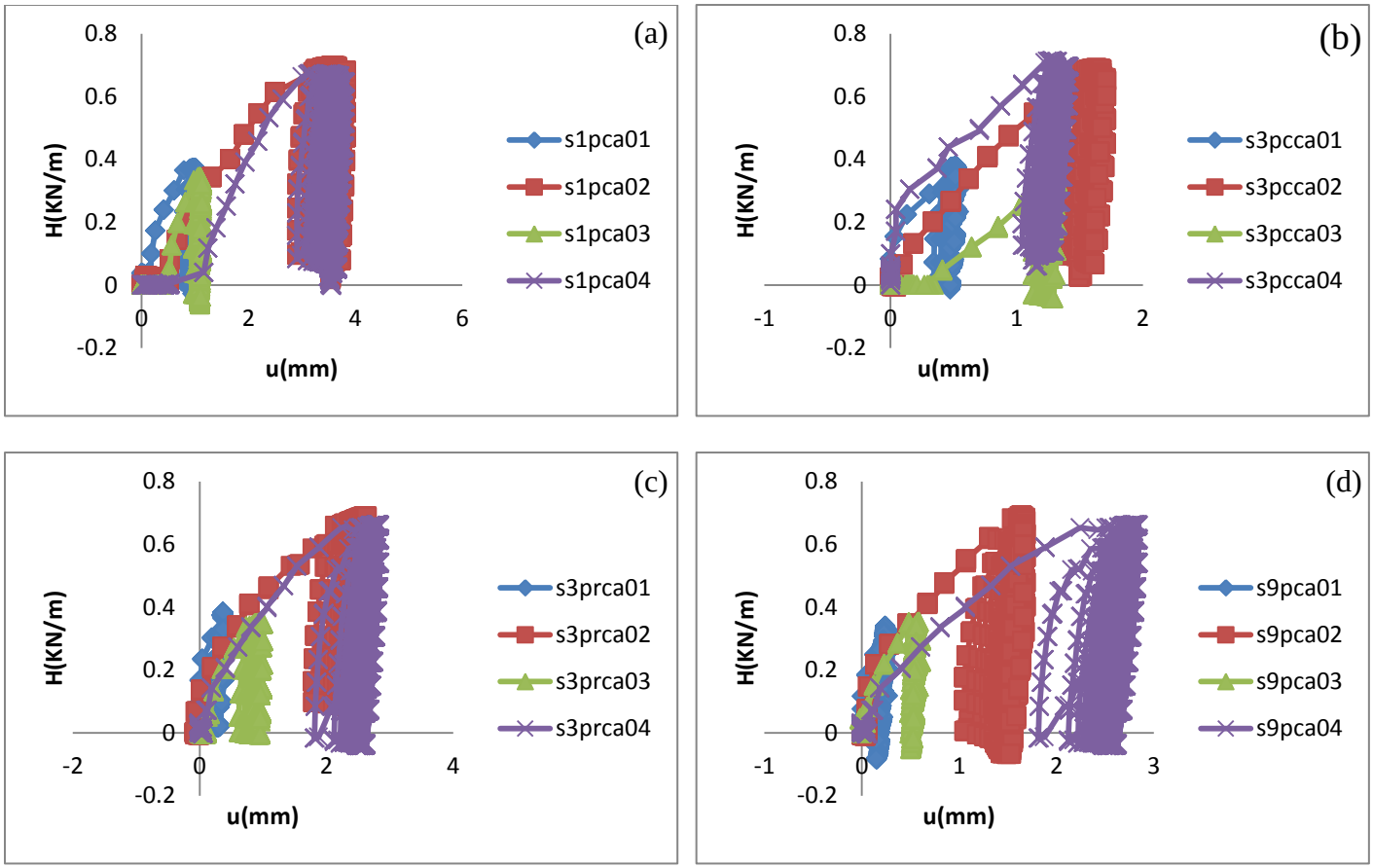

Figure 4-16: Load-displacement curves of the cyclic phase of the cyclic asymmetric tests (a) 1 pile, (b) 3 piles in a column, (c) 3 piles in a row, (d) 9 piles.

As it is previously mentioned by computing for each cycle of the tests the average stiffness, K_H, the dissipated energy, E_d, and the net vertical settlement (defined as the difference between v_{max} and the settlement corresponding with the first cycle v_1), related trends can be defined as a function of number of cycles. It must be noted that by considering the cyclic part of the load-displacement curves, some kind of drifting is visible due to the some machinery errors, but this is not affected on the value of stiffness and dissipated energy. The values of all the interpolating parameters defined in equations 4.5, 4.6 and 4.7 are reported in table 4-5 and figures 4-17a-d, 4-18a-d, 4-19a-d.

The kinematic of the system can be described by plotting the net cumulated horizontal displacement (u_{max}-u_1) versus the net cumulated vertical settlement (v_{max}-v_1) as shown in figures 4-20a-d. So in this case a constant pseudo-dilatancy can be defined with reference only to the cyclic phase based on equation 4.2 and the interpolating parameter is reported in table 4-5.

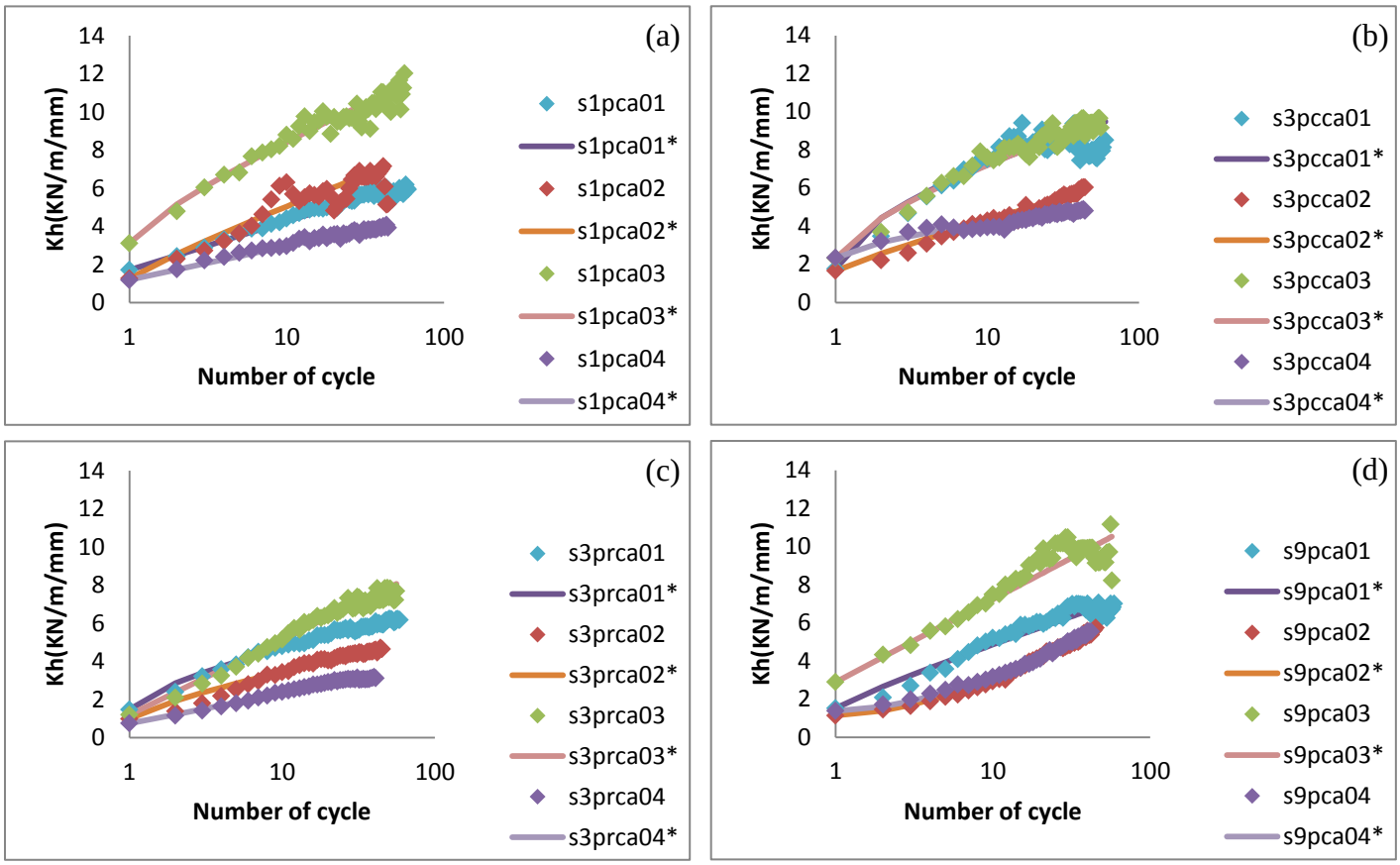

Figure 4-17: Evolution of the average stiffness; (a) 1 pile, (b) 3 piles in a column, (c) 3 piles in a row, (d) 9 piles.

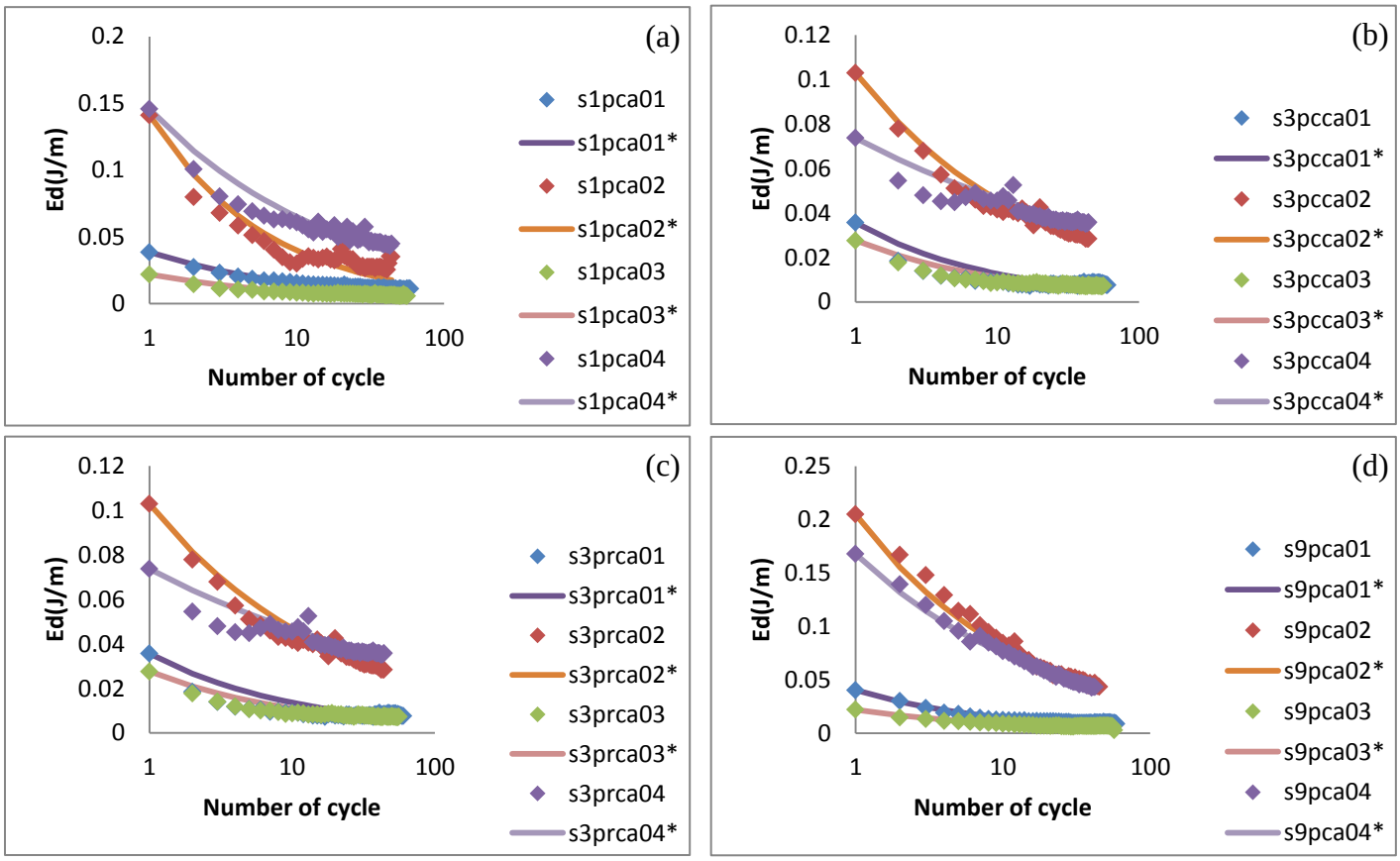

Figure 4-18: Evolution of the damped energy during cycling; (a) 1 pile, (b) 3 piles in a column, (c) 3 piles in a row, (d) 9 piles.

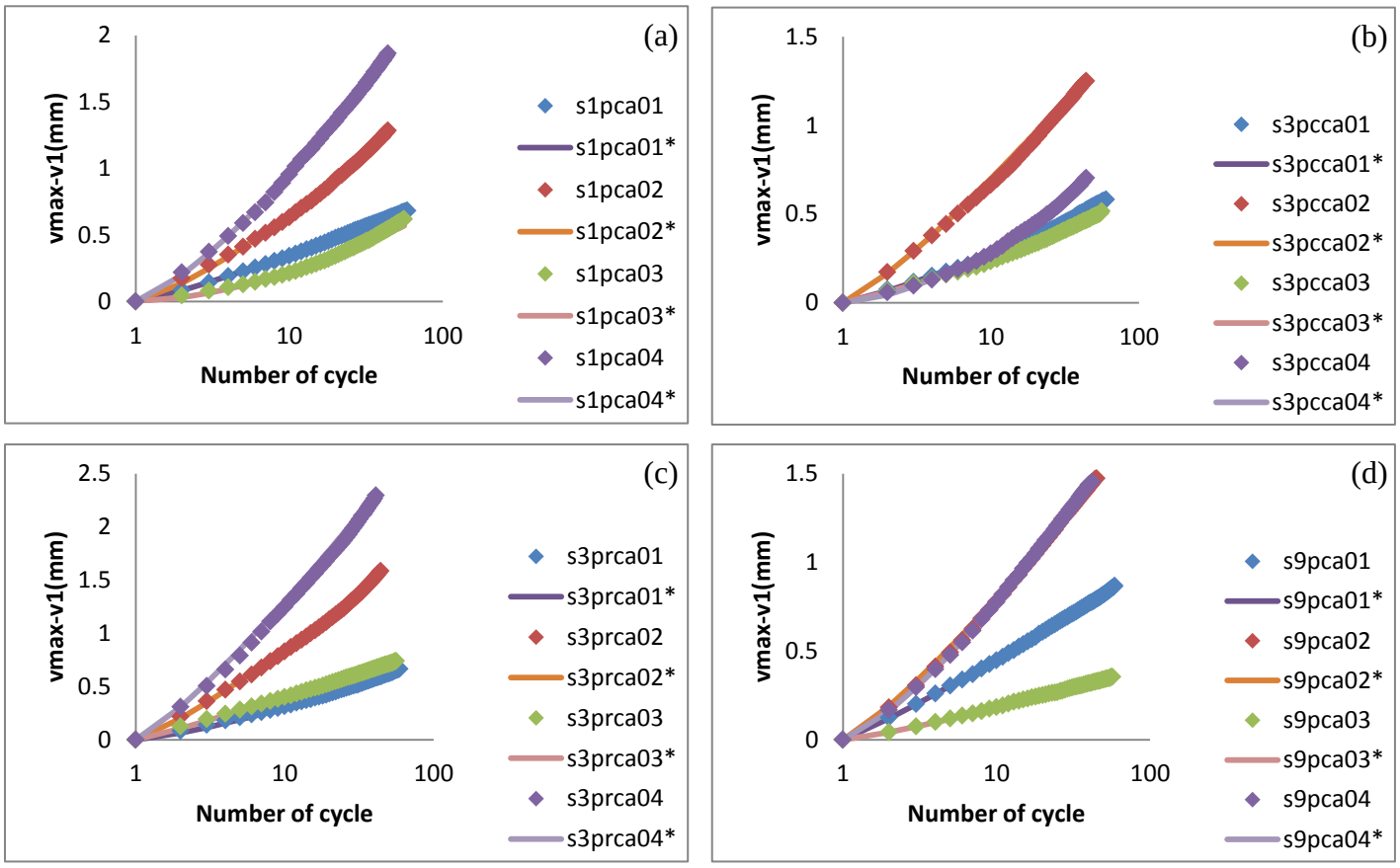

Figure 4-19: Evolution of the net cumulated vertical displacement during cycling; (a) 1 pile, (b) 3 piles in a column, (c) 3 piles in a row, (d) 9 piles.

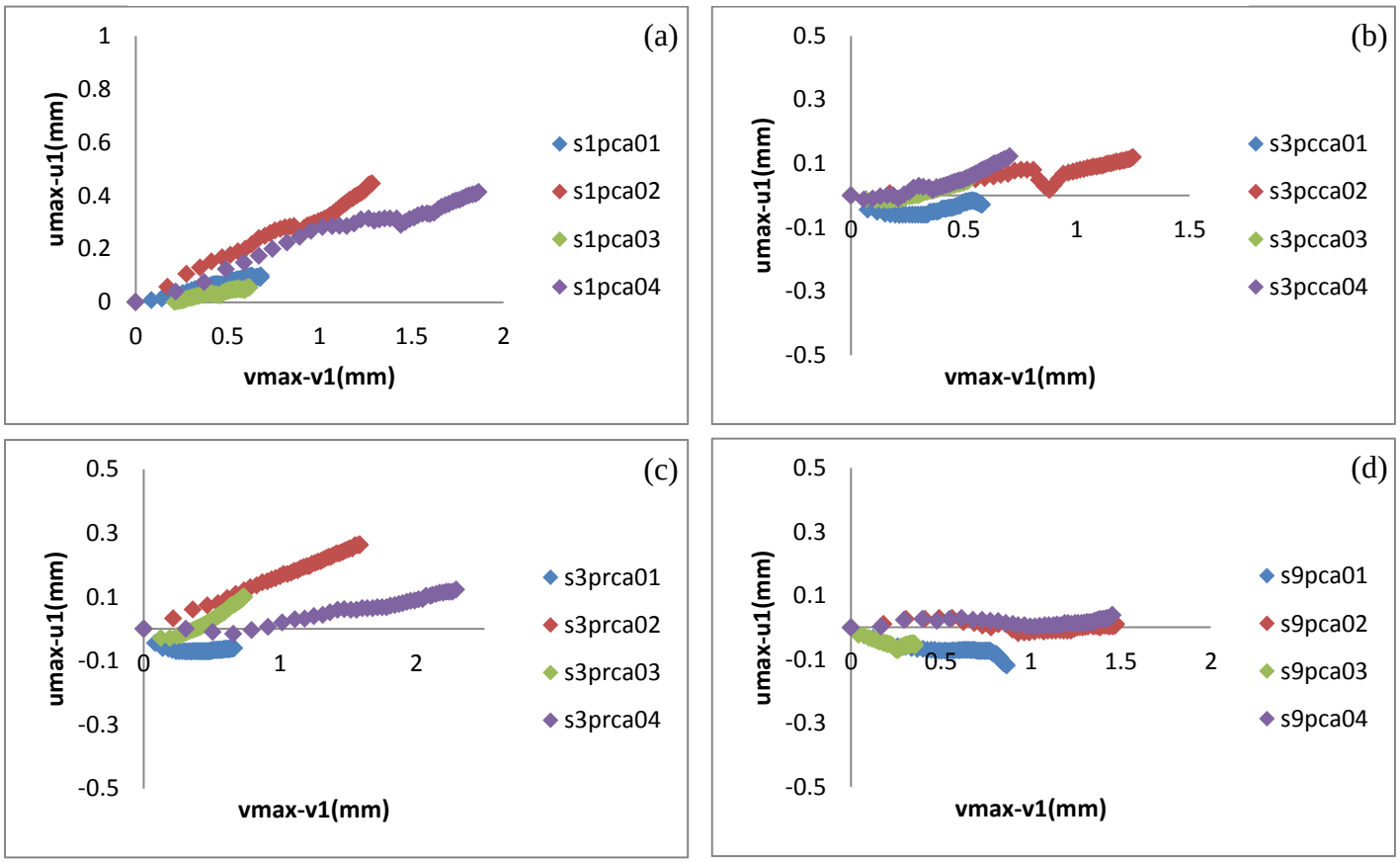

Figure 4-20: Evolution of the net cumulated horizontal displacement with respect to net cumulated vertical settlement; (a) 1 pile, (b) 3 piles in a column, (c) 3 piles in a row, (d) 9 piles.

load	Test Type	KH,1 [MPa]	α	n	$E_{d,1}$ [J/m]	b	βcyc	m	ψcyc
V170,H130	s1pca01	1.705	1.500	0.900	0.038	0.400	0.004	1.200	6.810
	s3pcca01	1.764	3.100	0.900	0.036	0.300	0.003	1.200	9.387
	s3prca01	1.464	2.200	0.900	0.036	0.400	0.003	1.300	9.236
	s9pca01	1.518	2.200	1.100	0.040	0.450	0.005	1.100	7.286
V170,H140	s1pca02	1.259	3.000	0.900	0.141	0.550	0.007	1.300	2.888
	s3pcca02	1.661	1.600	0.100	0.103	0.350	0.007	1.200	10.504
	s3prca02	0.985	2.500	0.900	0.103	0.5	0.009	1.200	6.004
	s9pca02	1.138	1.700	1.700	0.205	0.350	0.008	1.200	30.828
V210,H130	s1pca03	3.114	1.700	0.900	0.022	0.400	0.002	1.700	11.273
	s3pcca03	2.521	2.100	0.900	0.028	0.300	0.003	1.200	12.023
	s3prca03	1.191	3.300	1.000	0.028	0.400	0.004	1.100	7.390
	s9pca03	2.892	1.500	1.500	0.022	0.450	0.002	1.200	5.000
V220,H140	s1pca04	1.183	1.500	1.000	0.146	0.550	0.010	1.300	4.516
	s3pcca04	2.338	0.800	0.900	0.074	0.350	0.003	1.600	5.770
	s3prca04	0.744	2.100	1.000	0.074	0.500	0.013	1.200	18.803
	s9pca04	1.380	1.300	1.700	0.168	0.350	0.008	1.300	38.237

Table 4-5: Values of parameters for horizontal asymmetric cyclic tests for different foundation configuration.

- **Shallow foundation with 1 pile:**

In the figure 4-17(a) the average stiffness is shown, value of the *n* for the tests is equal to 1 that it shows these results are not related to the number of the cycles but completely affected by the horizontal loading amplitude. Generally the test with the lower amplitude of horizontal load has a higher stiffness (table 4-5). Figure 4-18(a) shows not only lower value for $E_{d,1}$ will be captured for the tests s1pca01 and s1pca03 with less horizontal loading amplitude, also minor changing in the dissipated energy will be captured for the tests with lower horizontal load and the value of b is equal to 0.4 (for these two mentioned tests) instead 0.55 for the tests with higher horizontal load (s1pca02 and s1pca04). The vertical displacement also shows that is more affected by the horizontal load and it is much higher for tests s1pca02 and s1pca04 which their horizontal load is higher than the other two tests (Figure 4-19a).

Figure 4-20(a) shows the quasi linear trend of the net cumulated horizontal displacement versus vertical displacement, so for each test a constant pseudo-dilatancy can be defined, and the value effected not only by the horizontal load, but also by the vertical load, which means the ψ_{cyc} will increase by increasing the vertical loading amplitude and on the other hand it will decrease by increasing the horizontal load (table 4-5).

- **Shallow foundation with 3 piles in a row**

In the figure 4-17(c) the stiffness is shown versus the number of cycles, here also the value of the parameter *n* for the tests is equal to 1, so it shows that this result is not affected by the number of the cycles. Here the results not only affected by the horizontal loading amplitude, but even affected by the vertical loading amplitude. While the tests with the lower amplitude of horizontal loading have a higher stiffness in total, on the other hand the tests with the same horizontal loading amplitude has a higher stiffness when the vertical load is lower. Figure 4-18(c) as well as previous part shows that less changing in the dissipated energy will be captured for the tests with lower horizontal load compare to the tests with higher horizontal loads (the value of b is equal to 0.4 for tests s3prca01 and s3prca03, instead b = 0.5 for the tests with higher horizontal load). The vertical displacement is much higher for the tests s3prca02 and s3prca04 with the higher horizontal load higher than the other two tests (Figure 4-19c). Also in the case of a constant pseudo-dilatancy, the same behavior of the shallow foundation with 1 pile can be observed (figure 4-20c and table 4-5).

- **Shallow foundation with 3 piles in a column**

It this case similar trend can be seen in compare to the previous case. By considering the figures 4-16b and 4-16c it can be captured that the horizontal displacement (u) of the foundation with 3 piles in column is obviously less than the horizontal displacement in the case of foundation with 3 piles in row and it shows that position of piles is a dominant factor on the behavior of the foundation.

- **Shallow foundation with 9 piles**

In the figure 4-17(d) the stiffness is shown, here despite of the other configurations under cyclic asymmetric loading, the number of cycles has an effect on the average stiffness and this effect will be higher for the tests with the higher horizontal load. The value of n is equal to 1.7 for the tests with higher amplitude of horizontal loading (tests s9pca02 and s9pca04) and this will be reduced to 1.5 for the test s9pca03 and 1.1 for the test s9pca01 (table 4-5). In total it can be concluded that in this configuration also the system is stiffer when the smaller amplitude of the horizontal load will be applied. Figure 4-18(d) like the other foundation configurations shows that the less changing in the dissipated energy will be captured for the tests with lower horizontal load and the value of b is equal to 0.45 (for tests s9pca01 and s9pca03) instead 0.35 for the tests with higher horizontal load (s9pca02 and s9pca04). In this case also, higher vertical displacement can be captured for the tests with higher horizontal loading tests (Figure 4-20d). it must be mentioned that in this test there was a laboratory error but it had a negligible effect on results.

4.6.2.2 Horizontal symmetric cyclic tests

Five horizontal symmetric cyclic tests were performed for each foundation configuration, whose generalised stress paths are plotted in figure 4-21a-d, and the corresponding load displacement curve in figure 4-22 a-d. It is worth noting that the amplitude of the horizontal load for all the tests is quiet far from the theoretical limit value, analytically determined by means of equation 4.1. The shape of the cycles is quite regular and, differently from what it is usually observed in asymmetric cyclic tests, they do not show any S-shaped behaviour, witnessing that no reduction in stiffness takes place when the loading increment changes in sign. The shape of the graphs and also the corresponding calculation for the average horizontal stiffness K_H and the dissipated energy E_d as well as the horizontal displacement for each case, confirmed also the increasing in the stiffness, reduction in dissipated energy value and stabilization of the accumulated rate of irreversible displacement.

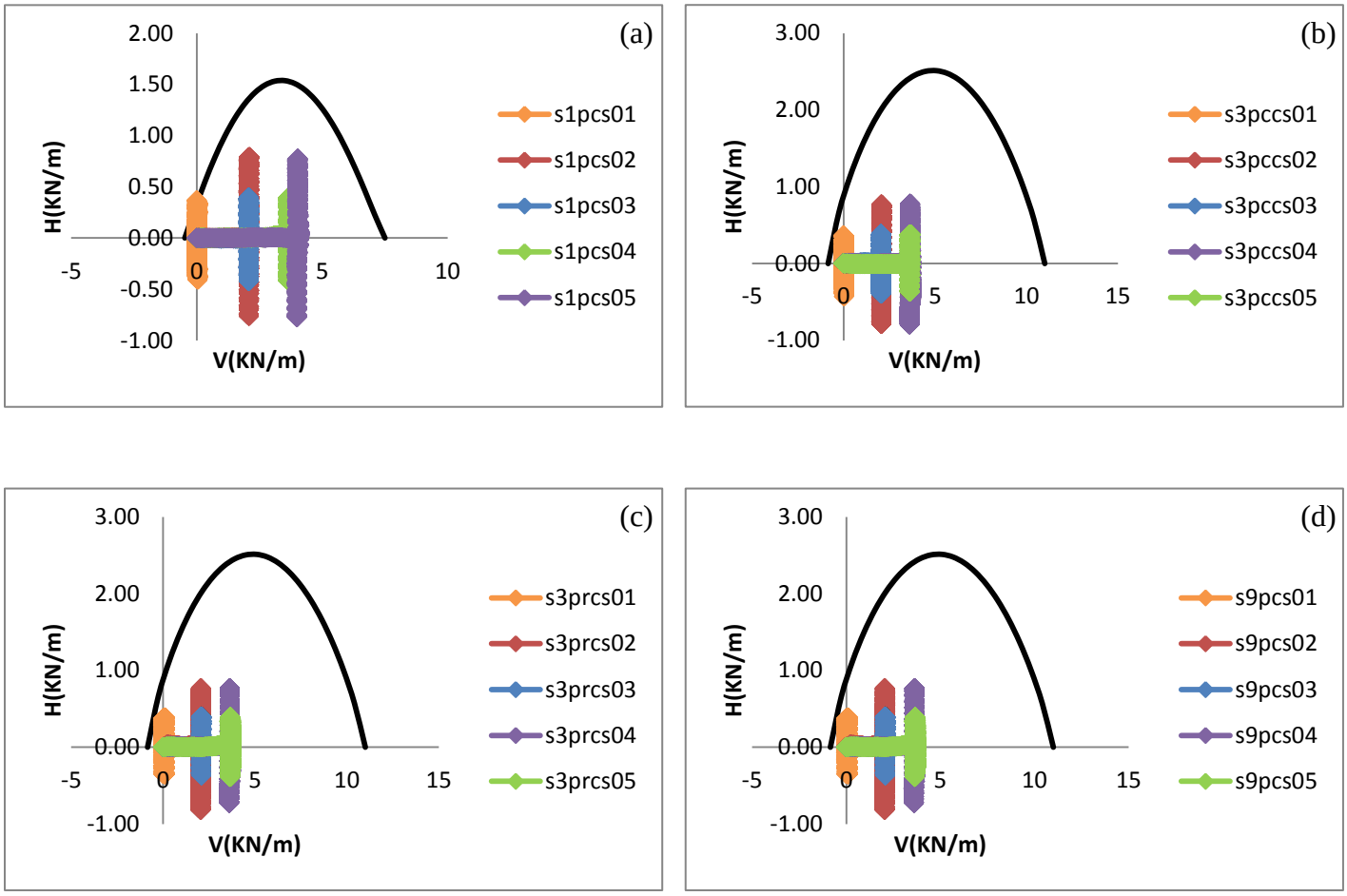

Figure 4-21: Imposed cyclic load paths for cyclic symmetric tests, black line represents the interaction domain; (a) 1 pile, (b) 3piles in a column (c), 3 piles in a row, (d) 9 piles.

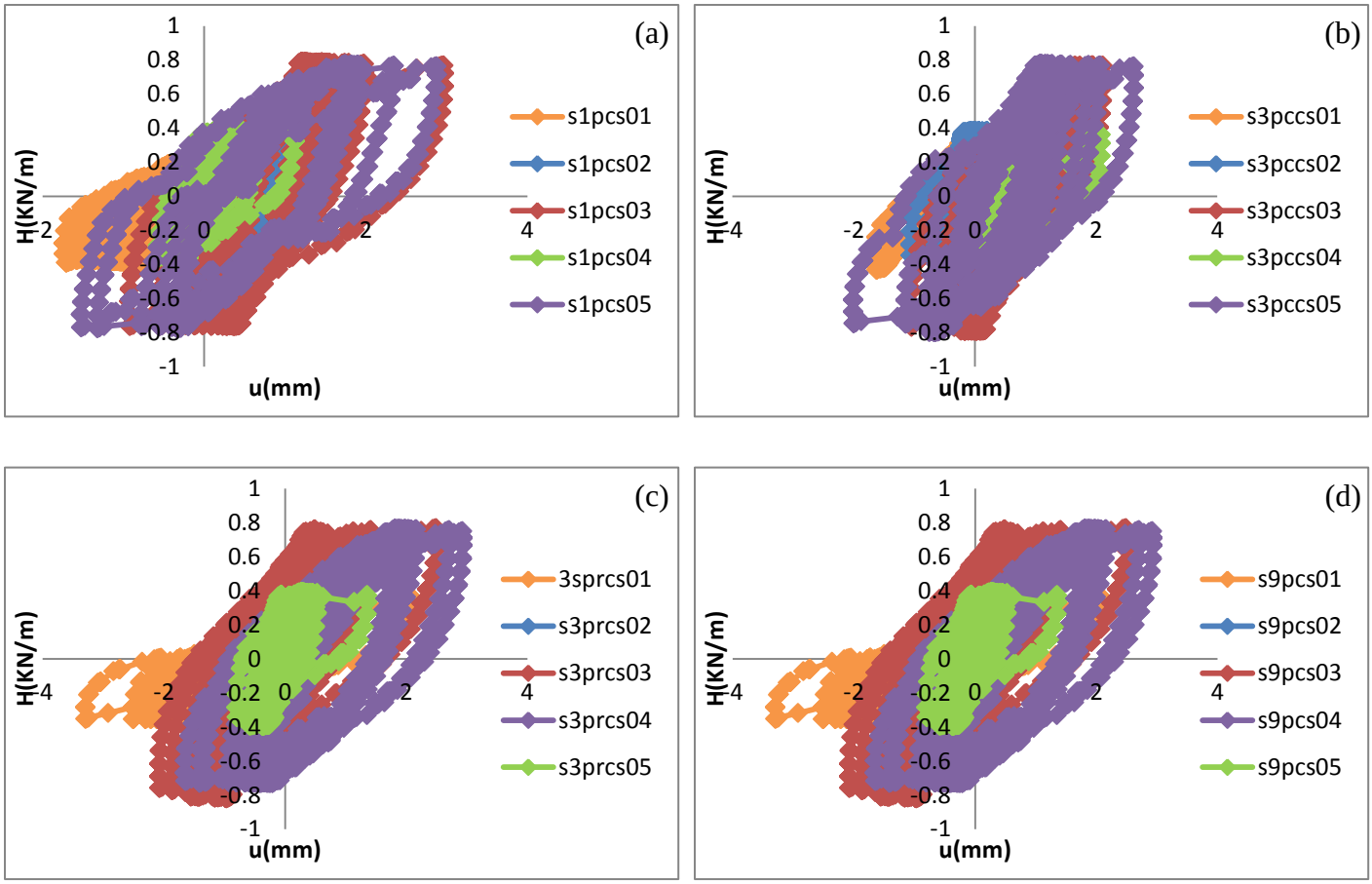

Figure 4-22: Load-displacement curves of the cyclic phase of the cyclic asymmetric tests; (a) 1 pile, (b) 3 piles in a column, (c) 3 piles in a row, (d) 9 piles.

An interesting point that can be captured from the cyclic part of the tests is the gap defined in figure 4-22a-d. This gap is caused by separation and re-attachment of the pile from the soil (Brown 2001, Takahashi et all 2008). This phenomenon is very well known in the cohesive materials and it is defined as a zero stiffness area but in the granular materials is due to a volume of reduced stiffness zone around the pile lateral surface. As it is reported by Takahashi et al. (2008) for dry sand the gap formed between the pile and adjacent soil in loading and unloading phase is filled with the reduced stiffness sand, so the normal stress acting on the pile cap did not reach zero when unloaded and shear stress was positive and kept more or less at a constant value equal to the beginning of unloading phase. In a simple manner this effect can describe the decreasing in the passive resistance of the soil, so the gap around the pile can be formed (Figure 4-23a, b). In this kind of test this may occur because of the kind of vertical load which is equal to zero, so it makes the minimum contact between the foundation and the soil, but in the other kinds of cyclic loading with deep foundation and deep foundation plus piles, which the vertical loading was applied, the presence of the plate has an important effect, so the gap effect will not happen.

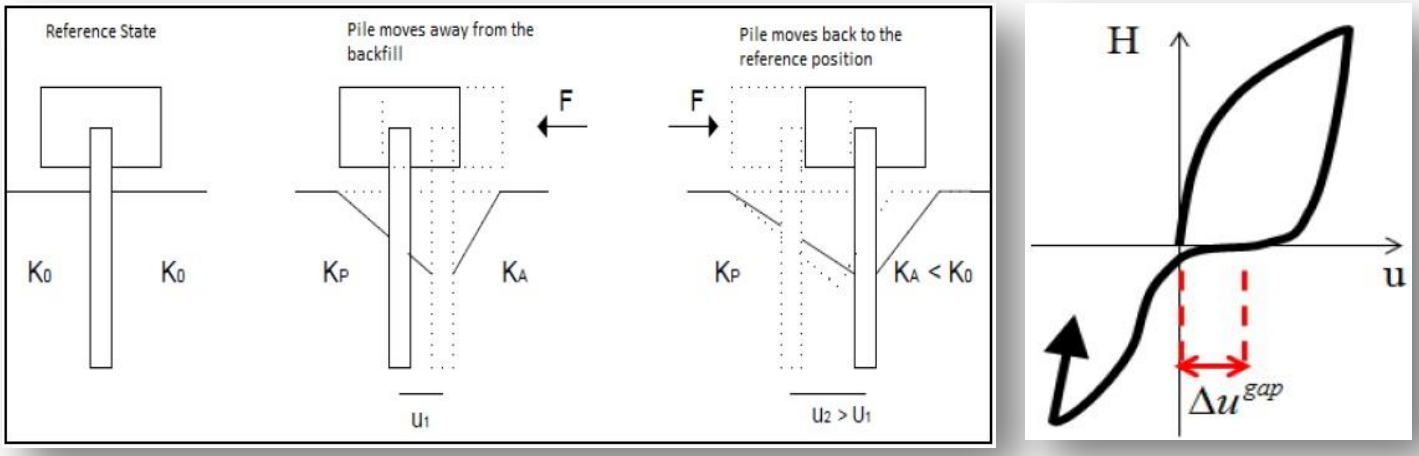

(a) (b)

Figure 4-23: Gap effect.

- **Shallow foundation with 1 pile:**

The shape of the graphs and also the corresponding calculation for the average horizontal stiffness K_H (Figure 4-24a) and the dissipated energy E_d (Figure 4-25a) as well as the vertical displacement (Figure 4-26a) for each case, confirmed increasing in the stiffness, reduction in dissipated energy value and stabilization of the accumulated rate of irreversible displacement which already discussed. The number of cycle in this kind of loading path despite of the cyclic asymmetric test is affected on the results of the horizontal stiffness (K_H), and this effect is less evident for the test with lower horizontal loading amplitude. For the tests s1pcs02 and s1pcs04 with n = 1.3 and it is lower compare to the tests with higher horizontal load with n = 1.5. The tests with lower horizontal loading amplitude (s1pcs02 and s1pcs04) as already discussed in the cyclic asymmetric tests have higher stiffness compare to the test with higher horizontal amplitude (table 4-6). In this kind of loading path as well as the cyclic asymmetric part, the value of the dissipated energy for the test with higher horizontal amplitude loading is higher than the other two tests (which means $E_{d,1}$ = 2.45 J/m over $E_{d,1}$ = 0.54 J/m). It is worth nothing that the vertical settlement for the tests with higher amplitude of horizontal loading is higher than the other two tests (Figure 4-26a). In cyclic symmetric tests value of the stiffness for the first cycle ($K_{H,1}$) is lower than the value of the stiffness obtained for the cyclic asymmetric test.

- **Shallow foundation with 3 piles in a row**

The corresponding calculation for the average horizontal stiffness K_H is plotted in Figure 4-24c and the dissipated energy E_d is illustrated in Figure 4-25c. In this configuration also the number of cycle in this kind of loading path despite of the cyclic asymmetric test is affected on the results of the horizontal stiffness (K_H), since the value of *n* is bigger than 1.
This effect is lower for the test with lower horizontal loading amplitude which means, tests

s3prcs02 and s3prcs04 with n = 1.3 compare to the test with higher horizontal load, s3prcs03 and s3prcs04 (n = 1.6). On the other hand the tests with lower horizontal loading amplitude (s3prcs02 and s3prcs04) have higher stiffness compare to the test with higher horizontal amplitude (table 4-6). In this kind of loading path as well as the cyclic asymmetric part, the value of the dissipated energy for the test with higher horizontal amplitude loading is higher than the other two tests (which mean 2.86 J/m and 2.45 J/m over 0.58 J/m). It is worth nothing that the vertical settlement for the test s3prcs03 and s3prcs05 with higher amplitude of horizontal loading is higher comparing to the two other tests are higher (Figure 4-26b).
In cyclic symmetric test value of the stiffness for the first cycle ($K_{H,1}$) is lower than the value of the stiffness obtained for the cyclic asymmetric test.

- **Shallow foundation with 3 piles in a column**

It this case similar trend can be seen in compare to the previous case. By considering the figures 4-22b and 4-22c it can be captured that the horizontal displacement (u) of the foundation with 3 piles in column is more or less equal to the horizontal displacement in the case of foundation with 3 piles in row.

- **Shallow foundation with 9 piles**

The corresponding calculation for the average horizontal stiffness K_H is plotted in Figure 4-24d and the dissipated energy E_{dH} is in Figure 4-25d. In this configuration as well as the other configurations with shallow foundation plus piles, the number of cycle in contrary of the cyclic asymmetric tests is affected on the results of the horizontal stiffness (K_H), and the value of the *n* is bigger than 1. Here also this effect is less effective for the test with lower horizontal load amplitude which means, tests s9pcs02 and s9pcs04 with n = 1 and 1.2 respectively compare to the tests with higher horizontal load, s9pcs03 and s9pcs05 (n = 1.5). On the other hand the tests with lower horizontal loading amplitude as already discussed so far, has higher stiffness compare to the test with higher horizontal amplitude (table 4-6). In this kind of loading path, same as the cyclic asymmetric loading path, the value of the dissipated energy for the test with higher horizontal amplitude loading is higher than the other two tests (which mean 2.14 J/m over 0.45 J/m). It is worth nothing that the vertical settlement for the tests with higher amplitude of horizontal loading is higher than the two other tests (Figure 4-26d). In cyclic symmetric test value of the stiffness for the first cycle ($K_{H,1}$) is much lower than the value of the stiffness obtained for the cyclic asymmetric test.

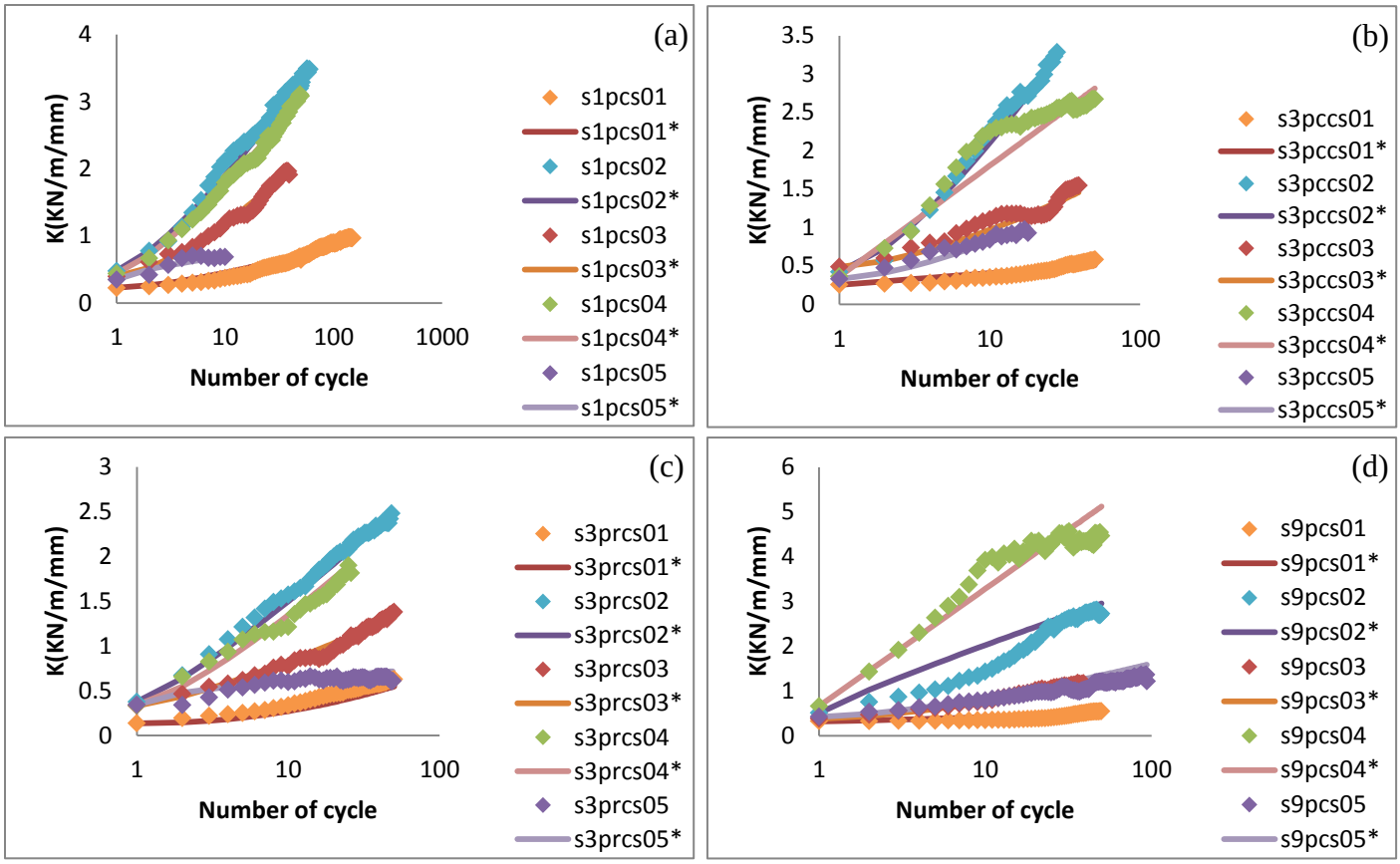

Figure 4-24: Evolution of the average stiffness; (a) 1 pile, (b) 3 piles in a column, (c) 3 piles in a row, (d) 9 piles.

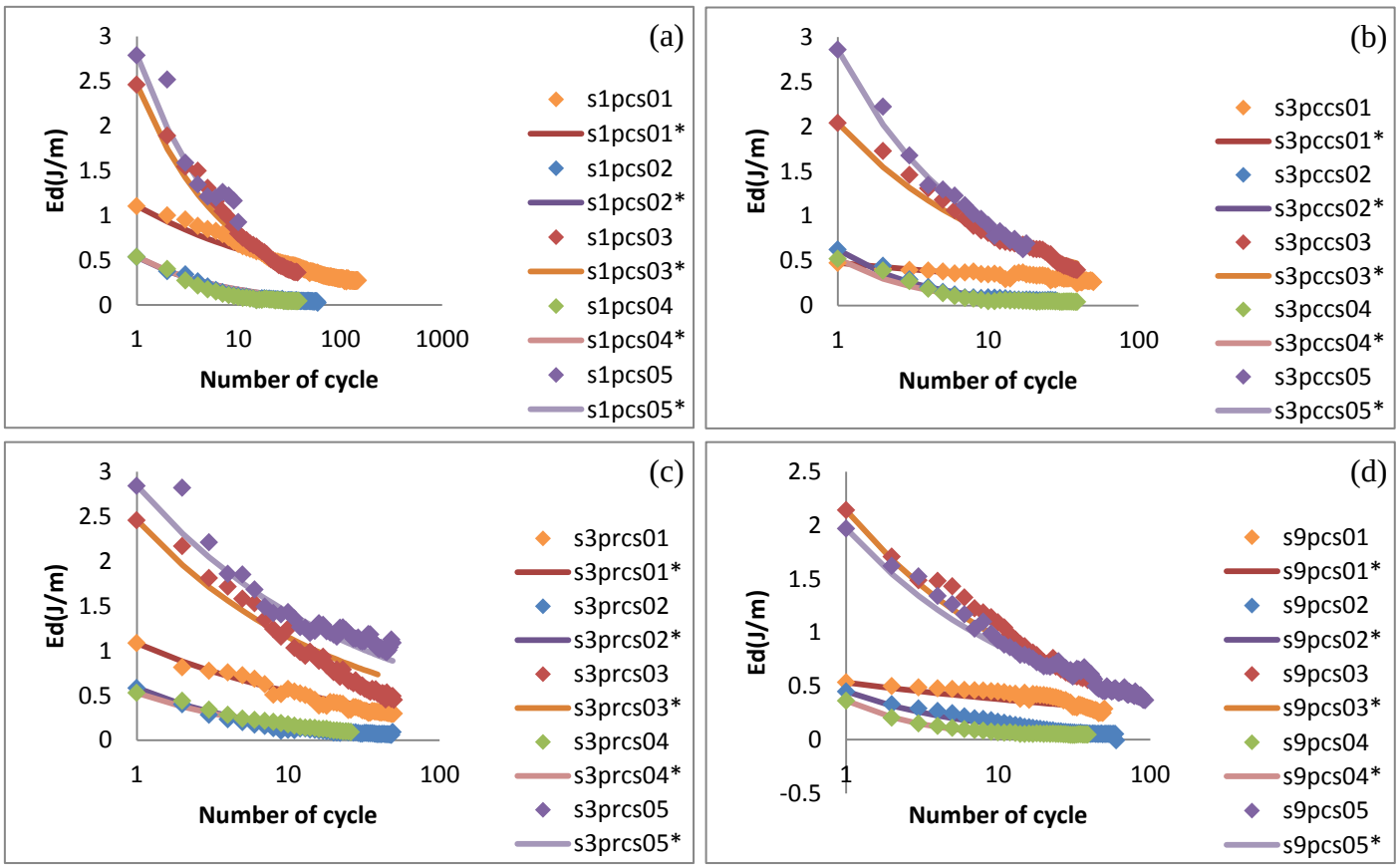

Figure 4-25: Evolution of the damped energy during cycling; (a) 1 pile, (b) 3 piles in a column, (c) 3 piles in a row, (d) 9 piles.

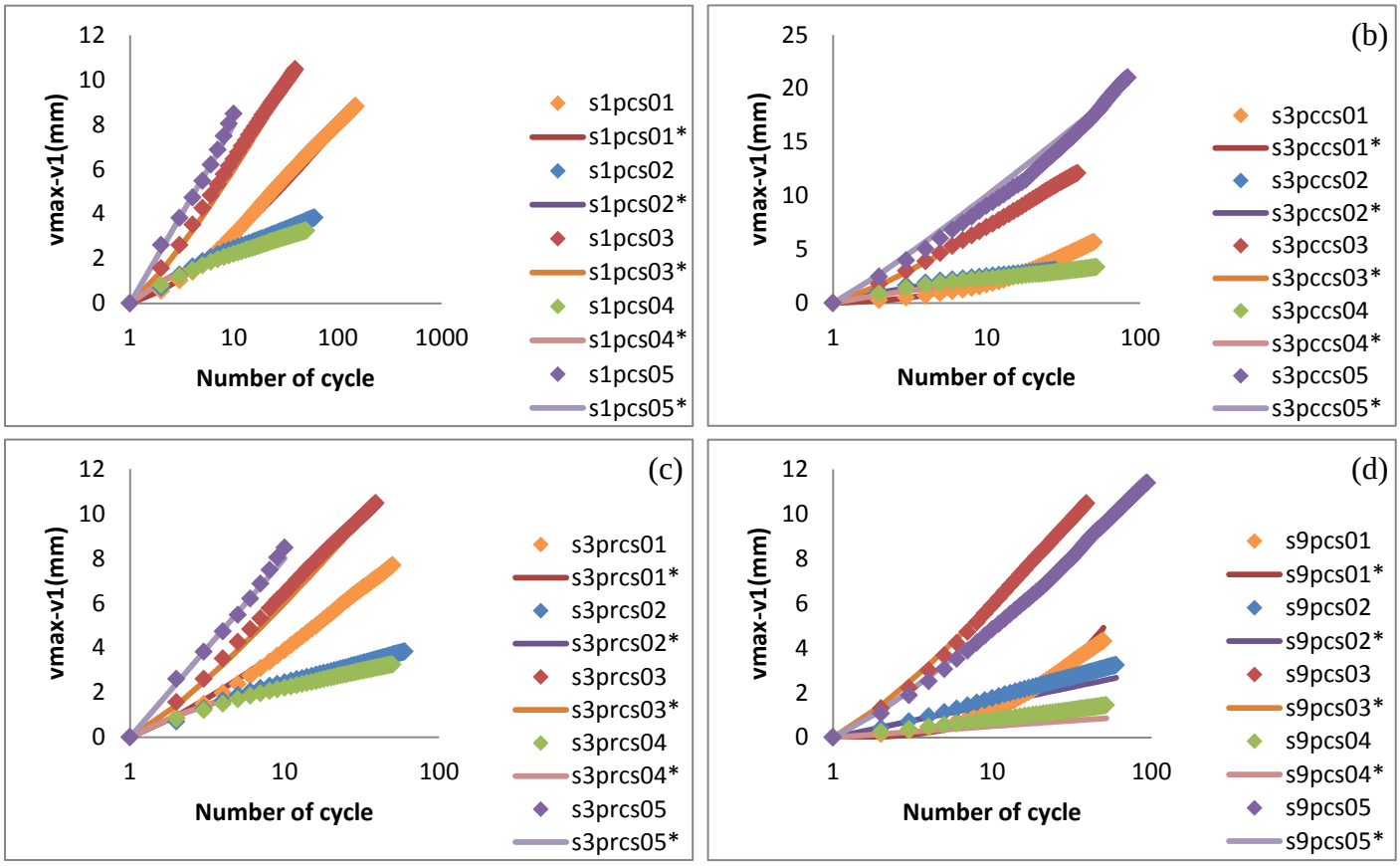

Figure 4-26: Evolution of the net cumulated vertical displacement during cycling; (a) 1 pile, (b) 3 piles in a column, (c) 3 piles in a row, (d) 9 piles.

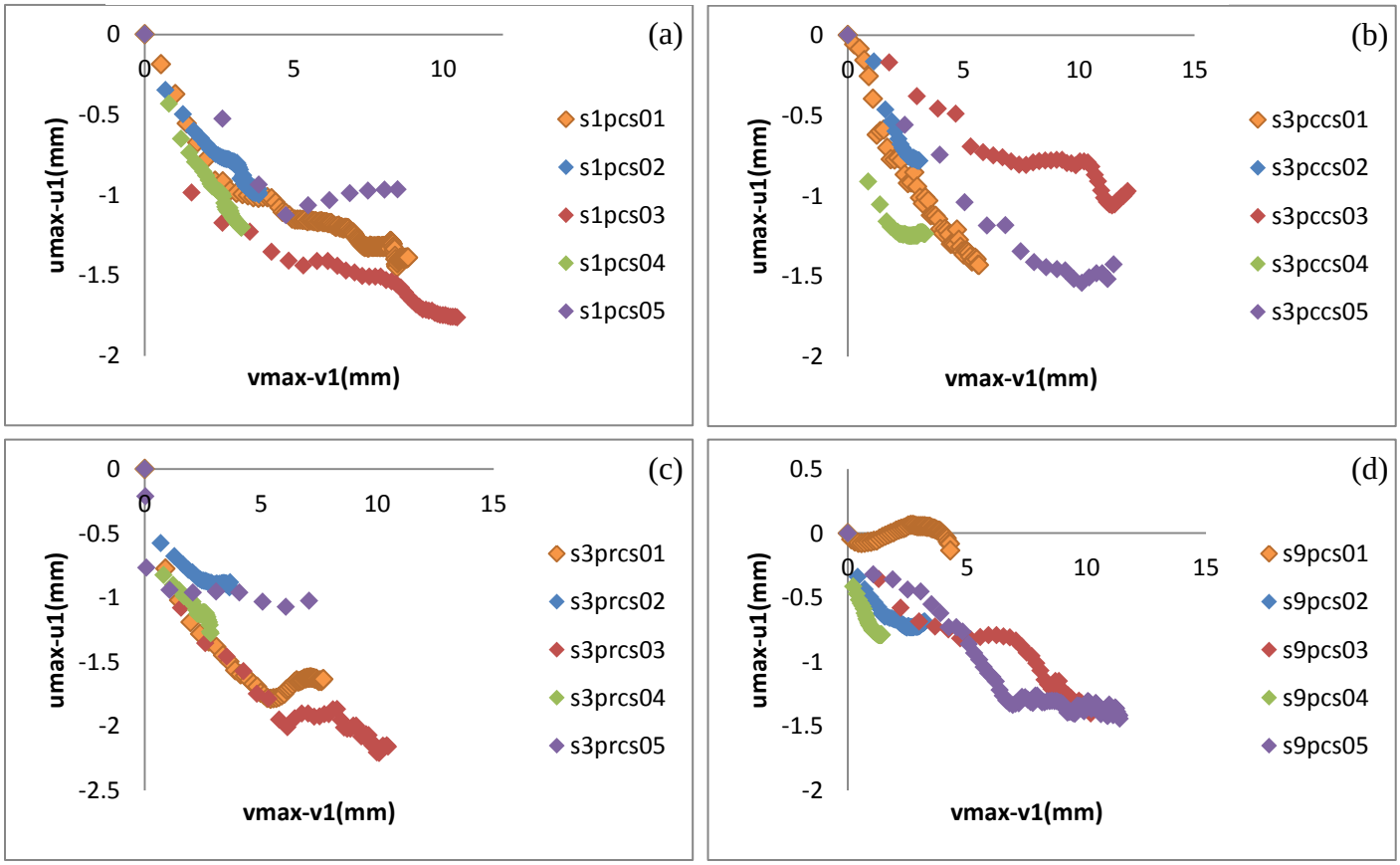

Figure 4-27: Evolution of the net cumulated horizontal displacement with respect to net cumulated vertical settlement; (a) 1 pile, (b) 3 piles in a column, (c) 3 piles in a row, (d) 9 piles.

load	Test Type	KH,1 [MPa]	α	n	$E_{d,1}$ [J/m]	b	βcyc	m	ψcyc
V0,H130	s1pcs01	0.225	1.000	1.500	1.103	0.250	0.030	1.400	6.088
	s3pccs01	0.253	0.600	1.000	0.476	0.150	0.020	2.000	3.969
	s3prca01	0.135	1.000	2.100	1.082	0.300	0.040	1.200	4.300
	s3pcs01	0.318	0.300	1.200	0.534	0.150	0.010	3.000	31.896
V170,H130	s1pcs02	0.475	3.000	1.300	0.533	0.500	0.025	0.800	3.840
	s3pccs02	0.485	4.000	1.400	0.623	0.500	0.025	0.800	3.972
	s3prcs02	0.375	3.000	1.300	0.582	0.550	0.025	0.800	4.152
	s9pcs02	0.506	3.000	1.000	0.449	0.500	0.015	1.000	4.405
V170,H140	s1pcs03	0.395	2.000	1.500	2.457	0.550	0.060	1.200	5.942
	s3pccs03	0.421	1.000	1.500	2.036	0.800	0.070	1.200	13.697
	s3prcs03	0.331	1.500	1.600	2.455	0.600	0.060	1.200	4.735
	s9pcs03	0.377	1.000	1.500	2.139	0.650	0.060	1.200	8.022
V210,H130	s1pcs04	0.439	3.000	1.300	0.536	0.500	0.025	0.800	2.697
	s3pccs04	0.361	4.000	1.400	0.623	0.500	0.020	0.800	3.301
	s3prcs04	0.336	3.000	1.300	0.576	0.500	0.025	0.800	2.544
	s9pcs04	0.656	4.000	1.200	0.364	0.500	0.005	1.000	1.726
V220,H140	s1pcs05	0.349	1.000	1.500	2.458	0.550	0.080	1.000	7.528
	s3pccs05	0.327	1.500	1.500	2.857	0.800	0.100	1.100	7.463
	s3prcs05	0.341	0.800	1.600	2.841	0.600	0.080	1.000	6.586
	s9pcs05	0.420	1.000	1.500	1.968	0.650	0.050	1.200	7.894

Table 4-6: Values of parameters for horizontal symmetric cyclic tests for different foundation configuration.

4.7 Summary

It was tried in this chapter to present all the results from monotonic and cyclic tests by considering shallow foundation with different configuration of piles and calculates different parameters that were the aim of these test best on different equations and compare the results in order to make the make the conclusion in the following chapter.

5

Conclusion

This thesis deals with soil-foundation interaction by considering shallow foundation with piles under cyclic and monotonic loads. The work is divided into two main parts, experimental tests and analytical interpolation.

The experimental part has been performed by means of the small scale experimental set up available at the geotechnical laboratory of the department of the civil and environmental engineering at Politecnico di Milano. The experimental works refereeing to shallow foundation with piles interacting with loose sand. Several types of monotonic and cyclic tests were performed. The tests have been performed with the aims of (i) defining the failure condition of the system (i.e. the interaction domain of the foundation in the generalized stress space V-H), (ii) describing the coupling between horizontal and vertical directions during monotonic tests, and (iii) analyzing the cyclic behavior of the system. The influence of the foundation geometry has been analyzed for these three points.

By studying initially about monotonic tests results, it is possible to analytically define the interaction domain in the V-H space. Nova-Montarsio macro-element formula has been used for the case of shallow foundation, but this formula has been modified for the case of shallow foundation with piles.

Since different interaction mechanism takes place for different loading direction, different stiffness and limit values for the load-displacement curves as well as various size of failure locus for each type of foundation configuration were obtained. For example, by considering a vertical upward loading path, higher value of initial stiffness was observed with respect to the downward vertical loading. This is due to presence of the plate which is a dominant factor affecting the behavior of the system. Similar results are observed for the horizontal loading tests, since the position of the piles plays an important role. The limit value of the horizontal load for zero vertical loads is equal for the case with 3 piles in a column (piles in a side by side position in front of the horizontal load and without shallow foundation) and 9 piles (piles in a box arrangement and without shallow foundation). On the other hand, when the case with shallow foundation plus 9 piles were considered, the interaction of the piles and the plate is playing a significant role and the value of the maximum horizontal load increases

significantly and the behavior of the system becomes similar to that of a single block.

The coupling between vertical and horizontal direction is even evident by studying the kinematic of the system. It can be found that all the tests show a positive vertical settlement during the horizontal load. A sort of pseudo-dilatancy (ψ) for the soil-foundation system was defined as the ratio of the net cumulated horizontal displacement (u_{max}-u_1) versus the net cumulated vertical settlement (v_{max}-v_1).The values of ψ are almost constant during the horizontal loading phase and, as a consequence, ψ can be assumed to be mainly dependent on the current applied vertical load V. The ψ -V relationship shows an increasing trend, and it was interpolated by means of simple linear function. This increasing trend for the ψ -V relationship was observed for all types of foundations, except for the case with the shallow foundation plus 9 piles, which is working as a single block. For the cyclic asymmetric tests, the cyclic pseudo-dilatancy (ψ_{cyc}) for each test is different but in general conclusion for each foundation configuration, by increasing the horizontal load, this value will be decreased while it will be increased by increasing the amplitude of vertical loading. For symmetric tests, moreover, differently for what it was observed for asymmetric tests, the mentioned trends are opposite.

The point which is interesting to mention here is that the value of ψ_{cyc} will increase significantly, by increasing the number of piles compare to shallow foundation. It means that by imposing horizontal load, higher displacement in vertical direction in case of shallow foundation with piles would happen compare to the case with using only shallow foundation and it can be interpreted as a coupling effect. It may be due to using relatively loose sand, which may cause sort of soil compaction and also disturbance in large depth under the pile after applying cyclic horizontal loads.

After defining the interaction domain, a deeper investigation on the response of the system to several cyclic loading paths, combining vertical and horizontal loads, has been presented. The analysis of the cycles shows that a progressive accumulation of displacement in horizontal direction takes place. In case of cyclic symmetric tests, the shape of the cycles is quite regular but for the cyclic symmetric tests, the shape of the cycles illustrate sort of gap effect. This phenomenon in the granular materials is due to a reduced stiffness zone around the pile lateral surface.

The experimental results were interpreted in terms of the average stiffness and of the damped energy of each cycle, as well as in terms of the accumulation of permanent displacements during cycling. A clear increase in stiffness and decay in dissipated energy were observed after applying number of cycles. From practical point of view, simple interpolating formulas and simple parameters for the stiffness and the dissipated energy values as well as vertical displacement were proposed, and their dependence on the vertical and horizontal load and on the type of the test was discussed for the different type of foundation configuration. These

results show that for a foundation interacting with loose sand, the mechanical response of the system during cycling is highly affected by the direction of loading, and it is characterized by a remarkable decrease of the mechanical properties (i.e. the stiffness along the vertical direction) and a significant increase in settlement and damped energy, when the loading direction changes from purely vertical to inclined.

The response of the system is also greatly influenced by the type of the loading. Lower stiffness value, higher displacement and damped energy will be observed for the cyclic symmetric tests compare to the cyclic asymmetric tests. Even the influence of the number of cycles depends on the type of the loading, and it is lower for the case of cyclic asymmetric tests.

In general conclusion, the value of stiffness will decrease, while settlement and damped energy will increase, by increasing the amplitude of horizontal loading. Instead by increasing the amplitude of vertical loading, the value of stiffness will increase and this has a reverse effect on the values of the displacement and damped energy.

References

1. Al Tabbaa A., W. D. M. (1989). An experimental based 'bubble' model for clay. *NUMOG 3, Niagara Falls.*

2. Anagnostopoulos, C., & Georgiadis, M. (1993). Interaction of Axial and Lateral Pile Responses. *Journal of Geotechnical Engineering-Asce, 119*(4), 793-798.

3. Anastasopoulos, I., Gazetas, G., Loli, M., Apostolou, M., & Gerolymos, N. (2010). Soil failure can be used for seismic protection of structures. *Bulletin of Earthquake Engineering, 8*(2), 309-326.

4. Bellotti R., Jamiolkowski M, Lo Presti D.C.F. and. Neill D.A. (1996), "Anisotropy of Small Strain Stiffness in Ticino Sand", *Geotechnique* 46, No.1, pp. 115-131.

5. Brown, D. A., Morrison, C., & Reese, L. C. (1988). Lateral Load Behavior of Pile Group in Sand. *Journal of Geotechnical Engineering-Asce, 114*(11), 1261-1276.

6. Brown, D. A., Morrison, C., & Reese, L. C. (1988). Lateral Load Behavior of Pile Group in Sand. *Journal of Geotechnical Engineering-Asce, 114*(11), 1261-1276.

7. Brown, D. A., Reese, L. C., & Oneill, M. W. (1987). Cyclic Lateral Loading of a Large-Scale Pile Group. *Journal of Geotechnical Engineering-Asce, 113*(11), 1326-1343.

8. Butterfield, R. (1980). A simple analysis of the load capacity of rigid footing on granular materials. *Geotechnique,* 128 - 134.

9. Butterfield, R., & Gottardi, G. (1994). A Complete 3-Dimensional Failure Envelope for Shallow Footings on Sand. *Geotechnique, 44*(1), 181-184.

10. Calogni G., Savoldi A. (2000). Analisi Sperimentale del Comportamento Meccanico di Fondazioni Superficiali Poste su Sabbia Rinforzata Mediante Geosintetici. *(PhD thesis), Politecnico di Milano.*

11. Calvetti, F. (1997). Experimental and numerical analysis of a 2-D granular material. *Numerical Models in Geomechanics - Numog Vi*, 39-44.

12. Calvetti, F., & di Prisco, C. (2010). Discrete numerical investigation of the ratcheting phenomenon in granular materials. *Comptes Rendus Mecanique, 338*(10-11), 604-614. 1292-1299.

13. Capozza A., Generali, S., (1999), *"Mechanical behaviour of shallow foundations on loose sand under inclined cyclic loading ", in Italian,* Degree Thesis, Dipartimento di Ingegneria Strutturale, Milan University of Technology.

14. Chatzigogos, C. T., Figini, R., Pecker, A., & Salencon, J. (2011). A macroelement formulation for shallow foundations on cohesive and frictional soils. *International Journal for Numerical and Analytical Methods in Geomechanics, 35*(8), 902-931.

15. Chatzigogos, C. T., Pecker, A., & Salencon, J. (2009). Displacement-Based Design of Shallow Foundations with Macroelement. *Soils and Foundations, 49*(6), 853-869.

16. Chatzigogos, C. T., Pecker, A., & Salencon, J. (2009). Macroelement modeling of shallow foundations. *Soil Dynamics and Earthquake Engineering, 29*(5), 765-781.

17. Cremer, C., Pecker, A., & Davenne, L. (2001). Cyclic macro-element for soil-structure interaction: material and geometrical non-linearities. *International Journal for Numerical and Analytical Methods in Geomechanics, 25*(13), 1257-1284.

18. Cremer, C., Pecker, A., & Davenne, L. (2002). Modelling of nonlinear dynamic behavior of a shallow strip foundation with macro-element. *Journal of Earthquake Engineering, 6*(2), 175-211.

19. Di Prisco, C. (2012). Creep Versus Transient Loading Effects in Geotechnical Problems. Mechanical Behaviour of Soils under Environmentally Induced Cyclic Loads, 534, 227-261.

20. Di Prisco, C., Galli, A., & Vecchiotti, M. (2009). Cyclic and Dynamic Mechanical Behaviour of Shallow Foundations on Granular Deposits. Coupled Site and Soil-Structure Interaction Effects with Application to Seismic Risk Mitigation, 139-150.

21. Di Prisco, C., Montanelli, F., Caloni, G., & A., S. (2003). Shallow foundations on geo- reinforced sand layers: experimental results and theorical observations. Founsup International Symposium.

22. Di Prisco, C., Nova, R., & Sibilia, A. (2003). Shallow footing under cyclic loading: experimental and constitutive modelling. *In: Geotechnical analysis of seismic vulnerability of monuments and historical sites. M. Maugeri & R. Nova editors, Bologna, Patron editore.*

23. Di Prisco, C., & Pisano, F. (2011). Seismic response of rigid shallow footings. European Journal of Environmental and Civil Engineering, 15, 185-221. *Geoengineering, 4*(2), 109 - 122.

24. Figini, R., Paolucci, R., & Chatzigogos, C. T. (2012). A macro-element model for non-linear soil-shallow foundation-structure interaction under seismic loads: theoretical development and experimental validation on large scale tests. *Earthquake Engineering & Structural Dynamics, 41*(3), 475-493.

25. Gajan, S., & Kutter, B. L. (2009). Contact Interface Model for Shallow Foundations Subjected to Combined Cyclic Loading. *Journal of Geotechnical and Geoenvironmental Engineering, 135*(3), 407-419.

26. Gottardi, G., Houlsby, G. T., & Butterfield, R. (1999). Plastic response of circular footings on sand

under general planar loading. *Geotechnique, 49*(4), 453-469.

27. Grange, S., Kotronis, P., & Mazars, J. (2008). A macro-element for a shallow foundation to simulate Soil-Structure Interaction considering uplift. *Comptes Rendus Mecanique, 336*(11-12), 856-862.

28. Houlsby, G. T., Cassidy, M. J., & Einav, I. (2005). A generalised Winkler model for the behaviour of shallow foundations. *Geotechnique, 55*(6), 449-460.

29. Jamiolkowski, M., Lo Presti, D. C. F., Puci, I., Negro, P., Verzeletti, G., Molina, J. F., Morabito, P. (1999). Large scale geotechnical experiments on soil-foundation interaction. *Pre-Failure Deformation Characteristics of Geomaterials, Vol 1*, 749-757.

30. Karthigeyan, S., Ramakrishna, V. V. G. S. T., & Rajagopal, K. (2006). Influence of vertical load on the lateral response of piles in sand. *Computers and Geotechnics, 33*(2), 121- 131. Lanier, J., & Calvetti, F. (1997). Evolution of microstructure in granular materials: Experimental results. *Powders & Grains 97*, 275-278.

31. Leblanc, C., Houlsby, G. T., & Byrne, B. W. (2010). Response of stiff piles in sand to long- term cyclic lateral loading. *Geotechnique, 60*(2), 79-90.

32. Martin, C. M., & Houlsby, G. T. (2001). Combined loading of spudcan foundations on clay: numerical modelling. *Geotechnique, 51*(8), 687-699.

33. Montrasio, L., & Nova, R. (1997). Settlements of shallow foundations on sand: Geometrical effects. *Geotechnique, 47*(1), 49-60.

34. Nova, R., & Montrasio, L. (1991). Analysis of Settlements of Shallow Foundations on Sand. *Deformation of Soils and Displacements of Structures : X Ecsmfe, Vol 2*, 505-509.

35. Nova, R., & Montrasio, L. (1991). Settlements of Shallow Foundations on Sand. *Geotechnique, 41*(2), 243-256.

36. Paolucci, R., & Pecker, A. (1997). Soil inertia effects on the bearing capacity of rectangular foundations on cohesive soils. *Engineering Structures, 19*(8), 637-643.

37. Pecker, A., Chatzigogos, C. T., & Salencon, J. (2010). A Dynamic Macro-Element for Performance-Based Design of Foundations. *Advances in Performance-Based Earthquake Engineering, 13*, 103-112.

38. Pecker, R. P. a. A. (1997). Seismic bearing capacity of shallow strip foundations on dry soils. *soils and foundations, Japanese Geotechnical Society, 37*(3), 95 - 105.

39. Poulos, H. G. (2001). Piled raft foundations: design and applications. *Geotechnique, 51*(2), 95-113.

40. PWRI. (2005). Experimental study on the residual displacements of shallow foundations. *Public Work Research Institute, Technical Note*.

41. Reese, L. C., Isenhower, W. M., & Wang, S. T. (2006). Analysis of Pile Groups. *Analysis and Design of Shallow and Deep Foundations*, 503-536.

42. Reese, L. C., Isenhower, W. M., & Wang, S. T. (2006). Geotechnical Design of Shallow Foundations. *Analysis and Design of Shallow and Deep Foundations*, 235-269.

43. Remaud, D., Garnier, J., & Frank, R. (1998). Laterally loaded piles in dense sand: Group effects. *Centrifuge 98, Vol 1*, 533-538.

44. Salencon, J., & Pecker, A. (1995). Ultimate Bearing Capacity of Shallow Foundations under Inclined and Eccentric Loads .1. Purely Cohesive Soil. *European Journal of Mechanics a-Solids, 14*(3), 349-375.

45. Salencon, J., & Pecker, A. (1995). Ultimate Bearing Capacity of Shallow Foundations under Inclined and Eccentric Loads .2. Purely Cohesive Soil without Tensile-Strength. *European Journal of Mechanics a-Solids, 14*(3), 377-396. *Geotechnique, 29*(1), 47 -65.

46. Takahashi, A., Sugita, H., & Tanimoto, S. (2008). Mobilisation of Earth Pressure Acting on Pile Caps under Cyclic Loading. *Soils and Foundations, 48*(6), 741-754. *Environmentally Induced Cyclic Loads, 534*, 137-226.

47. Vesic A. (1973), "Analysis of ultimate loads of shallow foundations". *Journ. Geotech. Engng. ASCE*, 99, 45-73.

48. Wood, D. M. (2012). Macroelement Modelling. *Mechanical Behaviour of Soils under Environmentally Induced Cyclic Loads, 534*, 399-439.

POLITECNICO DI MILANO
Department of Civil and Environmental Engineering
Master of Science in Civil Engineering

EXPERIMENTAL INVESTIGATION ON SOIL-FOUNDATION INTERACTION UNDER CYCLIC AND MONOTONIC LOADING

- Master thesis is submitted to the Department of Civil and Environmental Engineering in partial fulfillment of the requirements for the degree of Master of Science in Civil Engineering for Environmental Risk Mitigation.

Submitted by:

Ehsan Sanglakh Ghouchan Atigh
Student ID: 779966

Supervised by:

Prof. Andrea Galli
Department of Civil & Environmental Engineering, Politecnico di Milano

Piazza L. da Vinci, 32, I-20133, Milan

Academic Year 2013-2014